

**DYNAMIC ASPECTS OF SIGNALING IN
DISTRIBUTED NEURAL SYSTEMS**

Vinod Menon

Department of Computer Sciences
The University of Texas at Austin
Austin, Texas 78712-1188

TR-90-36

November 1990

Dynamic Aspects of Signaling in
Distributed Neural Systems

APPROVED BY

SUPERVISORY COMMITTEE:

Robert E. Wyatt

W. B. ...

W. W. ...

Michael P. ...

...

...

Copyright
by
Vinod Menon
1990

To my dear parents

**Dynamic Aspects of Signaling in
Distributed Neural Systems**

by

Vinod Menon, B.Sc. (Hons.)

DISSERTATION

Presented to the Faculty of the Graduate School of
The University of Texas at Austin
in Partial Fulfillment
of the Requirements
for the Degree of

DOCTOR OF PHILOSOPHY

THE UNIVERSITY OF TEXAS AT AUSTIN

December, 1990

Acknowledgments

I am grateful to Dr. J. C. Browne and Dr. R. E. Wyatt for their help and encouragement in pursuing this dissertation; but above all, for the kindness they have shown me. I also thank Dr. Wyatt for getting me started in the field of neural networks and his financial support during '88 through grants from the Welch Foundation and Cray Research Foundation.

I am grateful to Dr. D. S. Tang for giving me the opportunity to work with him, and his patient support and friendship. I thank Dr. W. W. Bledsoe, Dr. R. van de Geijn and Dr. M. P. Marder for their interest in the dissertation. I thank Dr. R. Miikkulainen for a careful reading of, and detailed remarks on the dissertation.

I am deeply grateful to Mario Cosenza for his kind and affectionate friendship. It is a pleasure to thank Anish Arora, Sumit Ganguly, Govind Menon, B. Ramachandran, and Elizabeth Thomas for their warm friendship.

I know of no words to thank my parents and sisters, Sudha and Prema, for their immeasurable love and affection.

Vinod Menon

The University of Texas at Austin

December, 1990

**Dynamic Aspects of Signaling in
Distributed Neural Systems**

Publication No. _____

Vinod Menon, Ph.D.

The University of Texas at Austin, 1990

Supervising Professors: J. C. Browne and R. E. Wyatt

A distributed neural system consists of localized populations of neurons – neuronal groups – linked by massive reciprocal connections. Signaling between neuronal groups forms the basis of functioning of such a system. In this thesis, fundamental aspects of signaling are investigated mathematically with particular emphasis on the architecture and temporal self-organizing features of distributed neural systems.

Coherent population oscillations, driven by exogenous and endogenous events, serve as autonomous timing mechanisms and are the basis of one possible mechanism of signaling. The theoretical analysis has, therefore, concentrated on a detailed study of the origin and frequency-amplitude-phase characteristics of the oscillations and the emergent features of inter-group reentrant signaling.

It is shown that a phase shift between the excitatory and inhibitory components of the interacting intra-neuronal-group signals underlies the gener-

ation of oscillations. Such a phase shift is readily induced by delayed inhibition or slowly decaying inhibition. Theoretical analysis shows that a large dynamic frequency-amplitude range is possible by varying the time course of the inhibitory signal.

Reentrant signaling between two groups is shown to give rise to synchronization, desynchronization, and resynchronization (with a large jump in frequency and phase difference) of the oscillatory activity as the latency of the reentrant signal is varied. We propose that this phenomenon represents a correlation dependent non-Boolean switching mechanism. A study of triadic neuronal group interactions reveals topological effects – the existence of stabilizing (closed loop) and destabilizing (open loop) circuits.

The analysis indicates (1) the metastable nature of signaling, (2) the existence of time windows in which correlated and uncorrelated activity can take place, and (3) dynamic frequency-amplitude-phase modulation of oscillations. By varying the latencies, and hence the relative phases of the reentrant signals, it is possible to dynamically and selectively modulate the cross-correlation between coactive neuronal groups in a manner that reflects the mapping topology as well as the intrinsic neuronal circuit properties. These mechanisms, we argue, provide dynamic linkage between neuronal groups thereby enabling the distributed neural system to operate in a highly parallel manner without clocks, algorithms, and central control.

4. Synchronization and Delay Induced Switching	59
4.1 Introduction	59
4.2 Mathematical Model	62
4.3 Illustrative Results	65
4.4 Frequency-Amplitude-Phase Relations	70
4.5 Nonlinear Theory	73
4.6 Other Models	90
4.7 Discussion	91
5. Topological Effects	96
5.1 Introduction	96
5.2 Mathematical Model	98
5.3 Analytic and Numerical Results	103
5.3.1 Triangular Reentry	105
5.3.2 Series Reentry	116
5.4 Discussion	120
6. Summary, Predictions, and Concluding Remarks	128
6.1 Summary	128
6.2 Predictions	131
6.3 Concluding Remarks	132
6.3.1 Information in the Oscillations	132
6.3.2 Switching and Gating	133
6.3.3 Time Delays and Memory	134
6.3.4 Time and Time Perception	135

A.	137
A.1	137
A.2	139
A.3	141
A.4	143
B.	145
B.1	145
Glossary	148
Bibliography	153
Vita	

Chapter 1

Introduction

Artificial intelligence has heretofore concentrated on the description of information processing problems at a high level, for example, in terms of symbols and programs and mathematical and logical operations (Charniak and McDermott, 1985; Winston and Brown, 1979). However, for certain tasks, such as pattern or even character recognition, this is not adequate: a computer system can recognize predetermined character sets rather well but even small distortions can cause a complete loss of recognition. The problem is that we do not know how characters, patterns, and symbols are represented. A different problem arises in robotics where the issue is reducing a large number of degrees of freedom to a few relevant ones to execute a particular task (Bernstein, 1967). A table matching strategy (Raibert, 1986) soon breaks down when the complexity of the task increases. In this case, as in several physical systems, it is the nonlinearity that causes a reduction in the number of degrees of freedom (see, for example, Kelso and Tuller, 1984).

In recent years, the problems of information processing have also been pursued in several areas of connectionist and cognitive science (Rumelhart and McClelland, 1986; Feldman and Ballard, 1982). However, these models simplify the architecture, ignore the self-organizing features of neural systems, and invoke ad hoc assumptions about signal processing. To gain an understanding of these problems it is necessary to pursue their organic basis, and since

the brain is the source of what we regard as ‘intelligence’, the biological issues cannot be neglected (Reeke and Edelman, 1988). In the present study, we pursue the biological approach rigorously, particularly with regard to its spatial and temporal self organizing features, in order to understand the fundamental processes underlying the functioning of complex neural systems.

The organization of the brain reflects the tendency of all complex non-linear systems to clump into coherent structures. A growing wealth of experimental data suggests that the brain is a distributed system with functionally segregated units (Mountcastle, 1978; Alexander et al., 1986; Goldman-Rakic, 1988; Zeki and Shepp, 1988). Repertoires of these units form a distributed system which transcends the notion of hierarchy (Mountcastle, 1978). Each module in this system is a localized population of tightly connected neurons termed neuronal groups (Edelman, 1978). The neuronal group serves as the fundamental input/output unit imposing transforms determined by its circuit properties, as well as its extrinsic connections (Mountcastle, 1978). For example, groups such as the cortical columns, serve as redundant and degenerate elements (von Neumann, 1956; Winograd and Cowan, 1963) which ensure that signals and their variants are recognized in a reliable manner (Edelman, 1987).

Such a distributed system serves a distributed function – because no single region receives or processes all aspects of the input (or endogenous activity), recognition of and the response to the external world has to be achieved by signaling between the fundamental units. Signaling between the neuronal groups, therefore, forms the basis of functioning of the system. Signaling has to perform many functions: integration and linkage of disjunctive aspects of the input, association and disassociation (von der Malsburg and Schneider, 1986), switching and gating (Evarts et al., 1984), maintenance of spatiotempo-

ral continuity of objects and events (Reeke et al., 1989), and conflict resolution (Finkel and Edelman, 1989), among others. Signaling is a real time process in distributed systems; the temporal aspects of this process are the subject of the present study.

It is the physical process of signaling and the emergent features thereof, not the specific tasks which are performed that is given importance in this thesis. Such an approach may be contrasted with models of neural computation such as the logical calculus that emerges from neural activity when neurons perform a thresholding function (McCulloch and Pitts, 1943), the approach to a fixed point of interacting symmetrically connected neurons (Hopfield, 1982; Hopfield, 1984), the minimization of error between the expected output and actual output for a class of inputs that has been determined a priori in the parallel distributed programming (PDP) models (Rumelhart and McClelland, 1986), the search for specific computations that are necessary in carrying out a task such as edge or motion detection in visual perception (Marr, 1982), and the analog computations arising from complex biophysical interactions at the level of neurons, synapses, dendrites, and spines (Koch and Poggio, 1987). There is growing evidence to suggest that the underlying operations are correlative and associational and not computational in the algorithmic sense.

It is believed that a basic study of signaling would then be useful in studying the more complex problems of co-ordination, memory, adaptive behavior, and learning, none of which are addressed here. Symbols, meaning, logic, reasoning, language etc. (the basis of cognition) arise at a much higher level than the ones we consider and are beyond the scope of this thesis.

Implicit in the approach we have taken is the view that signaling cannot be understood in terms of some nuance of an impulse; rather, it is the

result of the simultaneous cooperative interaction of impulses (Bernstein, 1967). Such a view is consistent with the notion of spatial self-organization discussed above. The physical basis of signaling, its nature, origin, and characteristics are studied analytically and augmented with numerical studies.

Physiological (Brazier, 1977), theoretical (Wiener, 1961), and psychological (Poppel, 1978) considerations suggest the rhythmic organization of temporal phenomena in the brain. Recent experiments and computer simulations (Traub et al., 1988; Traub et al., 1989; Gray and Singer, 1989) indicate that oscillations generated by localized populations of neurons underlie the process of signaling in neural systems. Oscillations in spatially separated parts of the visual cortex have been found to reflect global stimulus properties (Gray et al., 1989).

The present study has, therefore, focussed on the origin, generation, and characteristics of oscillations and the inter-group interaction of oscillatory signals. An analytical study allows us to underpin the critical aspects of the dynamics of interacting oscillatory signals in the distributed system and look for novel emergent phenomena. The mathematical models we use are derivations and extensions of the Wilson-Cowan model (Wilson and Cowan, 1972; Wilson and Cowan, 1973) for the functional dynamics of interacting subpopulations of excitatory and inhibitory neurons in localized populations of neurons.

A distributed system necessarily involves time delays. In a distributed system, access to specific signals can be deferred in time thereby serving as memory and ensuring temporal continuity in representation of the signals from the external world. Therefore, in the analytical models we consider, particular importance has been given to latency in the transmission and transduction of specific signals. In the present study, fundamental and qualitative changes in

the dynamics are found when synaptic and transmission delays are introduced. Whereas in computer systems, time delays are a nuisance that have to be compensated for, in neural systems, time courses of signals dynamically controlled by neurotransmitters and neuromodulators, may serve very useful roles, as the present thesis seeks to show. The complex phasic effects, arising from the delays of signals, are shown to give rise to a diverse set of phenomena which are studied in some detail.

Neuronal groups provide a stable locus for the cooperative spatiotemporal interaction of excitatory and inhibitory neurons to generate coherent oscillatory signals. It is shown that a particularly robust method for generating the oscillations is delayed inhibition or slowly decaying inhibition which causes a phase shift between the excitatory and inhibitory components of the interacting intra-neuronal-group signals. Theoretical analysis of the oscillations shows that a large range of frequency and amplitude is possible by varying the time course of the inhibitory signal.

The analysis is then extended to study the interaction of oscillatory signals between two groups. The results indicate a correlation dependent switching involving synchronization, desynchronization, and resynchronization of the oscillatory activity. By varying the latencies of the reentrant signals (modulated by neurotransmitters) it may be possible to dynamically control the cross-correlation between coactive neuronal groups. The logic expressed by such dynamics, it may be argued, is correlation dependent and hence non-Boolean.

A study of triadic neuronal group interactions reveals topological effects in signaling in distributed systems. Signals from the third group can dynamically control the diadic cross-correlation in a robust and selective man-

ner. The existence of stabilizing and destabilizing global mapping topologies is suggested. The cross-correlation of co-active groups is dependent, therefore, on the mapping topology as well as the intrinsic neuronal circuit properties.

In short, the results indicate the metastable nature of signaling in distributed neural systems and the dynamic manner in which the cross-correlation of co-active groups can be modulated.

In the following Chapter, the nature of the distributed system and the nature of signaling are elaborated along with the theoretical framework for the analysis pursued in the present study. The generation of robust oscillations in a localized population of neurons due to delayed inhibition is discussed in Chapter 3. These coherent oscillatory signals form the basis of reentrant signaling between neuronal groups. The emergent features of signaling, in particular the effects of delayed reentry on diadic and triadic neuronal group interactions are the topics of Chapters 4 and 5 respectively. The results and their implications are summarized in Chapter 6.

Chapter 2

Nature of Signaling in Distributed Neural Systems

There are fundamental differences between signaling in computer and neural systems. An important feature of the von Neumann architecture is the separation of logical aspects from circuit design. A consequence of this separation is the need for an external clock and the physical and conceptual separation of the processing unit from memory in computer systems. The clock, whose (fixed) frequency is controlled by a crystal oscillator, drives the basic processing elements – switches such as *AND*, *NAND*, and *OR* gates. In such a system, all operations including error correction follow a strictly Boolean algebra. The basic process, then, involves the fetch-execute-store operation on a sequence of instructions which are a subset of the algorithm (program) under execution.

It is somewhat odd that some of these features had their origin in the neural network model of McCullough and Pitts (1943) (see Aspray and Burks, 1987 pgs. 7 and 32). For, neural systems possess autonomous timing mechanisms, driven both by endogenous and exogenous events. Furthermore, in these systems, the underlying process is statistical, nonlinear, non-algorithmic, and adaptive.

In seeking to develop a general theory of automata, von Neumann (1956) had already noted the need for ‘highly mathematical and more specifically analytical theory of automata’ in view of the refractory nature of logical

analysis and emphasized in particular the need for a ‘deeper mathematical study of the nervous system’. Wiener (1961), in developing the theory of cybernetics, had noted several neurophysiological details which emphasized the role of nonlinear feedback processes for control and error correction.

Given the progress in neuroscience over the past few decades, it is possible to pose the issues related to the functioning of complex neural systems in terms of the architecture and self-organizing features of neural systems. In this chapter, we elaborate on one important mechanism of signaling in distributed neural systems. Such a consideration explains the particular theoretical formulation followed and developed in this thesis.

2.1 Nature of the Distributed System

In distributed neural systems, there are functionally specialized units which process specific attributes of exogenous or endogenous signals or events. For example, in the visual system, there are regions specialized for processing motion, form, and color (Zeki and Shepp, 1988; DeYoe and van Essen, 1988). Specialized structures which represent signals topographically, for example in the sensory cortex, (Mountcastle, 1978) and columns for orientation or ocular dominance in the visual cortex (Hubel and Wiesel, 1977) are well known.

The basic unit of this distributed system has been conjectured to be a neuronal group (Edelman, 1978). The neurons in such a group are tightly connected, i.e., the mean intra-group synaptic strength and density are greater than the mean inter-group synaptic strength and density respectively. In the primary receiving areas, these groups serve as elementary recognizers to map and represent signals from the external world. For example, an orientation column in the visual cortex may recognize an object with a particular orientation.

In the higher areas, the processing is more abstract and not well understood (Mountcastle, 1978).

In reviewing the nature of the distributed system, Mountcastle (1978) has noted that ‘... the processing function of neocortical modules is qualitatively similar in all neocortical regions. Put shortly, there is nothing intrinsically motor about the motor cortex, nor sensory about the sensory cortex. Thus, the elucidation of the mode of operation of the local modular circuit anywhere in the neocortex will be of great generalizing significance’. However, in conjunction with this observation, it is also important to note that such a neuronal group is constantly interacting with other groups.

2.2 Reentrant Signaling

One of the ubiquitous features of such a distributed system is the presence of reciprocal connections between the groups forming the distributed system. These connections, like the recurrent connections within the groups, have a quasi-random character. The reciprocal connections need not be neuron specific. For example, neuron A in group G may be connected to neuron A' in G' which may in turn be linked to A through an intermediary neuron C in G . Such multiple pathways provide redundancy in signaling.

Signaling now becomes a statistical process because no longer is the correlated firing of two neurons required. Thus, if specific neurons are refractory, signaling need not be disrupted since there exist multiply connected pathways ensuring *redundancy* in the signaling process. Signaling itself is then the result of cooperative nonlinear interactions within and between neuronal groups.

It is instructive to compare such a schema with the proposal of Hebb

(1949). Hebb proposed the idea of cell assemblies in which diffusely connected neurons form a closed loop when activated by specific inputs. However, given the considerable feedforward and feedback connectivity in neural systems, such point to point signaling between neurons would be difficult to achieve and indeed such a mechanism of communication would easily lose specificity. Signals may spread out diffusively rendering the reverberating pathway structurally unstable. Moreover, it is easy to see that such a system does not possess redundancy – if a neuron in one of the closed loops is refractory, signaling would be completely disrupted.

2.3 Organization of Temporal Phenomena

A variety of physiological and psychological experiments and observations suggests the rhythmic organization of temporal phenomena in the neural systems. The well known EEG oscillations (Brazier, 1977), oscillations in the central pattern generator in the motor system (Cohen et al., 1987), oscillations in the olfactory cortex (Bressler and Freeman, 1980), the thalamic oscillations (Steriade et al., 1990) and the recently observed cortical oscillations (Gray and Singer, 1989; Eckhorn et al., 1988), all affirm this.

The rhythmic organization of temporal phenomena in the brain is also suggested by studies of reaction times to visual stimuli (Poppel and Logothetis, 1986) and several neuropsychological experiments on speech production, delivery, and related cognitive phenomena (Poppel, 1978). With respect to motor activity, Bernstein (1967) has noted that a diversity of rhythmical human movements may be interpreted to a great accuracy with the sum of three or four harmonics in the oscillations.

2.4 Role of Oscillations in Signaling

Oscillations (see section 2.5) could serve as the basis of coherent signaling and as autonomous timing mechanisms. Wiener (1961) noted that oscillations could serve to gate specific inputs – thus, for example, signals arriving within a certain time gap are likely to be combined. Based on several psychological experiments and observations, it has been noted that sensory integration is likely to be aided by oscillations transduced by the different sensory modalities (Poppel et al., 1990). Integration of new and unexpected signals such as those required to take into account reactive phenomena in motion are likely to be aided by oscillations (Bernstein, 1967). Oscillations also serve as the basis for establishing dynamical correlations for sensory segmentation underlying pattern recognition (von der Malsburg and Schneider, 1986).

Oscillations provide a particularly effective mechanism to create a spatiotemporally continuous representation of objects or events – the so-called perceptual update – (Edelman, 1978; Reeke et al., 1989) in view of its own cyclic and continuous nature. Globally mapped oscillatory signals may also be involved in neural control of state (in the sleep-wake cycle, for example) as well (Hobson and Steriade, 1986).

These observations have been given an impetus by recent experiments on the cat visual cortex (Gray and Singer, 1989; Gray et al., 1989; Eckhorn et al., 1988) indicating that oscillations in the frequency range 20 – 80 Hz. occur in several areas of the neocortex when the animal directs its attention to meaningful stimuli. The oscillations, occurring in spatially separated regions, can be synchronized in a manner that reflects global stimulus properties. These experiments suggest an important role for oscillations in overall integration in distributed systems in order to obtain a coherent reconstruction of visual scenes.

2.5 Population Nature of the Oscillations

While individual neurons can fire rhythmically (Llinas, 1988), it is unlikely that given the massive recurrent connections between neurons this represents the dominant mode of signaling in a distributed neural system. On theoretical grounds, it may be argued that the oscillations must represent collective phenomena (Wilson and Cowan, 1972). Such oscillations have the advantage of being robust and stable to random fluctuations.

The computer simulations of Traub et al. (1988, 1989) have recently elucidated the nature of the population oscillations. The work of these scientists on the CA3 slice of the hippocampus indicates that the temporal activity consists of rhythmic population oscillations in which the number of neurons firing per unit time oscillates synchronously, even though single neurons may fire asynchronously. The firing of single neurons is largely stochastic and unpredictable. The amplitude and frequency of this emergent rhythmic activity depend on intrinsic cellular properties, such as refractoriness, as well as delay in the inhibitory feedback and the connectivity and strength of both excitatory and inhibitory synapses. An important indication of the population nature of the activity is that the population firing rate (the fraction of neurons firing per unit time) can be faster than the refractory period of single neurons. Furthermore, when the model slice is cut laterally, it is found that a certain minimum size is needed to sustain coherent oscillations. Variable levels of excitation and inhibition and their relative timings are found to be critical in determining the characteristics (in particular the frequency and amplitude) of the oscillation.

Experimental evidence also suggest that cellular firing is usually less well correlated with the EEG than are synaptic potentials (Traub et al., 1989). Eckhorn et al. (1988) have noted the difficulty of detecting rhythmic oscillations

in single unit activity even when the local field potential and multi-unit activity indicate coherent oscillatory activity. Therefore, it is unlikely that the critical character of the oscillations is likely to be understood by considering the firing of single neurons, or even a few interacting neurons.

2.6 Approach to Theoretical Analysis

An important characteristic of complex systems is that nonlinearity serves to decrease the number of degrees of freedom. This allows us to represent the aggregate dynamics by a few state variables. Such an approach is necessary to pursue a theoretical and analytical study of signaling. It allows us to provide a theoretical underpinning of several recent complex experiments and computer simulations, besides looking for qualitatively new phenomena. Even computer simulations of a thousand neurons in some detail requires considerable resources to explore even a limited parameter range.

The experiments of Traub et al. (1988, 1989) suggest that the relevant population variables are the fraction of excitatory and the fraction of inhibitory neurons firing per unit time. A mathematical framework for studying the functional dynamics of populations of neurons was developed by Wilson and Cowan (1972, 1973). In the subsequent chapters this model and its variants are used to study the generation of population oscillations within a neuronal group and the reentrant signaling between neuronal groups. It would, however, be a mistake to interpret the present approach in terms of neuronal fields (Arbib and Amari, 1989) since we study the interaction of *coherent signals* within and between localized segregated populations of neurons.

An important modification of the Wilson-Cowan model that has been introduced in the present study is delay in the transmission and transduction

of specific signals. Delays in models of physiological control systems have been found to result in important qualitative and quantitative differences (Murray, 1989). In most theoretical models of neural systems, delay has been neglected although its importance has been noted by von Neumann (Aspray and Burks, 1987).

It is important to note here that the spatial effects of connectivity within the neuronal group have been somewhat sidelined since in a distributed system the most important topological effects are thought to arise from mapping between neuronal groups. The connectivity within a localized population of neurons is statistical and the collective phenomena are more or less independent of the precise wiring. From such a systems point of view, the main problem is to study the frequency-amplitude-phase characteristics of the oscillatory activity and the effect of reentrant signaling on inter-group activity cross-correlation.

Chapter 3

Theoretical Analysis of Population Oscillations

3.1 Introduction

The mathematical study of the firing characteristics of a single neuron itself presents enormous difficulties (Tuckwell, 1988). The behavior of a single neuron is extremely complex – it is a highly nonlinear element which has several voltage gated channels controlling its membrane potential and hence its activity. When we consider that this neuron is interacting with several hundred other neurons through synaptic and dendritic interactions that are themselves gated by complex voltage gated channels and receptors coupled to second messenger systems (Shepherd, 1988b), the complexity becomes enormous.

In spite of this complexity, the firing pattern of a population of neurons must have a simpler characteristic in order that the signaling be coherent. Nonlinear interactions, between excitatory and inhibitory neurons in a localized population, give rise to collective behavior thereby serving to reduce the extreme variability that is possible in the firing of single neurons. Such population oscillations obviate the need for control and precise timing of individual impulses.

As we have seen, on several grounds it may be argued that the neuron is unlikely to be the fundamental unit of signaling in neural systems. There is evidence that the fundamental I/O unit in neural systems (at least complex ones) is likely to be a neuronal group (Mountcastle, 1978; Edelman, 1978).

The neurons in a group are tightly coupled, i.e., the synaptic strength within a group is much stronger than that between groups. Therefore, the neuronal group could serve as a stable locus for spatiotemporal signaling in a distributed system. Within this stable unit, a great deal of dynamic control of the oscillations is possible by varying, for example, the time courses of activation of neurotransmitters and synaptic strengths, as the simulations of Traub et al. (1988, 1989) have shown. Moreover, a large variety of neurotransmitters provides mechanisms to dynamically change the characteristics of the oscillations of the same circuit (Marder et al., 1987).

In light of the experimental and computational results discussed above, indicating the stochastic nature of firing of single neurons, we take a statistical approach to study the origin and characteristics of coherent oscillations generated by interacting excitatory and inhibitory neurons. The model we consider was proposed by Wilson and Cowan (1972) to study temporal phenomena in a localized population of interacting excitatory and inhibitory neurons and is based on the technique of renormalization which is widely used to study collective phenomena in the physical sciences (see, for example, Frohlich, 1983).

The redundant and the quasi-random nature of the circuitry in a neuronal group allows us to represent the mean temporal activity by renormalized variables for the fraction of excitatory and inhibitory neurons firing per unit time (Wilson and Cowan, 1972). In the present model, the actual renormalization step consists of replacing the summation of excitatory and inhibitory potentials on the membrane of a neuron by the summation of excitatory and inhibitory signals from interacting subpopulations of excitatory and inhibitory neurons (Cowan, 1971). This approach is useful in studying the dynamics of the aggregate, particularly when cellular refractoriness is not negligible com-

pared to the other time scales in the problem. The model therefore deals with coherent interacting excitatory and inhibitory signals. Such an approach may be contrasted with the EEG related studies of interacting neuronal oscillators (Freeman and Skarda, 1985; Li and Hopfield, 1988) and studies of the rhythmic response of central pattern generators using ‘phase models’ (Kopell, 1988; Rand et al., 1988).

The focus of the present chapter is in exploring the role of delayed inhibition and a slowly decaying inhibitory signal in inducing robust oscillations in neural systems. The time courses of inhibition, mediated by, for example, the slow and fast neurotransmitters $GABA_A$ and $GABA_B$, play a critical role in regulating the frequency-amplitude characteristics of the oscillations (Traub et al., 1989). Our aim here is to analytically underpin the basis of such dynamic response.

One of the reasons it has been difficult to analytically study the frequency-phase-amplitude characteristics of the Wilson-Cowan model is that without delay in the inhibition or a slowly decaying inhibition, strong feedback is needed to generate oscillations. Strong feedback results in the generation of strong harmonics which makes it difficult to carry out any detailed theoretical analysis. This problem has been overcome in the present study.

The organization of this Chapter is as follows: in Section 3.2 we describe the mathematical model of Wilson and Cowan and propose a simple extension to study temporal activity due to delayed inhibitory signals. In Section 3.3 the asymptotic stability of the linearized equations is considered. It is found that for a wide range of parameters delay in feedback from the inhibitory neurons can destroy stability of the fixed points, thereby inducing limit cycle oscillations. To study periodic solutions, the method of harmonic

balance is briefly described in Section 3.4, and in Section 3.5 this method is used to derive nonlinear algebraic equations governing the frequency, amplitude, and phase of oscillations for the piece-wise linear sigmoid. In Section 3.6 it is shown that a linear approximation is inadequate to study the oscillations. We consider a detailed nonlinear theory in Section 3.7. Section 3.8 summarizes the main results.

3.2 Mathematical Model

The aim of the mathematical model we consider in this and the following two chapters is to “give an expression to the statistical nature of the interaction of neurons” (Cowan, 1971). The model does not refer to the firing or activity of single neurons but to the collective behavior of localized populations of neurons. Such an approach is consistent with the experimental and computational results indicating the population nature of the oscillatory activity (Traub et al., 1989; Eckhorn et al., 1988; Sporns et al., 1989). The main problem that this model addresses is the nonlinear interaction of excitatory and inhibitory signals originating from the more complex spatiotemporal interaction of individual neurons.

Figure 3.2.1 is a schematic representation of the model. External input and recurrent excitation drive the activity of the excitatory subpopulation. The inhibitory subpopulation is activated by the excitatory subpopulation and possibly by external input. The activated inhibitory subpopulation then inhibits the activity of both inhibitory and excitatory neurons usually with a latency.

The nonlinear summation of voltages at the membrane of a neuron can be renormalized to represent the response of excitatory and inhibitory subpop-

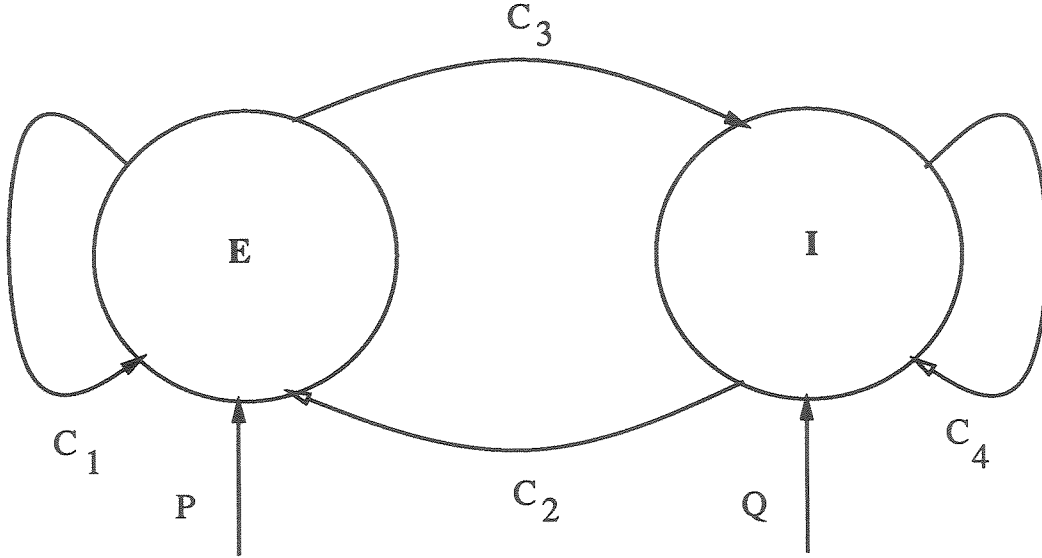


Figure 3.2.1: A schematic of interacting subpopulations of excitatory E and inhibitory I neurons in a neuronal group. External inputs P and Q drive the activity of the neurons. C_1 , C_2 , C_3 , and C_4 are the mean synaptic strengths mediating the inter- and intra-subpopulation interactions. Filled arrows indicate the excitatory effect, and unfilled arrows, the inhibitory effect of one subpopulation on the other or itself.

ulations in a localized population of neurons (Cowan, 1971). This represents a parsing of the complex circuitry within a neuronal group. The interactions between the subpopulations may then be modeled by the following time coarse grained and spatially averaged nonlinear differential equations, (Wilson and Cowan, 1972), for $f_e(t)$ and $f_i(t)$, the fraction of excitatory and inhibitory neurons firing per unit time at time t ,

$$T_e \dot{f}_e(t) = -f_e(t) + [1 - \int_{t-r_e}^t f_e(t') dt'] \sigma_e(x_e) \quad (3.2.1)$$

$$T_i \dot{f}_i(t) = -f_i(t) + [1 - \int_{t-r_i}^t f_i(t') dt'] \sigma_i(x_i) \quad (3.2.2)$$

$$x_e = C_1 f_e(t) - C_2 f_i(t) + P$$

$$x_i = C_3 f_e(t) - C_4 f_i(t) + Q$$

Condition 2 ensures that there is only one fixed point, and condition 1 implies that the fixed point is unstable. These conditions require that there be a strong negative feedback ($C_2C_3 \gg C_1C_4$). We will show that limit cycle oscillations exist for a much wider range of parameters than implied by the above results.

Eqns. 3.2.1 and 3.2.2 ignore delay in the expression of the inhibitory signal at the synapse (Hille and Catterall, 1989). Such delays are a typical feature of inhibitory interneurons and have been shown to be critical for oscillations – blocking slow inhibition can prevent partially synchronized bursts (Traub et al., 1988; Traub et al., 1989). If we denote the time course of the inhibitory postsynaptic potentials developing onto the excitatory and inhibitory subpopulations by $\alpha(t)$, Eqns 3.2.1, 3.2.2 are modified to

$$T_e \dot{f}_e(t) = -f_e(t) + [1 - \int_{t-r_e}^t f_e(t') dt'] \sigma_e(C_1 f_e(t) - C_2 \int_{-\infty}^t \alpha(t'') f_i(t-t'') dt'' + P) \quad (3.2.3)$$

$$T_i \dot{f}_i(t) = -f_i(t) + [1 - \int_{t-r_i}^t f_i(t') dt'] \sigma_i(C_3 f_i(t) - C_4 \int_{-\infty}^t \alpha(t'') f_i(t-t'') dt'' + Q) \quad (3.2.4)$$

Approximating the time course by the delta function, $\alpha(t) = \delta(t - t_d)$, where t_d is the delay in the inhibitory feedback, the above equations are,

$$T_e \dot{f}_e(t) = -f_e(t) + [1 - \int_{t-r_e}^t f_e(t') dt'] \sigma_e(C_1 f_e(t) - C_2 f_i(t - t_d) + P) \quad (3.2.5)$$

$$T_i \dot{f}_i(t) = -f_i(t) + [1 - \int_{t-r_i}^t f_i(t') dt'] \sigma_i(C_3 f_i(t) - C_4 f_i(t - t_d) + Q) \quad (3.2.6)$$

In the next section we show that Eqns. 3.2.5 and 3.2.6 display limit cycle oscillations for a wide range of parameters when the inhibitory signal delay, t_d , is non-zero.

3.3 Asymptotic Stability of Linearized Equations

The role of delay in inducing oscillations has been explored in other neural network models (an der Heiden, 1980; Marcus and Westervelt, 1989). The aim here is to consider specifically the role of delayed inhibition in a model with renormalized nonlinear summation of excitatory and inhibitory signals. In this section, we consider the stability of the fixed points of Eqns. 3.2.5 and 3.2.6 in order to study the effect of delay in the inhibitory signal. A different view of the origin of the oscillations will be described when a nonlinear theory is described.

A necessary condition for the existence of oscillations is that at least one of the fixed points is unstable. Proving existence of limit cycle oscillations for delay differential equations is quite complicated and no attempt is made to do so here. However, for the problem at hand, we will interpret the instability of all the fixed points to mean that oscillations could exist, although this is a much stronger condition than is actually needed. Numerical experiments indicate that the only limit sets that occur are fixed points and periodic orbits.

For the stability of a fixed point of the nonlinear functional differential Eqns. 3.2.5 and 3.2.6 a necessary and sufficient condition is the stability of the linearized equations (Kolmanovskii and Nosov, 1986). The fixed points, \bar{f}_e and \bar{f}_i , are given by

$$\bar{f}_e = (1 - r_e \bar{f}_e) \sigma_e (C_1 \bar{f}_e - C_2 \bar{f}_i + P) \quad (3.3.1)$$

$$\bar{f}_i = (1 - r_i \bar{f}_i) \sigma_i (C_3 \bar{f}_e - C_4 \bar{f}_i + Q) \quad (3.3.2)$$

Linearizing around the fixed point gives the following characteristic equation for small r_e and r_i (see Appendix A.1 for details)

$$\lambda^2 + G\lambda + H + \lambda J e^{-t_d \lambda} + I e^{-t_d \lambda} = 0 \quad (3.3.3)$$

where

$$\begin{aligned}
G(\bar{x}_e) &= (\kappa_e + \kappa_i - \alpha_e \sigma'_e(\bar{x}_e) C_1) \\
H(\bar{x}_e) &= \kappa_i (\kappa_e - \alpha_e \sigma'_e(\bar{x}_e) C_1) \\
I(\bar{x}_e, \bar{x}_i) &= \sigma'_e(\bar{x}_e) \sigma'_i(\bar{x}_i) \alpha_e \alpha_i (C_2 C_3 - C_1 C_4) \\
J(\bar{x}_i) &= \sigma'_i(\bar{x}_i) \alpha_i C_4 \\
\sigma'_e(\bar{x}_e) &= \beta_e / (4 \cosh^2(-\beta_e(\bar{x}_e - \chi_e))) \\
\sigma'_i(\bar{x}_i) &= \beta_i / (4 \cosh^2(-\beta_i(\bar{x}_i - \chi_i))) \\
T_e \kappa_e &= 1 + r_e \sigma_e(\bar{x}_e) \\
T_i \kappa_i &= 1 + r_i \sigma_i(\bar{x}_i) \\
T_e \alpha_e &= 1 - r_e \bar{f}_e \\
T_i \alpha_i &= 1 - r_i \bar{f}_i \\
\bar{x}_e &= C_1 \bar{f}_e - C_2 \bar{f}_i + P \\
\bar{x}_i &= C_3 \bar{f}_e - C_4 \bar{f}_i + Q
\end{aligned} \tag{3.3.4}$$

The quasi-polynomial (Eqn. 3.3.3) has an infinite number of roots. A necessary and sufficient condition for the stability is that $Re \lambda < 0$, for all roots. $\sigma'_e(\bar{x}_e)$ and $\sigma'_i(\bar{x}_i)$, are the slopes of the sigmoid at the fixed point. σ' lies between 0 and $\frac{\beta}{4}$ and its maximum value is at the threshold.

The following theorems, proven in Appendix A.2, indicate the nature of the solutions to the characteristic equation. Here we will discuss only the implications of the theorems.

Theorem 3.3.1 *For sufficiently large delay t_d the fixed point is unstable if $H < 0$.*

Theorem 3.3.2 *A set of sufficient conditions for stability of a fixed point is: (i) $t_d(H + I) > 0$ and (ii) $G - J > t_d|I|$*

Theorem 3.3.3 *If $t_d^2(H + I) < 0$, the fixed point is unstable.*

The following results indicate when limit cycle oscillations could occur and the critical delay for which this happens:

(1) If $\sigma'_e(\bar{x}_e) = 0$ and $\sigma'_i(\bar{x}_i) = 0$ then the fixed point is stable.

Proof: Let $\sigma'_e(\bar{x}_e) = \sigma'_i(\bar{x}_i) = 0$. Then $G = \kappa_e + \kappa_i$, $H = \kappa_e \kappa_i > 0$, $I = 0$ and $J = 0$, from Eqns. 3.3.4. From Theorem 3.3.2 it then follows that the fixed point is stable.

Hence, oscillations cannot occur for any value of delay if the slope of the sigmoid at all of the fixed points is zero for both the excitatory and the inhibitory components. Typically, the slope of the sigmoids is zero when either the driving input is too strong or too weak compared to the threshold for excitation.

(2) An interesting case arises when the sigmoid is a step function so that the slope is zero everywhere except the threshold where it is infinite. The result derived in (1), above, indicates that no oscillations are possible in such a case since the slope is zero almost everywhere. Thus, variance in the subpopulation, implying a non-step-function sigmoid, may be essential in generating stable oscillations. Numerical experiments indicate this to be true. Note however that this result has not been proved rigorously.

(3) If $H < 0$, which necessarily requires $\sigma'_e(\bar{x}_e) \neq 0$, there is a time delay, τ , such that for $t_d > \tau$, all fixed points are unstable. This follows directly from Theorem 3.3.1. This result indicates that for a wide range of parameters, all the fixed points are unstable, and therefore limit cycle oscillations occur for large enough delay. When $r_e = r_i = 0$ and $T_e = T_i$, for $H < 0$, it is necessary

that $C_1 > \frac{1}{\sigma'_e(\bar{x}_e)}$. If the fixed point is near the threshold this simply requires $C_1 > \frac{4}{\beta_e}$.

(4) If $H + I < 0$ for all fixed points, then from Theorem 3.3.3, arbitrarily small delays can cause the fixed points to be unstable. This result is particularly important for $I \propto C_2C_3 - C_1C_4 = 0$, i.e., there is no dominant feedback. Hence, if the condition $C_1 > \frac{4}{\beta_e}$ derived in (3), above, is satisfied, even arbitrarily small delay can cause oscillations. An example of this is illustrated in Fig. 3.3.1.

(5) On the other hand, if $H + I > 0$, condition (ii) of Theorem 3.3.2, $G - J > |I|t_d$, gives the delay times for which the fixed point is stable:

$$t_d^{cr} = [\kappa_e + \kappa_i - \alpha_e \sigma'_e(\bar{x}_e)C_1 - \sigma'_i(\bar{x}_i)\alpha_i C_4] / [\sigma'_e(\bar{x}_e)\sigma'_i(\bar{x}_i)\alpha_e\alpha_i(C_2C_3 - C_1C_4)]$$

For $t_d < \max(t_d^{cr})$, where \max is the maximum over all fixed points, every fixed point is guaranteed to be stable and no oscillations are possible. For $r_e = r_i = 0$, it is easy to see that for a wide range of parameters, stability is difficult to guarantee.

(6) The role of refractoriness in the excitatory neurons in inducing oscillations is indicated by the following argument. Let $\sigma_e(x_e) = \sigma_i(x_i) = 1$ (hence $\sigma'_e(\bar{x}_e) = 0$ and $\sigma'_i(\bar{x}_i) = 0$), as we have seen, even large delays cannot destabilize the fixed point. Consider parameters such that when $r_e = r_i = 0$, $f_e = 1$. f_e decreases when $r_e \neq 0$. This follows straightforwardly from Eqn. 3.3.1, $f_e = \frac{\sigma_e(\bar{x}_e)}{1+r_e\sigma_e(\bar{x}_e)} < 1$. Now, with a smaller value of f_e , $\sigma_e(\bar{x}_e)$ can be less than 1 thereby increasing $\sigma'_e(\bar{x}_e)$ to non-zero values, whence delay can induce oscillations.

(7) Oscillations can occur even if the delay t_d is zero and there is no dominant feedback, but the inhibitory decay time is greater than the excitatory decay time, $T_i > T_e$. From Eqn. 3.3.3, when $t_d = 0$, it is easy to see

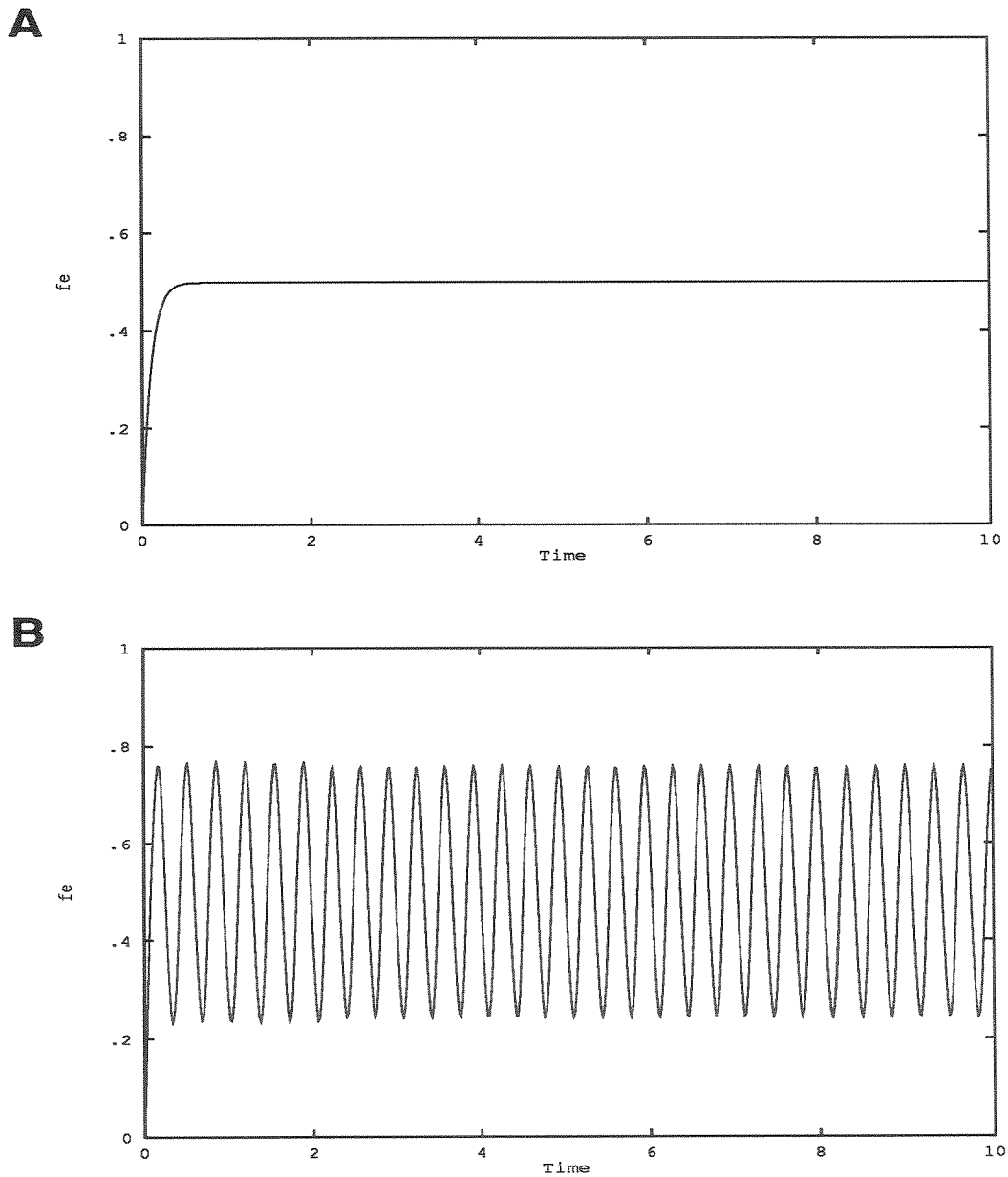


Figure 3.3.1: The fixed point can become unstable when a small delay is introduced in the inhibitory feedback thereby inducing limit cycle oscillations. (A) The fraction of excitatory neurons firing per unit time $f_e(t)$ for inhibitory delay $t_d = 0$ illustrates stabilization to a fixed point. (B) $f_e(t)$ for delay $t_d = 0.05$ indicates destabilization of the fixed point leading to robust oscillations. Results are obtained from the numerical simulation of Eqns. 3.2.5 and 3.2.6. Similar results hold for the inhibitory component.

that if $G + J < 0$, the characteristic equation has a positive real part and hence the fixed point is unstable. From Eqns. 3.3.4, since $J \sim \frac{1}{T_i}$ and $G \sim \frac{1}{T_e}(1 + \frac{T_e}{T_i} - \sigma'_e(\bar{x}_e)C_1)$, the effect of small excitatory decay time T_e and large inhibitory decay time T_i is to decrease $G + J$, thereby causing the fixed point to be unstable. Fig. 3.3.2 illustrates an example of oscillations when $t_d = 0$ but $T_e < T_i$.

From these results we note that there exist a wide range of parameters for which delay in the inhibitory signal or a slowly decaying inhibitory signal can destabilize the fixed point. In particular, it is not necessary that the coupling be feedback dominated. Arbitrarily small delays can cause instability of the fixed points and hence oscillations.

3.4 Method of Harmonic Balance

To study periodic solutions of Eqns. 3.2.5 and 3.2.6 we apply the method of harmonic balance, which reduces the problem of finding periodic solutions of differential equations to finding solutions of algebraic nonlinear equations (Mees, 1981). The method is closely related to the averaging technique (Guckenheimer and Holmes, 1983).

The solution of Eqns. 3.2.5 and 3.2.6 is taken to be of the form $f \sim \bar{f} + f_0 \sin(\omega t)$. Therefore, the input to the nonlinear sigmoid is of the form $x(t) = B + A \sin(\omega t + \theta)$ where B is the bias, A the amplitude, ω the frequency, and θ an appropriately determined phase. The main problem now is to obtain an approximate response of the nonlinear sigmoid. The crucial step here is to approximate the response of the nonlinear sigmoid by the Fourier transform of $\sigma(x)$ (Bogoliubov and Mitropolsky, 1961),

$$\sigma(x) \sim BF_B(\sigma, A, B) + AF_A(\sigma, A, B) \sin(\omega t + \theta)$$

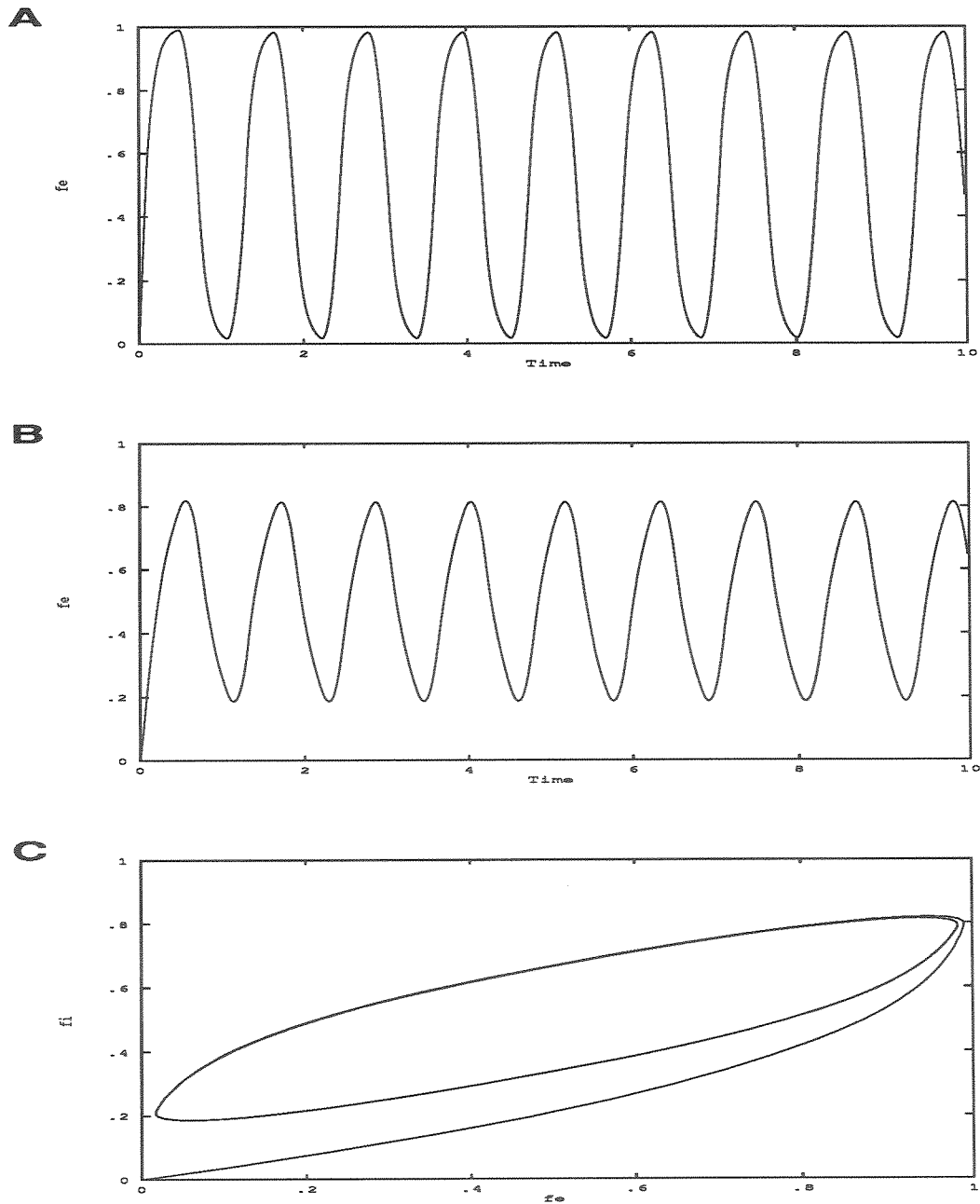


Figure 3.3.2: Even with zero inhibitory time delay, t_d , low frequency oscillations can be induced when the activity decay time scales, T_e and T_i , are disparate – $T_e < T_i$. (A) The fraction of excitatory neurons firing per unit time $f_e(t)$. (B) The fraction of inhibitory neurons firing per unit time $f_i(t)$. (C) The phase portrait showing non-zero phase between the excitatory and inhibitory components. In this example, $T_e = 0.1$ and $T_i = 0.25$. The other parameters are the same as in Fig. 3.3.1.

$$\begin{aligned}
& + AF_A^\dagger(\sigma, A, B) \cos(\omega t + \theta) \tag{3.4.1} \\
F_B(\sigma, A, B) &= \frac{1}{2\pi B} \int_0^{2\pi} \sigma(B + A \sin(\psi)) d\psi \\
F_A(\sigma, A, B) &= \frac{1}{\pi A} \int_0^{2\pi} \sigma(B + A \sin(\psi)) \sin(\psi) d\psi \\
F_A^\dagger(\sigma, A, B) &= \frac{1}{\pi A} \int_0^{2\pi} \sigma(B + A \sin(\psi)) \cos(\psi) d\psi
\end{aligned}$$

F_B , F_A , and F_A^\dagger are the nonlinear gain for the bias, sinusoidal, and co-sinusoidal components respectively. These gain functions are also referred to as describing functions (Gelb and Velde, 1967).

Using these approximations, the differential equations reduce to algebraic ones.

In the present problem, for the general form of the sigmoid, it is hard to evaluate the integrals above. However, the integrals can be easily evaluated by using the piecewise linear saturation function (Fig. 3.4.1)

$$\begin{aligned}
\sigma(x) = \quad & 1.0 & x > \chi + \delta \\
& 0.0 & x < \chi - \delta \\
& m(x - \chi) + 0.5 & |x - \chi| < \delta
\end{aligned}$$

where $\chi + \delta$ is the saturation point, and m is the slope of the sigmoid with $\delta m = \frac{1}{2}$.

The integrals simplify further for the symmetric version of the sigmoid

$$\begin{aligned}
\sigma^*(x) = \quad & mx & |x| < \delta \\
& 0.5 & x > \delta \\
& -0.5 & x < -\delta
\end{aligned} \tag{3.4.2}$$

The gain functions F_B , F_A , and F_A^\dagger for inputs of the form $x(t) =$

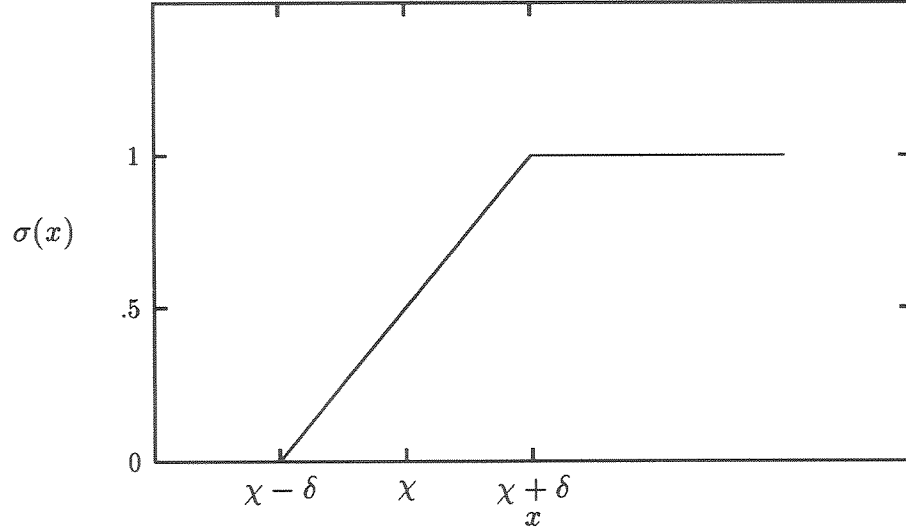


Figure 3.4.1: Piece-wise linear saturation nonlinearity, $\sigma(x)$. $\chi + \delta$ is the saturation point, m is the linear gain with $\delta m = \frac{1}{2}$.

$B + A \sin(\omega t + \theta)$ to σ^* can now be easily evaluated

$$F_B(B, A) = \frac{mA}{2B} [g(\frac{\delta+B}{A}) - g(\frac{\delta-B}{A})] \quad (3.4.3)$$

$$F_A(B, A) = \frac{m}{2} [f(\frac{\delta+B}{A}) + f(\frac{\delta-B}{A})] \quad (3.4.4)$$

$$F_A^\dagger(B, A) = 0 \quad (3.4.5)$$

where f and g are given by,

$$\begin{aligned} g(x) &= \frac{2}{\pi} (x \sin^{-1} x + \sqrt{1-x^2}) & |x| \leq 1 \\ &= |x| & |x| > 1 \end{aligned} \quad (3.4.6)$$

$$\begin{aligned} f(x) &= -1 & x < -1 \\ &= \frac{2}{\pi} (\sin^{-1} x + x \sqrt{1-x^2}) & |x| \leq 1 \\ &= 1 & x > 1 \end{aligned} \quad (3.4.7)$$

(Gelb and Velde, 1967).

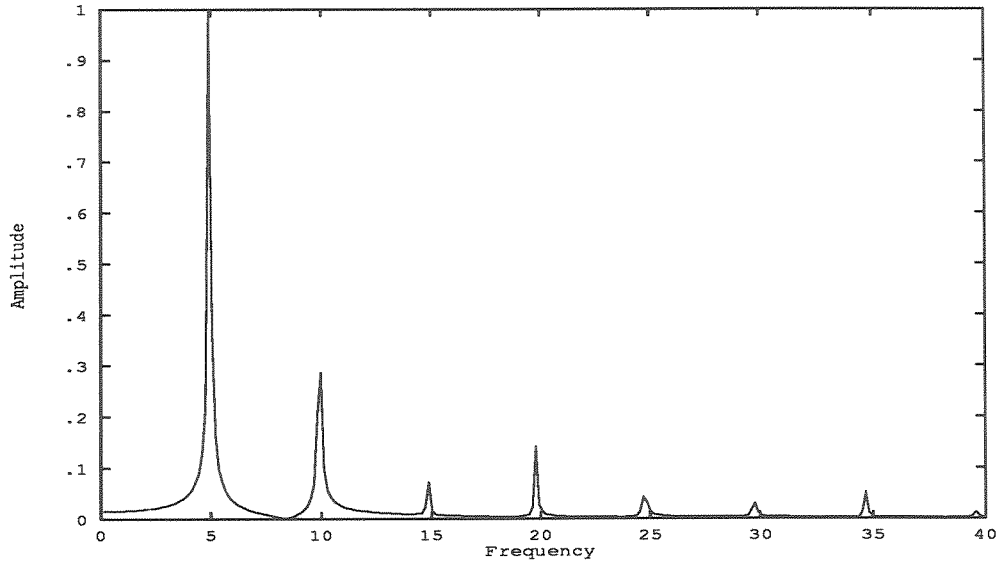


Figure 3.4.2: Strong harmonics can be generated when the input to the sigmoids is large. The strong even harmonics are due to refractoriness in the excitatory neurons. The primary frequency is $\Omega = 4.91$. $C = 20$, $T_e = 0.1$, $T_i = 0.2$, $r_e = 0.5$, and $t_d = 0.2$.

While in principle higher harmonics can be taken into account, the complexity of the problem has so far prevented us from tackling these. The existence of higher harmonics depends not only on the response of the nonlinear sigmoid but also the linear operator $(\frac{d}{dt})^{-1} \sim \frac{1}{\omega}$. Thus if the frequency is low, a pronounced generation of harmonics is possible. Fig. 3.4.2 indicates a general case where the harmonics can be strong. We will discuss the generation of harmonics as particular cases are considered in Section 3.7. For example, when the input to the sigmoid is very large, numerical experiments and theory indicate that the third harmonic can have an amplitude of about $\frac{1}{3}$ of the fundamental. In such cases, the approximation of taking the input to the nonlinear element as a bias plus sinusoid is incorrect.

In the next section, the method of harmonic balance discussed above is used to derive nonlinear algebraic equations governing periodic solutions of

Eqns. 3.2.5 and 3.2.6.

3.5 Frequency-Amplitude-Phase Relations

In this section we derive the frequency-amplitude-phase relations between the excitatory and inhibitory components of the following equations using the method of harmonics discussed in Section 4. For simplicity, we temporarily ignore cellular refractory periods and set $r_e = r_i = 0$.

$$T_e \dot{f}_e(t) = -f_e(t) + \sigma_e(C_1 f_e(t) - C_2 f_i(t - t_d) + P) \quad (3.5.1)$$

$$T_i \dot{f}_i(t) = -f_i(t) + \sigma_i(C_3 f_e(t) - C_4 f_i(t - t_d) + Q) \quad (3.5.2)$$

Shifting the origin to the threshold χ , Eqns. 3.5.1 and 3.5.2 are modified to

$$T_e \dot{f}_e(t) = -f_e(t) + 0.5 + \sigma_e^*(C_1 f_e(t) - C_2 f_i(t - t_d) + P - \chi_e) \quad (3.5.3)$$

$$T_i \dot{f}_i(t) = -f_i(t) + 0.5 + \sigma_i^*(C_3 f_e(t) - C_4 f_i(t - t_d) + Q - \chi_i) \quad (3.5.4)$$

Neglecting the higher harmonics, solutions to these equations may be approximated by,

$$\begin{aligned} f_e(t) &= \bar{f}_e + f_{e0} \sin(\omega t) \\ f_i(t) &= \bar{f}_i + f_{i0} \sin(\omega t - \theta_i) \end{aligned} \quad (3.5.5)$$

where θ_i is the phase difference between f_e and f_i which has to be self-consistently determined from the solution. We assume θ_i to be constant.

Inserting Eqns. 3.5.5 in 3.5.3 and 3.5.4 gives,

$$\begin{aligned} \omega T_e f_{e0} \cos(\omega t) &= -\bar{f}_e - f_{e0} \sin(\omega t) + 0.5 + \\ &\sigma_e^*([C_1 \bar{f}_e - C_2 \bar{f}_i + P - \chi_e] \end{aligned}$$

$$\begin{aligned}
&+[C_1 f_{e0} \sin(\omega t) - C_2 f_{i0} \sin(\omega t - \theta_i - \omega t_d)] \\
\omega T_i f_{i0} \cos(\omega t - \theta_i) &= -\bar{f}_i - f_{i0} \sin(\omega t - \theta_i) + 0.5 + \\
\sigma_i^* &([C_3 \bar{f}_e - C_4 \bar{f}_i + Q - \chi_i] \\
&+[C_3 f_{e0} \sin(\omega t) - C_4 f_{i0} \sin(\omega t - \theta_i - \omega t_d)]) \quad (3.5.6)
\end{aligned}$$

The input to the sigmoid σ^* can be cast into a more elegant form with a single sinusoidal component. Writing the argument of the excitatory sigmoid σ_e^* as $x_e = B_e + A_e \sin(\omega t + \theta_{ae})$ the following can be inferred:

$$\begin{aligned}
B_e &= C_1 \bar{f}_e - C_2 \bar{f}_i + P - \chi_e \\
A_e^2 &= C_1^2 f_{e0}^2 + C_2^2 f_{i0}^2 - 2C_1 C_2 f_{e0} f_{i0} \cos(\theta_i + \omega t_d) \\
A_e \sin(\theta_{ae}) &= C_2 f_{i0} \sin(\theta_i + \omega t_d) \\
A_e \cos(\theta_{ae}) &= C_1 f_{e0} - C_2 f_{i0} \cos(\theta_i + \omega t_d) \\
\tan(\theta_{ae}) &= \sin(\theta_i + \omega t_d) / \left(\frac{C_1 f_{e0}}{C_2 f_{i0}} - \cos(\theta_i + \omega t_d) \right)
\end{aligned} \quad (3.5.7)$$

Similarly, writing the argument of σ_i^* as $x_i = B_i + A_i \sin(\omega t + \theta_{ai})$,

$$\begin{aligned}
B_i &= C_3 \bar{f}_e - C_4 \bar{f}_i + Q - \chi_i \\
A_i^2 &= C_3^2 f_{e0}^2 + C_4^2 f_{i0}^2 - 2C_3 C_4 f_{e0} f_{i0} \cos(\theta_i + \omega t_d) \\
A_i \sin(\theta_{ai}) &= C_4 f_{i0} \sin(\theta_i + \omega t_d) \\
A_i \cos(\theta_{ai}) &= C_3 f_{e0} - C_4 f_{i0} \cos(\theta_i + \omega t_d) \\
A_i \sin(\theta_{ai} + \theta_i) &= C_3 f_{e0} \sin(\theta_i) + C_4 f_{i0} \sin(\omega t_d) \\
A_i \cos(\theta_{ai} + \theta_i) &= C_3 f_{e0} \cos(\theta_i) - C_4 f_{i0} \cos(\omega t_d) \\
\tan(\theta_{ai}) &= \sin(\theta_i + \omega t_d) / \left(\frac{C_3 f_{e0}}{C_4 f_{i0}} - \cos(\theta_i + \omega t_d) \right)
\end{aligned} \quad (3.5.8)$$

Eqns. 3.5.6 can now be written as

$$\omega T_e f_{e0} \cos(\omega t) = -\bar{f}_e - f_{e0} \sin(\omega t) + 0.5 +$$

$$\sigma_e^*(B_e + A_e \sin(\omega t + \theta_{ae})) \quad (3.5.9)$$

$$\begin{aligned} \omega T_i f_{i0} \cos(\omega t - \theta_i) = & -\bar{f}_i - f_{i0} \sin(\omega t - \theta_i) + 0.5 + \\ & \sigma_i^*(B_i + A_i \sin(\omega t + \theta_{ai})) \end{aligned} \quad (3.5.10)$$

Using the nonlinear gain functions described in Section 4, the nonlinear terms in the above equations can be written as,

$$\begin{aligned} \sigma^*(x_e) &= B_e F_{B_e} + A_e F_{A_e} \sin(\omega t + \theta_{ae}) \\ \sigma^*(x_i) &= B_i F_{B_i} + A_i F_{A_i} \sin(\omega t + \theta_{ai}) \end{aligned} \quad (3.5.11)$$

where the functions $F_B(B, A)$ and $F_A(B, A)$ are as in Eqns. 3.4.3 and 3.4.4. Substituting Eqns. 3.5.11 in 3.5.9 and 3.5.10 and equating the bias and coefficients of cos and sin to zero, we get

$$\bar{f}_e = 0.5 + B_e F_{B_e} \quad (3.5.12)$$

$$\omega T_e f_{e0} = A_e F_{A_e} \sin(\theta_{ae}) \quad (3.5.13)$$

$$f_{e0} = A_e F_{A_e} \cos(\theta_{ae}) \quad (3.5.14)$$

$$\bar{f}_i = 0.5 + B_i F_{B_i} \quad (3.5.15)$$

$$\omega T_i f_{i0} = A_i F_{A_i} \sin(\theta_{ai} + \theta_i) \quad (3.5.16)$$

$$f_{i0} = A_i F_{A_i} \cos(\theta_{ai} + \theta_i) \quad (3.5.17)$$

The nonlinear differential equations, Eqns. 3.5.3 and 3.5.4, have thus been reduced to algebraic equations, Eqns. 3.5.12 - 3.5.17. In what follows we attempt to gain some insight into the nonlinear oscillations by studying these equations. Modification of these equations to take into account refractoriness in the excitatory neurons is deferred to the latter part of Section 3.7.

3.6 Linear theory

We first seek the solution to small amplitude oscillations. These oscillations are unstable to small perturbations and almost never exist in real systems; however their study could shed light on the behavior of the nonlinear system. To solve Eqns. 3.5.12 - 3.5.17 for the frequency, phase, and ratio of excitatory and inhibitory neurons firing in the linear region, we first approximate the gain functions F_B and F_A , noting that $\frac{\delta \pm B}{A} \gg 1$. These approximations hold when δ is large and the amplitude and bias components of the input into the sigmoid are small. From Eqns. 3.4.3 - 3.4.7, it follows that $F_B \sim m$ and $F_A \sim m$ where $m = \frac{0.5}{\delta}$ is the slope of the sigmoid. This result would also follow from straightforward linearization. Eqns. 3.5.12 - 3.5.17 can now be written as,

$$\begin{aligned}
 \bar{f}_e &= 0.5 + B_e m_e \\
 \omega T_e f_{e0} &= A_e m_e \sin(\theta_{ae}) \\
 f_{e0} &= A_e m_e \cos(\theta_{ae}) \\
 \bar{f}_i &= 0.5 + B_i m_i \\
 \omega T_i f_{i0} &= A_i m_i \sin(\theta_{ai} + \theta_i) \\
 f_{i0} &= A_i m_i \cos(\theta_{ai} + \theta_i)
 \end{aligned} \tag{3.6.1}$$

Substituting for $A_e \cos(\theta_{ae})$, $A_e \sin(\theta_{ae})$, $A_i \cos(\theta_{ae} + \theta_i)$, $A_i \sin(\theta_{ae} + \theta_i)$ from Eqns. 3.5.7 and 3.5.8,

$$\omega T_e f_{e0} = m_e C_2 f_{i0} \sin(\theta_i + \omega t_d) \tag{3.6.2}$$

$$f_{e0} = m_e (C_1 f_{e0} - C_2 f_{i0} \cos(\theta_i + \omega t_d)) \tag{3.6.3}$$

$$\omega T_i f_{i0} = m_i (C_3 f_{e0} \sin(\theta_i) - C_4 f_{i0} \sin(\omega t_d)) \tag{3.6.4}$$

$$f_{i0} = m_i (C_3 f_{e0} \cos(\theta_i) + C_4 f_{i0} \cos(\omega t_d)) \tag{3.6.5}$$

Eliminating $\theta_i + \omega t_d$ from Eqns. 3.6.2 and 3.6.3 and θ_i from Eqns. 3.6.4 and 3.6.5,

$$\frac{f_{e0}^2}{f_{i0}^2} = \frac{m_e^2 C_2^2}{T_e^2 \omega^2 + (m_e C_1 - 1)^2} \quad (3.6.6)$$

$$\frac{f_{e0}^2}{f_{i0}^2} m_i^2 C_3^2 = (T_i \omega - m_i C_4 \sin(\omega t_d))^2 + (m_i C_4 \cos(\omega t_d) + 1)^2 \quad (3.6.7)$$

From these equations, the following relation for ω may be obtained

$$(T_i \omega - m_i C_4 \sin(\omega t_d))^2 + (m_i C_4 \cos(\omega t_d) + 1)^2 = \frac{m_e^2 m_i^2 C_2^2 C_3^2}{T_e^2 \omega^2 + (m_e C_1 - 1)^2} \quad (3.6.8)$$

Some simple results may be obtained when $t_d = 0$. In this limit, the frequency can be solved for,

$$\begin{aligned} \omega^2 &= -(\alpha^2 + \beta^2) + \sqrt{\omega_0^4 + (\alpha^2 + \beta^2)^2} \quad (3.6.9) \\ T_e T_i \omega_0^2 &= m_e m_i C_2 C_3 \\ T_e \alpha &= \frac{1}{\sqrt{2}} (m_e C_1 - 1) \\ T_i \beta &= \frac{1}{\sqrt{2}} (m_i C_4 + 1) \end{aligned}$$

The phase difference between the excitatory and inhibitory components is found to be $\tan(\theta_i) = \frac{\omega T_i}{m_i C_4 + 1}$. If feedback dominates, $C_2 C_3 \gg C_1 C_4$, then $\omega \sim \omega_0 = \sqrt{\frac{m_e m_i C_2 C_3}{T_e T_i}}$. The phase difference is $\tan(\theta_i) = \sqrt{\frac{T_i}{T_e}} \sqrt{m_e m_i C_2 C_3} \sim \frac{\pi}{2}$.

In numerical solution of the differential equations, we tested the theoretical frequency and phase results. It was found that the linear theory predicted much larger frequencies than the correct values. The phase difference between the components was also in disagreement. This leads us to conclude that linear theory is inaccurate and inadequate to study oscillations in the feedback system with delay. Furthermore, as the stability analysis of Section 3 has shown, linear oscillations can be unstable to even small time delays in the feedback.

3.7 Nonlinear Theory

As noted above, linear oscillations are guaranteed only in the low gain limit and are unstable not only to perturbations but also delay in feedback. Nonlinear saturation mechanisms then limit the response of the subpopulations. In addition, refractoriness of the neurons limits the number of neurons firing per unit time. Next, we study nonlinear oscillations using the method of harmonic balance discussed in Sections 3.4 and 3.5. The following equations were derived in Section 3.5 (Eqns. 3.5.12 - 3.5.17) neglecting the refractoriness in both excitatory and inhibitory neurons (a consideration of the effect of refractoriness in the excitatory neurons is deferred to the latter part of this section, see *Case 3* below).

$$\bar{f}_e = 0.5 + B_e F_{Be} \quad (3.7.1)$$

$$\omega T_e f_{e0} = A_e F_{Ae} \sin(\theta_{ae}) \quad (3.7.2)$$

$$f_{e0} = A_e F_{Ae} \cos(\theta_{ae}) \quad (3.7.3)$$

$$\bar{f}_i = 0.5 + B_i F_{Bi} \quad (3.7.4)$$

$$\omega T_i f_{i0} = A_i F_{Ai} \sin(\theta_{ai} + \theta_i) \quad (3.7.5)$$

$$f_{i0} = A_i F_{Ai} \cos(\theta_{ai} + \theta_i) \quad (3.7.6)$$

Some general observations may be made without explicitly solving the equations above.

(1) If $|\frac{\delta+B}{A}| > 1$ and $|\frac{\delta-B}{A}| > 1$ and these terms have opposite sign, $F_A = 0$ from Eqns. 3.4.4 and 3.4.7. No oscillations occur when $F_A = 0$. This implies that nonlinear oscillations, if they exist, must have a strong sinusoidal component (compared to the bias) to the input activity.

(2) The phase shift $\theta_0 = \theta_i + \omega t_d$, between the excitatory and inhibitory signals is critical for the oscillations. It has two components: θ_i originating from the feedback coupling and ωt_d from the time delay in feedback. The response from the nonlinear sigmoid is proportional to $A_e \sin(\theta_{ae}) F_{Ae} = F_{Ae} C_2 f_{i0} \sin(\theta_0)$. Since F_{Ae} is bounded by m_e , the slope of the sigmoid, the response is exactly zero when $\theta_0 = 0$. When $C_2 C_3 = C_1 C_4$, the phase difference θ_i , can be zero (this statement will be proved below) in which case it is necessary that the feedback time delay not be equal to zero. When $\theta_0 \sim \frac{\pi}{2}$, $A_e^2 = C_1^2 f_{e0}^2 + C_2^2 f_{i0}^2 - 2C_1 C_2 f_{e0} f_{i0} \cos(\theta_0) \sim (C_1^2 f_{e0}^2 + C_2^2 f_{i0}^2)$, hence the sinusoidal component of the input to the nonlinear sigmoid could be large, in which case the corresponding nonlinear response is non-zero.

(3) Inter- and intrasubpopulation asymmetries (for example, $C_1 C_4 \neq C_2 C_3$, or $P - \chi_e \neq Q - \chi_i$) can also result in nonzero phase differences between the excitatory and inhibitory signals. However, the results of Wilson and Cowan (see Section 3.2) show that rather stringent conditions are required on the asymmetry in feedback coupling to cause adequate phase shifts to induce oscillations in the present model.

(4) When the input P is large, no oscillations occur in the excitatory component because the effective gain from the nonlinear sigmoid for the oscillating component, F_{Ae} , is zero: for example consider P such that $(\delta - B_e)/A_e^{max} < -1$ and $(\delta + B_e)/A_e^{max} > +1$, i.e. the bias is very large, where A_e^{max} is $C_1 + C_2$, in which case $F_{Ae} = 0$. Therefore there exists a $P = P^{max}$ such that for $P > P^{max}$ no oscillations occur. A similar result holds for the inhibitory component.

(5) If the excitatory subpopulation receives subthreshold excitation, i.e., P is small compared to the threshold, χ_e , no oscillations occur. The reason is essentially the same as the one above: the input to the sigmoid has a large bias

component compared to the maximum possible oscillating component, thereby reducing the nonlinear gain for the sinusoidal component, F_A , to zero. Thus, the oscillations are input driven underscoring the strongly dissipative nature of the interaction in the absence of external drive.

(6) It is possible for oscillations in the inhibitory component to occur in the absence of oscillations in the excitatory component. This typically occurs when P is large so that $F_{Ae} = 0$, as discussed above, but the external input Q to the inhibitory neurons is close to the threshold and hence $F_{Ai} \neq 0$.

(7) The frequency of oscillation depends on the connectivities C_1, C_2, C_3, C_4 as well as the time scales t_d, T_e, T_i and the inputs P, Q .

It is extremely difficult to solve Eqns. 3.7.1 - 3.7.6 exactly. However, in the large amplitude limit, $\frac{B}{A} < 1$, the equations may be simplified as follows. The nonlinear gain is

$$\begin{aligned} F_B(B, A) &= \frac{mA}{2B} [g(\frac{\delta+B}{A}) - g(\frac{\delta-B}{A})] \\ F_A(B, A) &= \frac{m}{2} [f(\frac{\delta+B}{A}) + f(\frac{\delta-B}{A})] \end{aligned} \quad (3.7.7)$$

Let $|\frac{\delta+B}{A}| < 1$ and $|\frac{\delta-B}{A}| < 1$, then substituting for g and f from Eqns. 3.4.6 and 3.4.7,

$$\begin{aligned} F_B(B, A) &= \frac{mA}{B\pi} [(\frac{\delta+B}{A} \sin^{-1}(\frac{\delta+B}{A}) + \sqrt{1 - (\frac{\delta+B}{A})^2}) \\ &\quad + (\frac{\delta-B}{A} \sin^{-1}(\frac{\delta-B}{A}) - \sqrt{(1 - (\frac{\delta-B}{A})^2})] \\ F_A(B, A) &= \frac{m}{\pi} [(\sin^{-1}(\frac{\delta+B}{A}) + \frac{\delta+B}{A} \sqrt{1 - (\frac{\delta+B}{A})^2}) \\ &\quad + (\sin^{-1}(\frac{\delta-B}{A}) + \frac{\delta-B}{A} \sqrt{1 - (\frac{\delta-B}{A})^2})] \end{aligned} \quad (3.7.8)$$

Approximating $\sin^{-1}(x) \sim x$ and $\sqrt{1 - x^2} \sim (1 - x^2/2)$ above,

$$F_B(B, A) = \frac{2}{\pi A} \quad (3.7.9)$$

$$F_A(B, A) = \frac{2}{\pi A} - \frac{\delta(\delta^2 - 3B^2)}{2\pi A^3} \quad (3.7.10)$$

In making this approximation we are faced with a dilemma: without this approximation Eqns. 3.7.1 - 3.7.6 are very difficult to solve analytically; on the other hand, when the approximation is strictly valid the harmonic feedback is strong and therefore the bias plus sinusoid input to the nonlinear sigmoid is incorrect. The neglect of harmonics is valid only for moderately strong inputs into the nonlinear sigmoid, typically $A + |B| \leq 10\delta$, i.e., the maximum input into the sigmoid is within an order of magnitude of δ . Also, for $(\delta \pm B)/A > 0.6$, the approximations $\sin^{-1}(x) \sim x$ and $\sqrt{1-x^2} \sim (1-x^2/2)$ are incorrect. Within the regime suggested above, the approximations used do give correct results.

Neglecting the $O(\frac{1}{A^3})$ term in F_A , Eqns. 3.7.1 - 3.7.6 can be written as,

$$\bar{f}_e = 0.5 + B_e \frac{2}{\pi A_e} \quad (3.7.11)$$

$$\omega T_e f_{e0} = \frac{2}{\pi} \sin(\theta_{ae}) \quad (3.7.12)$$

$$f_{e0} = \frac{2}{\pi} \cos(\theta_{ae}) \quad (3.7.13)$$

$$\bar{f}_i = 0.5 + B_i \frac{2}{\pi A_i} \quad (3.7.14)$$

$$\omega T_i f_{i0} = \frac{2}{\pi} \sin(\theta_{ai} + \theta_i) \quad (3.7.15)$$

$$f_{i0} = \frac{2}{\pi} \cos(\theta_{ai} + \theta_i) \quad (3.7.16)$$

From the Eqns. 3.7.11 - 3.7.16, the following may be easily shown,

$$\begin{aligned} T_e \omega &= \tan(\theta_{ae}) \\ T_i \omega &= \tan(\theta_{ai} + \theta_i) \end{aligned} \quad (3.7.17)$$

where, from Eqns. 3.5.7 and 3.5.8,

$$\begin{aligned} \tan(\theta_{ae}) &= \frac{\sin(\theta_i + \omega t_d)}{\frac{C_1 f_{e0}}{C_2 f_{i0}} - \cos(\theta_i + \omega t_d)} \\ \tan(\theta_{ai}) &= \frac{\sin(\theta_i + \omega t_d)}{\frac{C_3 f_{e0}}{C_4 f_{i0}} - \cos(\theta_i + \omega t_d)} \end{aligned} \quad (3.7.18)$$

We consider here oscillations with $P \sim \chi_e$ and $Q \sim \chi_i$. The bias B then depends on the mismatch of the excitatory and inhibitory activity and not the actual value of the external input. Below, some of the characteristics of the oscillations for a few different cases are discussed. Except as noted, all the numerical values quoted are for the following default parameters: $C_1 = C_2 = C_3 = C_4 = 5.0$, $t_d = 0.1$, $T_e = T_i = 0.1$, $m_e = m_i = 0.5$, $P = Q = 4.0$, $\chi_e = \chi_i = 4.0$, $r_e = r_i = 0.0$. In *Case 3* below, $r_e \neq 0.0$.

Note on Method: The differential equations were solved by fourth-order Runge-Kutta method with step size 0.005. The numerical values of the theoretical results quoted were obtained by solving the simplified frequency-amplitude-phase relations using the symbolic manipulation program Mathematica (Wolfram, 1989).

Case 1 Let $C_1C_4 = C_2C_3$, so that there is no dominant feedback. and similar excitatory and inhibitory decay time scales, $T_e = T_i = T$. The following results may be shown:

(1) The phase difference θ_i between the excitatory and inhibitory components is equal to zero. From Eqns. 3.7.18, when $C_2C_3 = C_1C_4$, $\tan(\theta_{ae}) = \tan(\theta_{ai})$, and from Eqns. 3.7.17 if $T_e = T_i$, $\tan(\theta_{ae}) = \tan(\theta_{ai} + \theta_i)$. It follows that $\theta_i = 0$. Figs. 3.7.1 and 3.7.2 illustrate examples of phase locked oscillations. Note that the zero phase difference is due to the symmetry. In this case, oscillations exist only because of the ‘hidden phase shift’, ωt_d , caused by the delay in the inhibitory feedback.

(2) The excitatory and inhibitory components have the same amplitude, i.e., $\frac{f_{e0}}{f_{i0}} = 1$. From Eqns. 3.7.12 and 3.7.13 eliminating θ_{ea} , and from Eqns.

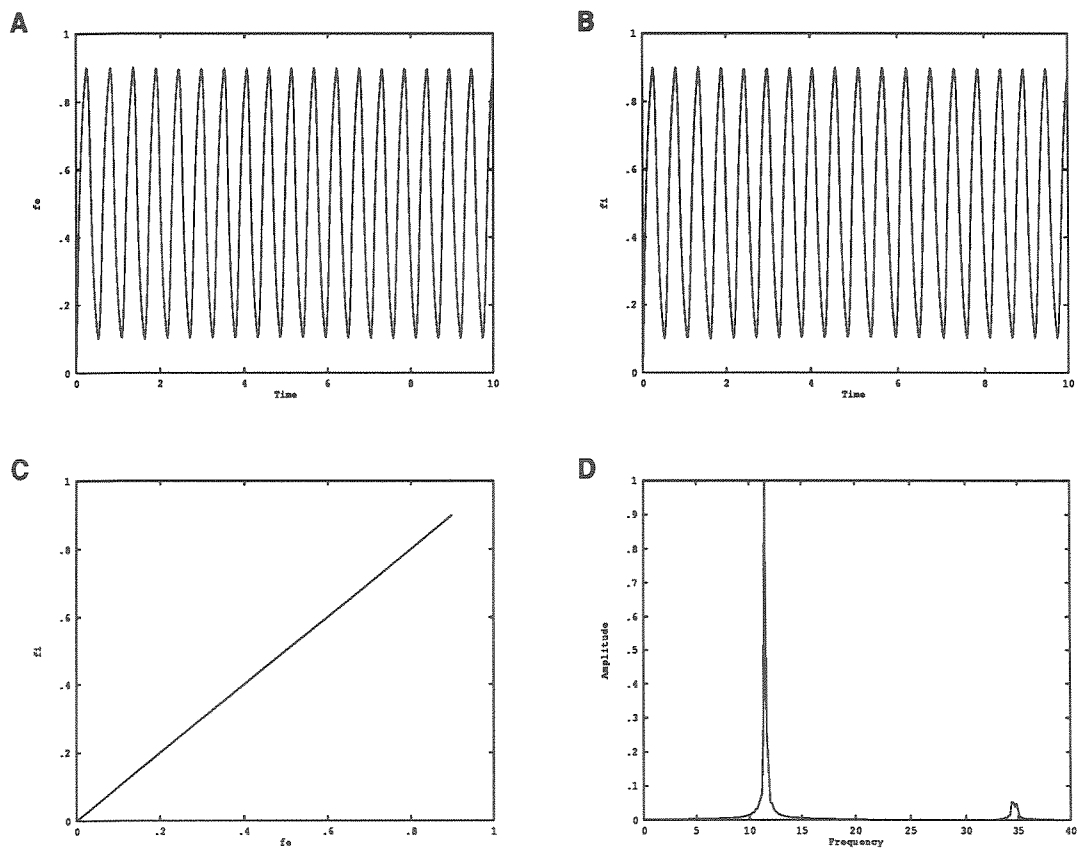


Figure 3.7.1: Oscillations with zero phase difference between the excitatory and inhibitory components can occur under certain symmetry constraints: $C_1C_4 = C_2C_3$, $T_e = T_i$ and $P = \chi_e$, and $Q = \chi_i$. Such zero phase difference oscillations cannot arise in the absence of delayed feedback. (A) Fraction of excitatory neurons firing per unit time, $f_e(t)$. (B) Fraction of inhibitory neurons firing per unit time, $f_i(t)$. (C) Phase portrait of the f_i and f_e shows zero phase difference. (D) The frequency spectrum showing a weak third harmonic. The frequency of oscillation is $\omega = 11.50$.

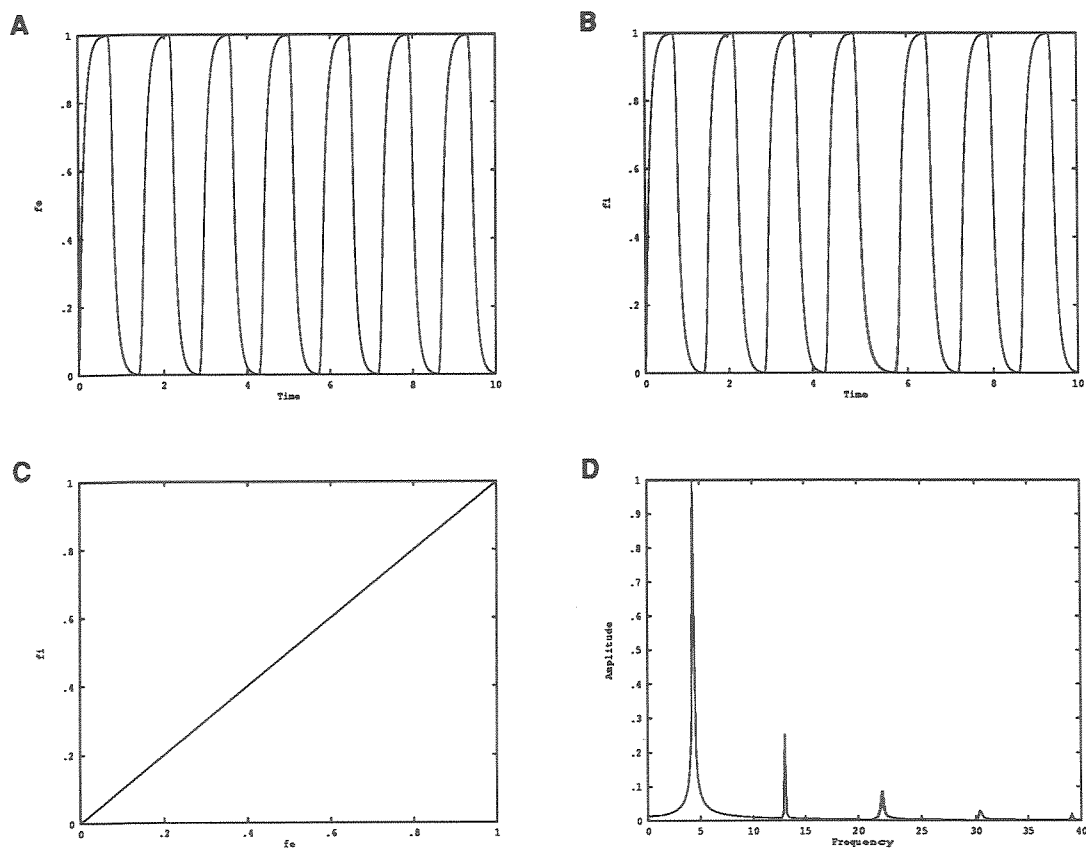


Figure 3.7.2: When the inhibitory delay is increased, the amplitude and frequency of the oscillations can change significantly. The number of neurons firing per unit time increases and the frequency decreases (compare with Fig. 3.7.1). (A) Fraction of excitatory neurons firing per unit time, $f_e(t)$. (B) Fraction of inhibitory neurons firing per unit time, $f_i(t)$. (C) The phase portrait once again indicates zero phase difference between the excitatory and inhibitory components. (D) The frequency spectrum showing the presence of moderately strong odd harmonics because the frequency of the oscillation is smaller ($\omega = 4.30$). The inhibitory delay is $t_d = 0.5$.

t_d	ω (num.)	ω (theory)
0.05	17.49	19.2
0.1	11.35	13.06
0.2	7.67	8.60
0.5	4.30	4.56
1.0	2.61	2.62
1.5	1.84	1.85
2.0	1.38	1.38
3.0	0.92	0.98

Table 3.7.1: The frequency of oscillation, ω , monotonically decreases with increasing inhibitory feedback delay t_d (comparison of theoretical and numerical results).

3.7.15 and 3.7.16 eliminating $\theta_{ai} + \theta_i$,

$$f_{e0}^2(1 + T_e^2\omega^2) = \frac{4}{\pi^2} \quad (3.7.19)$$

$$f_{i0}^2(1 + T_i^2\omega^2) = \frac{4}{\pi^2} \quad (3.7.20)$$

The two relations above give $\frac{f_{e0}}{f_{i0}} = 1$. The amplitudes, f_{e0} and f_{i0} , decrease with increasing oscillation frequency.

(3) With the above results, Eqn. 3.7.17 may be solved for the frequency of oscillation,

$$T\omega = \frac{\sin(\omega t_d)}{\frac{C_1}{C_2} - \cos(\omega t_d)} \quad (3.7.21)$$

For $C_1 = C_2$ this is simply $T\omega = \cot(\omega t_d/2)$. If this relation is cast in the form $\frac{2T}{t_d}\psi = \cot(\psi)$, where $\psi = \omega t_d$ it is easy to see that for fixed T the frequency is a monotonic decreasing function of the delay t_d . Table 3.7.1 compares the numerical and theoretical results for the variation of frequency with the inhibitory signal delay. The results are close, particularly for lower frequency. The time period of the oscillation is different from any time scale in the problem. As noted in Section 3.4, the harmonics become important when (1) the input to the nonlinear sigmoid is large and/or (2) the frequency is small. Fig. 3.7.1

C	ω (num.) $t_d = 0.1$	ω (num.) $t_d = 0.5$
5	11.35	4.29
10	9.66	4.14
20	8.13	3.83
200	5.21	3.07

Table 3.7.2: The frequency of oscillation decreases as the mean synaptic strength C is increased (numerical results), and its variation is much less when the frequency is small.

(D) indicates that the harmonics are small when the frequency is large and the input to the sigmoid is small. Fig. 3.7.2 (D) shows that even when the input to the sigmoid is small, harmonics can be generated because the nonlinear gain drops as only $\frac{1}{\omega}$. The theory and approximations used, however, do not capture the functional dependence of the frequency on C . This is partly because at larger values of C , the harmonic feedback becomes strong and this variation is not accounted for. The frequency decreases as the mean synaptic strength C is increased (Table 3.7.2). For lower frequencies, there is much less variation of frequency with C , presumably because harmonics are present even with small values (of C). For small C , the approximations $\sin^{-1} x \sim x$ and $\sqrt{1-x^2} \sim 1$ are no longer valid, and the frequency must be obtained by a detailed numerical solution of the transcendental equations. The frequencies obtained in that case approach the numerical results even more closely and is found to increase as C decreases. The details of the calculations are tedious, offer no particular insight, and therefore are not presented here.

(4) As shown above, when $C = C_1 = C_2 = C_3 = C_4$ and $T_e = T_i$, f_{e0} is equal to f_{i0} , therefore if $P = Q = \chi$, the biases B_e and B_i are zero. In Appendix A.3 it is shown that the even harmonic feedback is proportional to the bias. Hence the even harmonics are negligible. As the mean connection strength C

is increased, it is the odd harmonics that are important. In particular, the third harmonic can have an amplitude of $\frac{1}{3}$ of the fundamental (Eqn. A.3.8). However if, for example, P is increased beyond the threshold χ , the bias B_e will in general be non-zero and the even harmonics, in particular the second harmonic, would be present.

(5) To study how the frequency varies with $\frac{C_1}{C_2} = \frac{C_3}{C_4}$, a general result concerning the frequency of oscillation is proved next (we assume oscillations exist).

Theorem 3.7.1 *For $x > 0$, the frequency of oscillation given by $T\omega = \frac{\sin(\omega t_d)}{x - \cos(\omega t_d)}$ monotonically decreases as x increases.*

Proof: The expression for frequency is first cast into the form:

$$x(\psi) = \gamma \frac{\sin(\psi)}{\psi} + \cos(\psi) \quad (3.7.22)$$

where $\gamma = \frac{t_d}{T}$ and $\psi = \omega t_d$. Let ψ_0 be the root of the equation above. It is easy to see that ψ_0 satisfies $\frac{\pi}{2} < \psi_0 < \pi$. Now we show that for $0 < \psi < \psi_0$, $x(\psi)$ is a monotonically decreasing function. The turning point of $x(\psi)$ occurs when $x'(\psi) = 0$. Let this value be ψ_1 . Then, $\tan(\psi_1) = \frac{\gamma\psi_1}{\gamma + \psi_1^2}$. At $\psi_1 = 0$, $x = 1 + \gamma$, its maximum value. This implies that at $\psi_1 = 0$, $x(\psi)$ is a decreasing function. The next turning point occurs at ψ_1 such that $\pi < \psi_1 < \frac{3\pi}{2}$, which means that $\psi_1 > \psi_0$. Hence $x(\psi)$ is a monotonically decreasing function for $0 < \psi < \psi_0$. This completes the proof.

From this result it follows that as $\frac{C_1}{C_2}$ decreases, (maintaining $C_2C_3 = C_1C_4$) the frequency of oscillation increases. Table 3.7.3 compares the theoretically derived frequency with numerical results for $\frac{C_1}{C_2} = \frac{C_3}{C_4} = \frac{5}{6}$ and $\frac{C_1}{C_2} = \frac{C_3}{C_4} = \frac{2.5}{5}$ as a function of the delay t_d . Comparing Tables 3.7.1 and 3.7.3 we find that the frequency of oscillation increases with decreasing $\frac{C_1}{C_2}$. When

$\frac{C_1}{C_2}$	t_d	ω (num.)	ω (theory)
$\frac{C_1=5}{C_2=6}$	0.05	18.87	22.47
	0.1	12.27	14.30
	0.2	8.13	9.05
	1.0	2.61	2.66
$\frac{C_1=2.5}{C_2=5}$	0.1	15.03	16.67
	0.5	4.75	4.92
	1.0	2.76	2.74

Table 3.7.3: The frequency of oscillation increases as the ratio of the recurrent excitation to feedback inhibition, $\frac{C_1}{C_2}$, is lowered (a comparison of theoretical and numerical results). The constraint $C_1C_4 = C_2C_3$ is maintained.

$\frac{C_1}{C_2} \neq 1$, the mismatch between excitatory and inhibitory activity generates a bias, hence the oscillations contain odd as well as even harmonics.

Case 2 Consider next the case of disparate decay time scales, $T_i > T_e$, again with $C_2C_3 = C_1C_4$. The phase difference, θ_i , between the excitatory and inhibitory components is no longer zero, and $f_e \neq f_i$ as shown below:

(1) From $T_e\omega = \tan(\theta_{ae})$ and $T_i\omega = \tan(\theta_{ai} + \theta_i)$, of Eqn. 3.7.17 we now have,

$$\tan(\theta_i) = \frac{\omega(T_i - T_e)}{1 + T_eT_i\omega^2} \quad (3.7.23)$$

Thus the phase difference is no longer zero (see Fig. 3.7.3) but is dependent on the mismatch between the excitatory and inhibitory decay time scales as well as the other parameters through the frequency ω . We noted earlier the importance of the phase shift for oscillations to occur. From the expression for the phase difference, it is therefore possible that when $T_i > T_e$, oscillations may occur even when there is no time delay. In Section 3.3, we observed that such oscillations do occur (see Fig. 3.3.2).

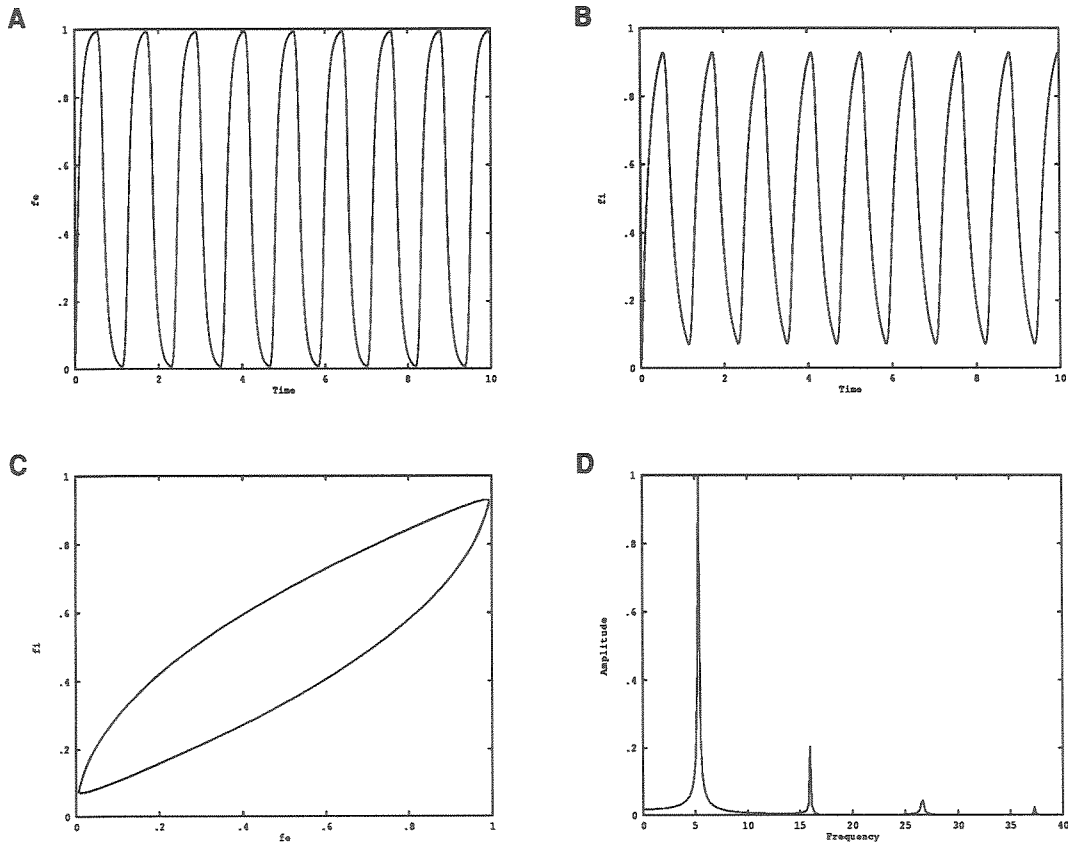


Figure 3.7.3: Oscillations with disparate decay time scales $T_e = 0.1$ and $T_i = 0.2$. (A) The fraction of excitatory neurons firing per unit time $f_e(t)$ and (B) the fraction of inhibitory neurons firing per unit time $f_i(t)$ indicate that the amplitude of the inhibitory component is smaller than the excitatory component as predicted theoretically. (C) The phase difference between the two components is no longer zero, the phase difference is about 18° . (D) The frequency spectrum shows the presence of odd harmonics, the third harmonic in particular is moderately strong. The frequency of oscillation is 5.37. The inhibitory delay is $t_d = 0.2$.

T_i	t_d	ω (num.)	ω (theory)
0.2	0.05	7.67	8.72
	0.1	6.60	8.34
	0.2	5.37	6.67
	0.5	3.53	4.01
	1.0	2.30	2.43
0.5	0.05	3.53	4.70
	0.1	3.22	4.74
	0.2	2.91	4.41
	0.5	2.30	3.14
	1.0	1.68	2.05

Table 3.7.4: The frequency of oscillation decreases with increasing inhibitory delay, t_d , and decay time, T_i .

(2) Proceeding as before, from Eqns. 3.7.11 - 3.7.16, the ratio of the amplitude of the oscillating components may be obtained, $\frac{f_{e0}}{f_{i0}} = \sqrt{\frac{1+T_i^2w^2}{1+T_e^2w^2}}$. The amplitude of the excitatory component is thus greater than that of the inhibitory component (Fig. 3.7.3).

(3) With the two results above, we can solve for the frequency,

$$T_e\omega = \frac{\sin(\tan^{-1}(\frac{\omega(T_i-T_e)}{1+T_eT_iw^2}) + \omega t_d)}{\frac{C_1}{C_2} \sqrt{\frac{1+T_i^2w^2}{1+T_e^2w^2}} - \cos(\tan^{-1}(\frac{\omega(T_i-T_e)}{1+T_eT_iw^2}) + \omega t_d)} \quad (3.7.24)$$

Although complicated, this expression for the frequency is a function of only one unknown and can be solved symbolically (see note above). Table 3.7.4 compares the numerical and theoretical frequencies for increasing inhibitory decay time T_i as a function of the delay t_d . We note (1) the frequencies progressively decrease as the T_i increases and the decay time scales become disparate, (2) the frequency monotonically decreases with the delay, and (3) the frequencies are quite different from any one of the time scales in the system.

(4) Since $f_{e0} \neq f_{i0}$, the bias is different from zero and in this case there are even as well as odd harmonics in the oscillation. When $T_i \gg T_e$, the frequency is small and, as discussed in Section 3.4, harmonic generation can be strong. In this case the bias plus sinusoid approximation is incorrect.

Case 3 The effect of refractoriness in the excitatory neurons on the oscillations is explored next. The refractoriness of the inhibitory interneurons is neglected. Once again we will consider sub-populations with $C_2C_3 = C_1C_4$. In Appendix 7B, the method of harmonics is used to obtain the following equations governing the periodic solutions in a manner analogous to the derivation in Section 3.5:

$$\bar{f}_e = 0.5(1 - \bar{f}_e r_e) + \frac{2B_e}{\pi A_e}(1 - \bar{f}_e r_e) \quad (3.7.25)$$

$$\omega T_e f_{e0} = \frac{2}{\pi}(1 - \bar{f}_e r_e) \sin(\theta_{ae}) \quad (3.7.26)$$

$$f_{e0} = \frac{2}{\pi}(1 - \bar{f}_e r_e) \cos(\theta_{ae}) \quad (3.7.27)$$

$$\bar{f}_i = 0.5 + \frac{2B_e}{\pi A_e} \quad (3.7.28)$$

$$\omega T_i f_{i0} = \frac{2}{\pi} \sin(\theta_{ai} + \theta_i) \quad (3.7.29)$$

$$f_{i0} = \frac{2}{\pi} \cos(\theta_{ai} + \theta_i) \quad (3.7.30)$$

These equations are valid if the harmonics, in particular the second and third, are weak. For $T_i \gg T_e$, this condition is not satisfied as discussed above. Furthermore, in order to concentrate on the critical effects of refractoriness in the excitatory neurons, the discussion here is restricted to the case of identical decay time scales, $T_e = T_i$. We may now show:

(1) The phase difference between the excitatory and inhibitory components is zero; this follows from $\tan(\theta_{ae}) = \tan(\theta_{ai})$, and $\tan(\theta_{ae}) = \tan(\theta_{ai} + \theta_i)$ as shown in *Case 1*.

(2) The amplitude of the excitatory neurons firing per unit time is less than the amplitude of the inhibitory neurons firing per unit time. When $T_e = T_i = T$, from Eqns. 3.7.26 and 3.7.27, $f_{e0} = \frac{2}{\pi\sqrt{1+\omega^2 T^2}}(1 - r_e \bar{f}_e)$ and from Eqns. 3.7.29 and 3.7.30, $f_{i0} = \frac{2}{\pi\sqrt{1+\omega^2 T^2}}$. Hence $\frac{f_{e0}}{f_{i0}} = 1 - r_e \bar{f}_e$. Therefore $\frac{f_{e0}}{f_{i0}} < 1$.

(3) The effect of refractoriness is to increase the frequency of oscillation. This result follows from the decrease of $\frac{f_{e0}}{f_{i0}}$ and Theorem 3.7.1, since the frequency is given by the same expression as in *Case 1*, $T\omega = \frac{\sin(\omega t_d)}{\frac{C_1 f_{e0}}{C_2 f_{i0}} - \cos(\omega t_d)}$.

(4) The amplitudes f_{e0}, f_{i0} both decrease as a result of refractoriness. This follows straightforwardly from the expressions for f_{e0} and f_{i0} derived in (2) and the increase of the frequency ω as shown in (3) above.

(5) If we assume that $\bar{f}_e \sim f_{e0}$, then approximate expressions for the amplitudes and frequency of the oscillation may be derived. With $\bar{f}_e \sim f_{e0}$, f_{e0} in (2) above can be solved for, $f_{e0} \sim \frac{2}{\pi} \frac{1}{\frac{2r_e}{\pi} + \sqrt{1+\omega^2 T^2}}$. Therefore,

$$\frac{f_{e0}}{f_{i0}} \sim \frac{1}{1 + \frac{2r_e}{\pi\sqrt{1+\omega^2 T^2}}} \quad (3.7.31)$$

It can now be shown that the frequency of oscillation is a nondecreasing function of r_e . A proof of this statement follows: consider the frequency of oscillation $T\omega = \frac{\sin(\omega t_d)}{\frac{C_1 f_{e0}}{C_2 f_{i0}} - \cos(\omega t_d)}$, and assume that the frequency of oscillation decreases with increasing r_e . Then $\frac{f_{e0}}{f_{i0}}$ as given by Eqn. 3.7.31 decreases. However, by Theorem 3.7.1, when $\frac{f_{e0}}{f_{i0}}$ decreases, the frequency increases. This contradicts our assumption that the frequency decreases with r_e . Hence the frequency of oscillation either increases or remains constant as r_e is increased. This completes the proof.

Consequently, it follows that the amplitudes, f_{e0} and f_{i0} , are nondecreasing functions of r_e . If $\omega T < 1$, as is typical in the present discussion, it follows that $\frac{f_{e0}}{f_{i0}} \sim \frac{1}{1+\kappa r_e}$, where $\frac{\sqrt{2}}{\pi} \leq \kappa \leq \frac{2}{\pi}$. Hence the ratio of the number of excitatory to inhibitory neurons firing per unit time scales inversely with the

t_d	r_e	ω (num.)	ω (theory)
0.1	0.05	11.66	13.20
	0.1	11.96	13.34
	0.5	12.73	14.20
	1.0	13.19	14.97
0.5	0.05	4.45	4.58
	0.1	4.45	4.60
	0.2	4.60	4.64
	0.5	4.75	4.74
	1.0	4.75	4.82
	1.5	4.75	4.89
	5.0	4.75	5.10

Table 3.7.5: The frequency of oscillation is a non-decreasing function of the refractory period of the excitatory neurons, r_e . Results are shown for two different values of the inhibitory delay, $t_d = 0.1$ and $t_d = 0.5$.

refractoriness in the excitatory neurons. With the expression for frequency of oscillation given by

$$T\omega = \frac{\sin(\omega t_d)}{\frac{C_1}{C_2} \frac{1}{1 + \frac{2r_e}{\pi\sqrt{1+\omega^2 T^2}}} - \cos(\omega t_d)} \quad (3.7.32)$$

we compare the numerical and theoretical results for the change of frequency with increasing r_e for two different values of delay t_d (Table 3.7.5). The frequency of oscillation either increases or is constant as predicted. It is also found that the amplitudes of the oscillation decrease and $\frac{f_{e0}}{f_{i0}} < 1$ (Fig. 3.7.4).

(6) The calculations in Appendix A.3 show that the effect of refractoriness is to introduce a second harmonic, from the product of the integral and the output from the sigmoid term in Eqn. 3.2.5. Additionally, from Appendix A.3, we note that the second harmonic feedback from the nonlinear sigmoid is proportional to the bias (Eqn. A.3.10). With $\frac{f_{e0}}{f_{i0}} < 1$ as shown above, the bias due to the mismatch between excitatory and inhibitory activity, $B \sim C_1 f_{e0} - C_2 f_{i0}$ is non-zero.

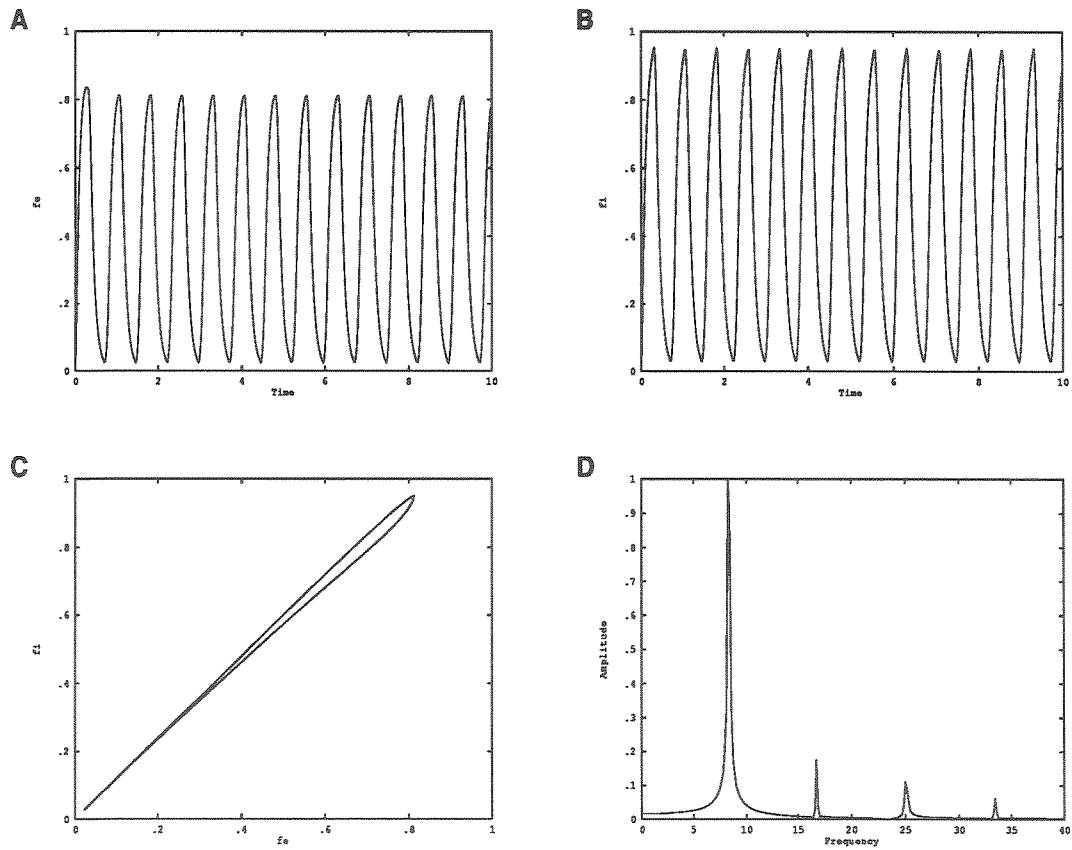


Figure 3.7.4: Oscillations when the refractoriness of the excitatory neurons is non zero ($r_e = 0.5$). (A) Refractoriness suppresses the fraction of excitatory neurons firing per unit time $f_e(t)$. (B) The fraction of inhibitory neurons firing per unit time $f_i(t)$. (C) The phase difference between the two components is almost zero. (D) The frequency spectrum shows the presence of odd as well as even harmonics as predicted. The frequency of the oscillation is 8.28. $T_e = T_i = 0.1$ and $t_d = 0.2$.

We conclude with a brief discussion on the case of strong feedback: $C_2C_3 \gg C_1C_4$. In this case, it is found that both the second and third harmonics are strong. From Eqn. A.3.10, the second harmonic is proportional to $\frac{B}{A}$. When $C_2C_3 \gg C_1C_4$, at least one of $B_e = C_1\bar{f}_e - C_2\bar{f}_i$ and $B_i = C_3\bar{f}_e - C_4\bar{f}_i$ is large so that the bias then generates a strong second harmonic. In addition a large sinusoidal input to the sigmoid produces a strong third harmonic as shown in Appendix A.4. In view of the presence of these harmonics, the method used in this section is inappropriate to study the case of dominant feedback.

3.8 Discussion

We have studied some aspects of nonlinear oscillations generated by interacting excitatory and inhibitory subpopulations of neurons in a neuronal group. As noted in the introduction, the problem with the generation of strong harmonics, the main hindrance to any detailed analysis of the oscillations, has been circumvented in the present analysis by introducing delay in the inhibitory signal. These delays are physiologically meaningful as well.

Delay in the inhibitory feedback can induce limit cycle oscillations by destroying the stability of fixed points. It is not necessary that the connection strength be feedback dominant. If the slopes of the sigmoids at all the fixed points are zero, stability is guaranteed for all feedback delay times, i.e., oscillations cannot occur. This indicates that for a step function sigmoid oscillations may not occur. This is interpreted to mean that synaptic and/or threshold variability is essential for oscillations. Oscillations can occur even when there is no delay, if the decay time period of the inhibitory activity is greater than that of the excitatory activity.

The frequency-amplitude-phase relations derived shed further light on

the role of delay. A non-zero phase shift between the excitatory and inhibitory components is essential for the oscillations. The phase shift has two components: one from asymmetry in feedback coupling or slowly decaying inhibitory signals (implying asymmetric decay rates) and the other explicitly due to delay. Only the former contributes to the recorded phase difference between the excitatory and inhibitory components. Delay and/or slowly decaying inhibitory signals cause a phase shift between the excitatory and inhibitory components; this phase shift underlies the origin of robust oscillations. Combining these results, we note that inhibition with time courses such as the alpha functions, $\alpha \sim \text{exp}(-t/\tau)$, used in the simulations of (Traub et al., 1989), would be ideally suited to generate oscillatory activity.

The oscillations are input driven and the ideal operating region is excitation close to the threshold. In the present model, too strong or too weak excitation is insufficient to induce oscillations as had already been noted (Wilson and Cowan, 1972). Mathematically, the reason for both of these phenomena is the same: the bias component of the input into the sigmoid is greater than the maximum possible sinusoidal component. Refractoriness in the excitatory neurons is an abetting factor in the existence of oscillations, because it causes suppression of excitatory activity and places the fixed point in a regime wherein the slope of the sigmoid at the fixed point is non-zero so that delayed inhibition can induce oscillations. In agreement with this observation, we have shown that ratio of the excitatory to inhibitory neurons firing per unit time, $\frac{f_{e0}}{f_{i0}}$, decreases with increasing excitatory refractory period r_e . The important effect of refractoriness in excitatory neurons has also been noted in detailed simulations (Sporns et al., 1989).

The frequency of oscillation is, in general, different from any time scale

in the system and depends on the delay, the time scales of decay of activity, the connection strengths, and the inputs. It is particularly important to note that even in the simplest approximation, it is not the inhibitory time delay that determines the frequency of the oscillation, indeed $\omega t_d \ll 2\pi$ for a wide range of parameters. The frequency decreases monotonically with, (1) the delay in inhibitory feedback, and (2) increasing inhibitory decay time. Phase locked oscillations can occur when there is a certain symmetry: the decay time periods are identical $T_e = T_i$, there is no feedback dominance $C_1 C_4 = C_2 C_3$, and both the excitatory and inhibitory sub-populations are driven at their respective thresholds. This zero phase difference would not be possible without delay in the inhibitory signal.

When the neurons are not refractory, the ratio of the amplitudes of the excitatory to inhibitory neurons firing per unit time, $\frac{f_{e0}}{f_{i0}}$, is 1, and both f_{e0} and f_{i0} decrease with increasing frequency. As the ratio of recurrent excitation to feedback inhibition $\frac{C_1}{C_2}$ decreases, the frequency of oscillation increases. When refractoriness in the excitatory neurons is introduced, the frequency of oscillation increases, and the ratio of the excitatory to inhibitory neurons firing per unit time, $\frac{f_{e0}}{f_{i0}}$, as well as the amplitudes, f_{e0} and f_{i0} , decrease with increasing excitatory refractory period r_e . The fraction of excitatory neurons firing per unit time scales as $\frac{1}{1+\kappa r_e}$, where, typically, $\frac{\sqrt{2}}{\pi} \leq \kappa \leq \frac{2}{\pi}$. These results are in agreement with the observation that, when the excitatory neurons have a large refractory period, only a small fraction ($\sim 2.8\%$) of excitatory neurons but a large fraction ($\sim 62\%$) of the inhibitory neurons fire in a population burst (Traub et al., 1989).

Strong harmonics, in particular the second and third, are generated when the frequency of the oscillation is small and/or the activity in the excita-

tory and inhibitory sub-populations is large. Harmonics with amplitudes up to (at least) a third of that of the fundamental can be present. Even harmonics are dominant when the excitatory refractory period is non-zero and the input to the sigmoid has a strong bias component due to the mismatch in excitatory and inhibitory activity. A recent experiment on tactile frequency discrimination in monkeys has confirmed that at low frequency strong second harmonics can be generated (Mountcastle et al., 1990); at high frequency the harmonics are absent.

It is interesting to consider why single cell firing has a stochastic characteristic to it while the population activity is synchronous. An important clue is the experimental evidence indicating that cellular firing is usually less well correlated with the EEG than are synaptic potentials (Traub et al., 1989). This suggests that it is the synaptic events that carry the underlying rhythm with the cell firing providing the drive. Indeed, if the cell firing is initiated as a cascade (see Fig. 5 in Traub et al. 1989), or more generally due to random fluctuations, a certain subset of the pathways will always be blocked as a result of cellular refractoriness. Consistent with this observation is the finding above that the fraction of excitatory neurons firing per unit time scales inversely with the refractoriness.

The redundant and quasi-random circuitry in a neuronal group with multiple pathways and variability at the cellular level may be the source of coherent population oscillations. The pattern of recurrent excitation and inhibition underlying such circuitry is present throughout several cortical areas (Shepherd, 1988a). The results discussed above indicate that robust oscillations occur when there is delay in the inhibitory feedback and/or a slowly decaying inhibitory signal. It is the separation of time scales along with the redun-

dant and quasi-random circuitry which may also justify the study of collective population oscillations with aggregate variables.

Dynamically controlled robust and stable population oscillations from locally redundant circuits reduce the variability in single cell firing and may play an important part in temporal signal processing in neural systems.

Chapter 4

Synchronization and Delay Induced Switching

4.1 Introduction

A distributed computer system consisting of communicating processors needs, (1) a protocol for communication, and (2) protocols to enable events to carry out any effective computation. Synchronization is both architecture and problem specific. Complex algorithms are necessary to coordinate inter-process communication and intraprocess events. This reflects the fact that an external clock drives the fetch-execute-store cycle, as we noted earlier. Neural systems, on the other hand, operate in a highly parallel manner without ‘clocks’, spatial markers and algorithms (Edelman and Finkel, 1984; Edelman, 1987). Synchronization and other emergent phenomena, in this case, reflect the physical process of signaling. In this chapter, we investigate signaling between two neuronal groups; an understanding of the underlying mechanisms is important in order to gain insight into the complex functions performed by neural systems.

In a distributed system it is necessary to reconstruct responses by global integration. Recent experiments suggest that such a function is performed by the interaction of localized oscillatory signals. Specifically, the experiments on the visual cortex indicate that spatially separated localized populations of neurons can synchronize their oscillatory activity, and the degree of synchronization reflects global stimulus properties (Gray et al., 1989; Eckhorn

et al., 1988).

In detailed computer simulations it has been demonstrated that the synchronization of the oscillatory activity in neuronal groups can be achieved by reentrant signaling (Sporns et al., 1989). In this model, the signature of phase locked oscillations is found, not in the firing of individual neurons which can fire asynchronously, but in the cross correlation (between groups) of the number of neurons firing per unit time which is proportional to the experimentally observed local field potential, in agreement with the observations on the hippocampus (Traub et al., 1988; Traub et al., 1989) and the visual cortex (Eckhorn et al., 1988; Gray et al., 1989).

The oscillations, as we noted in the previous chapter, are input driven due to the dissipative nature of the activity in an unexcited group (or one excited subthreshold). The frequency-amplitude-phase relations indicate that the frequency of oscillation of the number of neurons firing per unit time depends on several parameters – the delay in inhibition, the decay time periods of excitatory and inhibitory activity, the refractory period, the mean synaptic strengths, and the input. Due to variation in virtually all of these parameters, no two groups are likely to have exactly the same frequency of oscillation. This chapter is concerned with the nonlinear interaction of the excitatory and inhibitory components from two groups in order to study the origins and characteristics of synchronization and reentry delay induced desynchronization and resynchronization of oscillatory activity in distributed neural systems.

A critical aspect of signaling in a distributed neural system is the presence of time delays in the transmission and expression of signals. Delays in circulating signals would (1) allow differential access to signals in time and (2) provide mechanisms to ‘hold’ signals for memory related operations. Dis-

tributed mapping with delays in circulating oscillations would be particularly useful in maintaining spatiotemporal correlations of objects and events in the outside world (Reeke et al., 1989).

Such delays can arise from conduction delays and synaptic delays. The expression of various transmitters with different latencies and time courses (Marder et al., 1987) implies a large dynamic range for the latencies involved in inter-group signaling. Transmission delays are not negligible either: cortico-cortical axons have a considerably slower conduction speed ($1m/s$) than the faster geniculo-striate conduction speeds ($4 - 40m/s$) (Bullier et al., 1988). Moreover, Bullier et al. report highly specific feedback connections to laminae 2 and 3 of Areas 17 from Areas 18 and 19 with low latency jitter ($0.3ms$). Hence intracortical signals to Area 17 from Area 18 would have a mean delay of $5ms$, from Area 19 a mean delay of $10ms$, and to the temporal lobe a delay of $20-30$ ms in the transmission (Thorpe and Imbert, 1989). Since these time scales are much greater than the membrane or activity decay time scales they may not be neglected.

In the next section, an extension of the Wilson-Cowan model to take into account reentrant interactions between two groups of neurons is described. In Section 4.3, some of the phenomena we wish to study are illustrated. Approximate relations for the frequency, amplitude, and phases of the various excitatory and inhibitory components of the synchronized oscillatory activity are derived in Section 4.4. Using these relations, the characteristics of reentrant signaling and the resultant synchronization and desynchronization are studied in Section 4.5. In Section 4.6, we describe numerical studies of some other models for the aggregate behavior of groups, including ones with multiplicative (shunting) nonlinearities, in order to elucidate the critical ingredients

in establishing synchrony of different neuronal groups. Section 4.7 summarizes and concludes the discussion.

4.2 Mathematical Model

The mathematical model developed in the previous chapter is extended here to study reentrant signaling between two neuronal groups. Fig. 4.2.1 is a schematic illustration of the inter- and intragroup interactions between two neuronal groups G and G' , where E and I represent the excitatory and inhibitory subpopulations of G and E' and I' the corresponding subpopulations of G' . (*Notation:* Throughout this Chapter, the unprimed variables refer to the group G and the primed ones to G' .) The fraction of excitatory and inhibitory cells firing per unit time, $f_e(t)$, and $f_i(t)$ for the group G , and $f'_e(t)$, and $f'_i(t)$, for the group G' , at time t are given by the following time coarse-grained and spatially averaged nonlinear differential equations,

$$T_e \dot{f}_e(t) = -f_e(t) + (1 - \int_{t-r_e}^t f_e(t') dt') \sigma_e(x_e) \quad (4.2.1)$$

$$T_i \dot{f}_i(t) = -f_i(t) + (1 - \int_{t-r_i}^t f_i(t') dt') \sigma_i(x_i) \quad (4.2.2)$$

$$T'_e \dot{f}'_e(t) = -f'_e(t) + (1 - \int_{t-r'_e}^t f'_e(t') dt') \sigma'_e(x'_e) \quad (4.2.3)$$

$$T'_i \dot{f}'_i(t) = -f'_i(t) + (1 - \int_{t-r'_i}^t f'_i(t') dt') \sigma'_i(x'_i) \quad (4.2.4)$$

$$x_e(t) = C_1 f_e(t) + C'_{r1} f'_e(t - t'_r) - C_2 f_i(t - t_d) + P$$

$$x_i(t) = C_3 f_e(t) + C'_{r2} f'_e(t - t'_r) - C_4 f_i(t - t_d) + Q$$

$$x'_e(t) = C'_1 f'_e(t) + C_{r1} f_e(t - t_r) - C'_2 f'_i(t - t'_d) + P'$$

$$x'_i(t) = C'_3 f'_e(t) + C_{r2} f_e(t - t_r) - C'_4 f'_i(t - t'_d) + Q'$$

where x_e , x_i , x'_e , and x'_i are the activities and $\sigma_e(x_e)$, $\sigma_i(x_i)$, $\sigma'_e(x'_e)$, and $\sigma'_i(x'_i)$ are the responses (outputs) of the respective subpopulations. The sigmoids

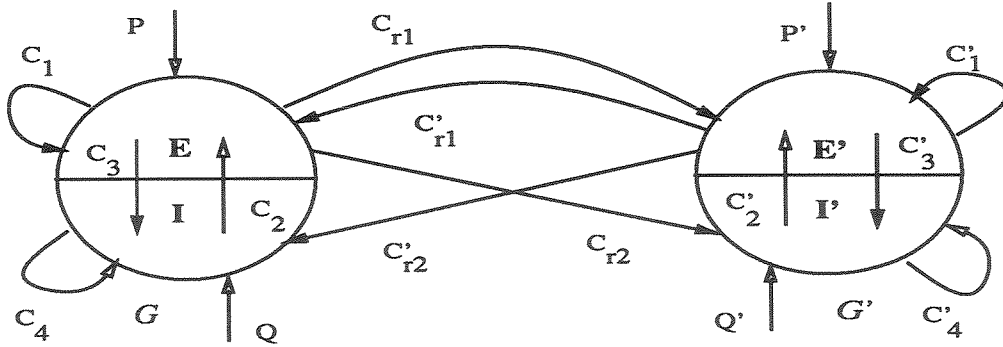


Figure 4.2.1: A schematic diagram of two interacting neuronal groups G and G' each consisting of excitatory and inhibitory subpopulations, E and I , and E' and I' respectively. External inputs P and Q , and P' and Q' activate the neurons. The mean synaptic strengths for the intragroup interactions of the excitatory and inhibitory subpopulations are C_1, C_2, C_3, C_4 for the group G , and C'_1, C'_2, C'_3, C'_4 for the group G' . Reciprocal excitatory connections C_{r1}, C'_{r1}, C_{r2} and C'_{r2} mediate reentrant signaling between the groups. Filled arrows indicate the excitatory effect, and unfilled arrows, the inhibitory effect of one subpopulation on the other or itself.

have the standard form,

$$\sigma(x) = \frac{1}{1 + \exp(-\beta(x - \chi))}$$

where β and χ are respectively the sigmoid nonlinearity and threshold.

Consider, for example, the equation for the fraction of excitatory cells firing per unit time, $f_e(t)$ (Eqn. 4.2.1) for the subpopulation represented by E . The time scale of decay of activity in the absence of external excitation is T_e , and r_e is the absolute refractory period of the excitatory cells. C_1, C_2 , and C'_{r1} are the mean synaptic strengths mediating the E to E , I to E , and E' to E subpopulation interactions respectively, and P is the (constant) external

input. The inhibitory signal arrives with a delay, t_d , and the reentrant signal with a delay, t'_r . The delay could be due to either synaptic latency, delay in transmission, or both. Typically, the inhibitory signals are delayed due to latency in chemical activation at the synapse (Hille and Catterall, 1989), and the excitatory signals are delayed due to the transmission time. Any delay in the recurrent excitation within the neuronal group has been ignored as small compared to the delay in the inhibitory and reentrant signals. Similar considerations hold for each of the other subpopulations. C_{r1} , C_{r2} , C'_{r1} , and C'_{r2} will be referred to as reentrant connections although only the mean synaptic strength is represented in the mathematical model we consider here.

Although synchronization of the activities of the groups is observed for a wide range of parameters, in order to keep the model analytically tractable, the following approximations are made: $C_1 = C_2 = C_3 = C_4 = C'_1 = C'_2 = C'_3 = C'_4 = C$, $C'_{r1} = C'_{r2} = C_{r1} = C_{r2} = C_r$, $r_e = r'_e$ and $r_i = r'_i$. The activities of the subpopulations, x_e , x_i and x'_e , x'_i simplify to,

$$x_e(t) = Cf_e(t) + C_r f'_e(t - t'_r) - Cf_i(t - t_d) + P \quad (4.2.5)$$

$$x_i(t) = Cf_e(t) + C_r f'_e(t - t'_r) - Cf_i(t - t_d) + Q \quad (4.2.6)$$

$$x'_e(t) = Cf_e(t) + C_r f_e(t - t_r) - Cf'_i(t - t'_d) + P' \quad (4.2.7)$$

$$x'_i(t) = Cf'_e(t) + C_r f_e(t - t_r) - Cf'_i(t - t'_d) + Q' \quad (4.2.8)$$

Consistent with the theory of neuronal group selection (Edelman, 1987), we assume that the mean intragroup synaptic strength is greater than the intergroup synaptic strength, i.e., $C > C_r$. Refractoriness in the inhibitory neurons is neglected, and is not critical for the phenomena we wish to study.

For the mathematical analysis of Eqns. 4.2.1 - 4.2.8, it is necessary

to approximate the sigmoid with a piecewise linear function as in Chapter 3:

$$\sigma(x) = \begin{cases} 1.0 & x > \chi + \delta \\ 0.0 & x < \chi - \delta \\ m(x - \chi) + 0.5 & |x - \chi| < \delta \end{cases} \quad (4.2.9)$$

where $\chi + \delta$ is the saturation point, and m is the slope of the sigmoid with $\delta m = \frac{1}{2}$. The approximation preserves the nonlinear saturation characteristics of the original sigmoid.

Two final notes are in order pertaining to the following discussion:

Parameters: Except as noted, the following default parameters are used in quoting the results of the numerical studies of Eqns. 4.2.1 - 4.2.8, $T_e = T_i = T'_e = T'_i = 0.1$, $m_e = m_i = m'_e = m'_i = 0.5$, $\chi_e = \chi_i = \chi'_e = \chi'_i = 4.0$, $P = Q = P' = Q' = 4.0$, $r_e = r'_e = 0.3$, $r_i = r'_i = 0.0$, $C = 5.0$, and $C_r = 2.0$.

Notation: The intrinsic frequencies of the two groups (without reentry) will be denoted by Ω and Ω' and the (common) synchronized frequency of the two groups by ω .

4.3 Illustrative Results

In this section, some results from numerical simulation of Eqns. 4.2.1 - 4.2.8 are described in order to illustrate the theoretical problem we wish to study in the following sections. The two neuronal groups discussed above can have different frequencies of oscillation depending on several parameters, important among which are the connection strengths, time periods of decay, and delay in activation, the refractory periods of excitatory neurons, and the external input (see Chapter 3). For a wide range of parameters, with the introduction of reentrant signaling, the oscillatory activity of the two groups are

phase locked. The phase portraits (Fig. 4.3.1) show that although there is coherent oscillatory activity within a group, the cross components have uncorrelated phases in the absence of reentrant signaling. However, after reentrant signaling is introduced, both the intra- and intergroup activities are correlated. Synchronization is typically established within a few cycles.

The intrinsic frequencies of the oscillatory activity in the two groups are $\Omega = 8.90$ and $\Omega' = 8.28$; after the introduction of reentrant signaling, the frequencies of the two groups are identical, $\omega = 7.67$. For small reentry delays, the frequency of the synchronized oscillation reduces by about 10% in agreement with the detailed computer simulations of (Sporns et al., 1989). The phase locking results in an increase in the cross correlation between the fraction of excitatory neurons firing per unit time (Fig. 4.3.2). Fig. 4.3.3 shows the oscillatory excitatory and inhibitory components from the two groups along with the (identical) frequency spectra after reentrant signaling is introduced.

Finally, we note that if both groups are excited close to the threshold, synchronized oscillations are possible even when only one-way intergroup connections exist. The reason is that, through such a connection, the phase difference between the excitatory components of the groups (see below) can still be adjusted in a manner such that the cross components are phase locked. However, the synchronization is less robust: (1) the intrinsic frequencies of the groups have to be within 10%, and (2) the phase difference between the groups is large. For these reasons, we restrict the discussion to reentrant signaling between G and G' where the signal from a group is continually mapped in a reentrant manner.

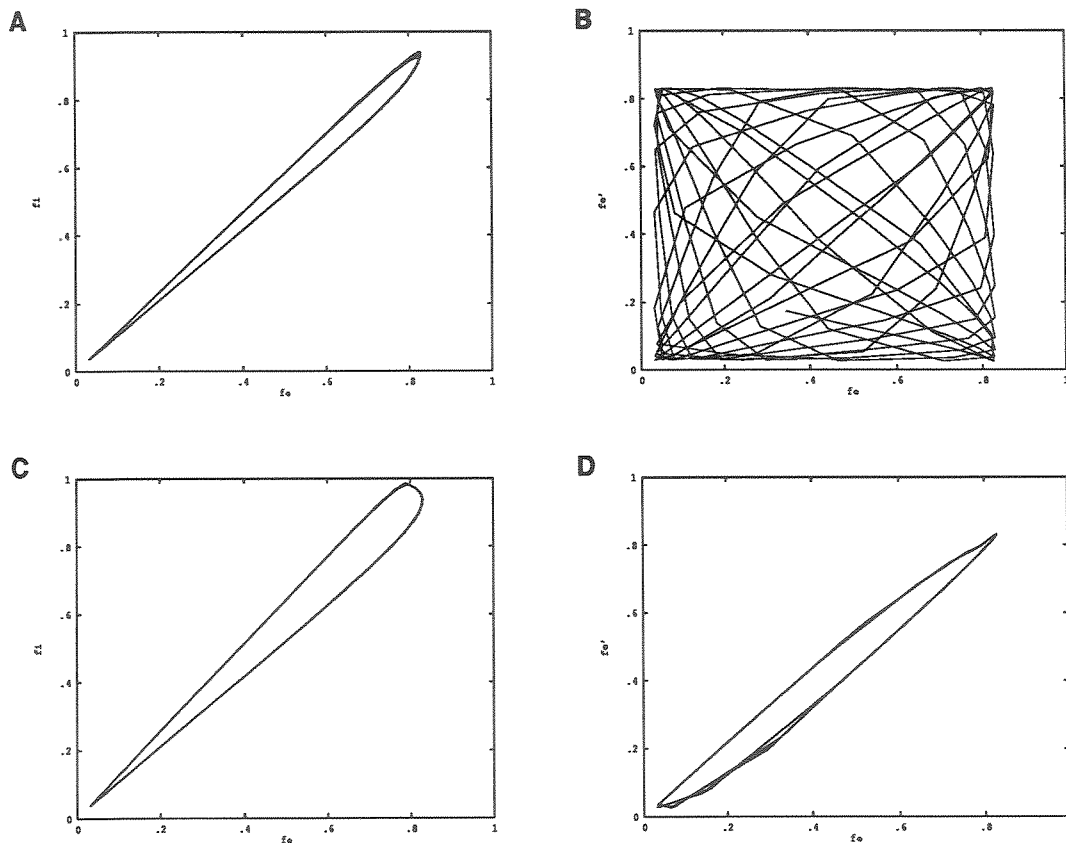


Figure 4.3.1: The phase portraits before and after the introduction of reentry indicate that reentrant signaling induces phase coherence in the intergroup excitatory components. Without reentry, the excitatory $f_e(t)$ and inhibitory $f_i(t)$ components within a group are correlated (A), but the cross components f'_e and f_e are uncorrelated, (B). After the introduction of reentry, both the intragroup (C), and the intergroup components are correlated (D). The intrinsic frequencies of the groups are $\Omega = 8.90$ corresponding to an inhibitory delay $t_d = 0.18$ and $\Omega' = 8.28$ corresponding to inhibitory delay $t'_d = 0.2$. The frequency of the synchronized oscillation drops to $\omega = 7.67$. Similar reductions in the frequency have been reported by Sporns et al. (1989).

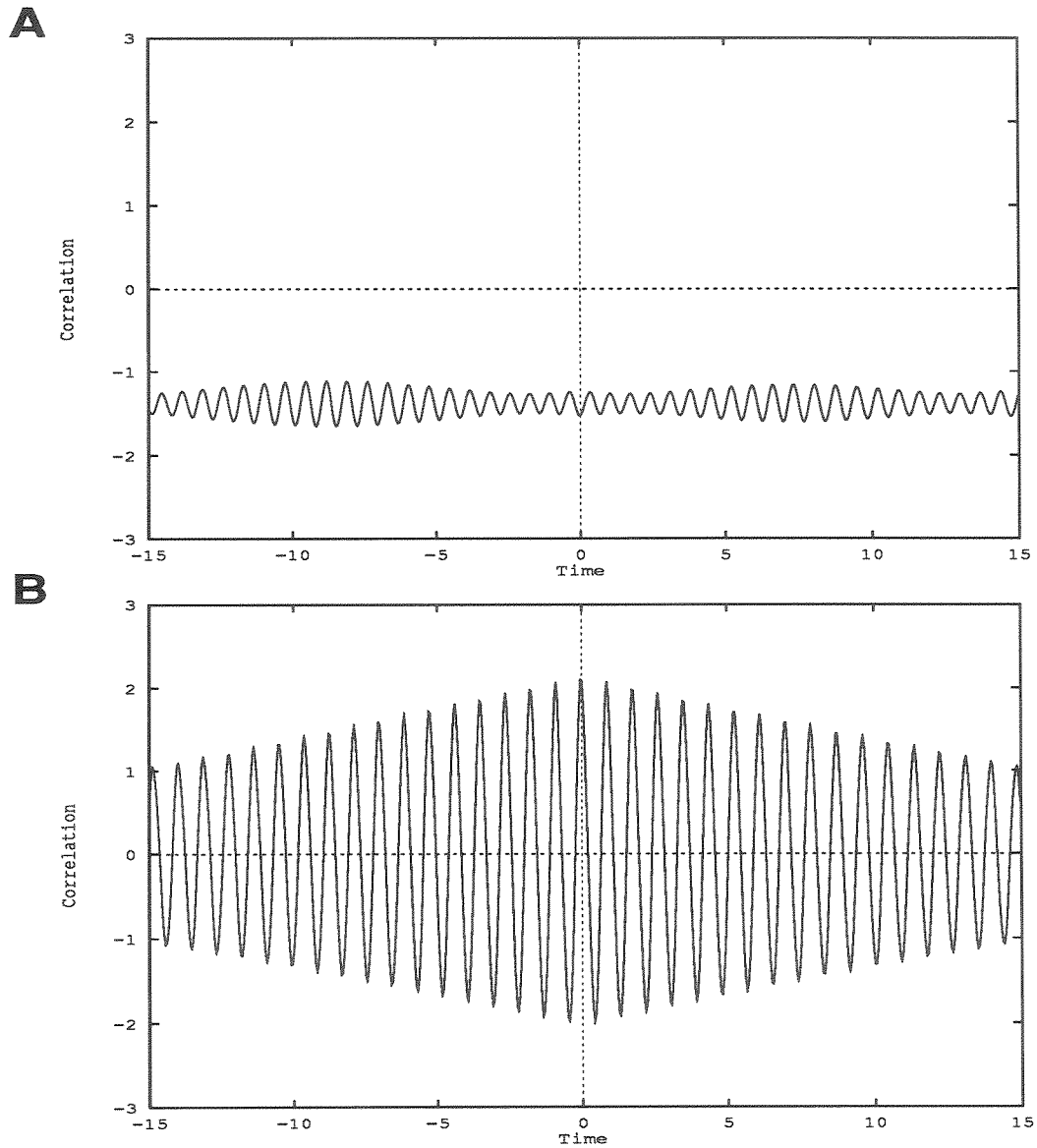


Figure 4.3.2: The cross correlation between the excitatory components, $f'_e(t)$ and $f_e(t)$, of the two groups increases after the introduction of reentry. (A) The cross correlation before, and (B) after the introduction of reentry. The cross correlations are normalized with respect to the mean and standard deviation of the activity after introduction of reentry (B). The intrinsic frequencies are the same as in Fig. 4.3.1.

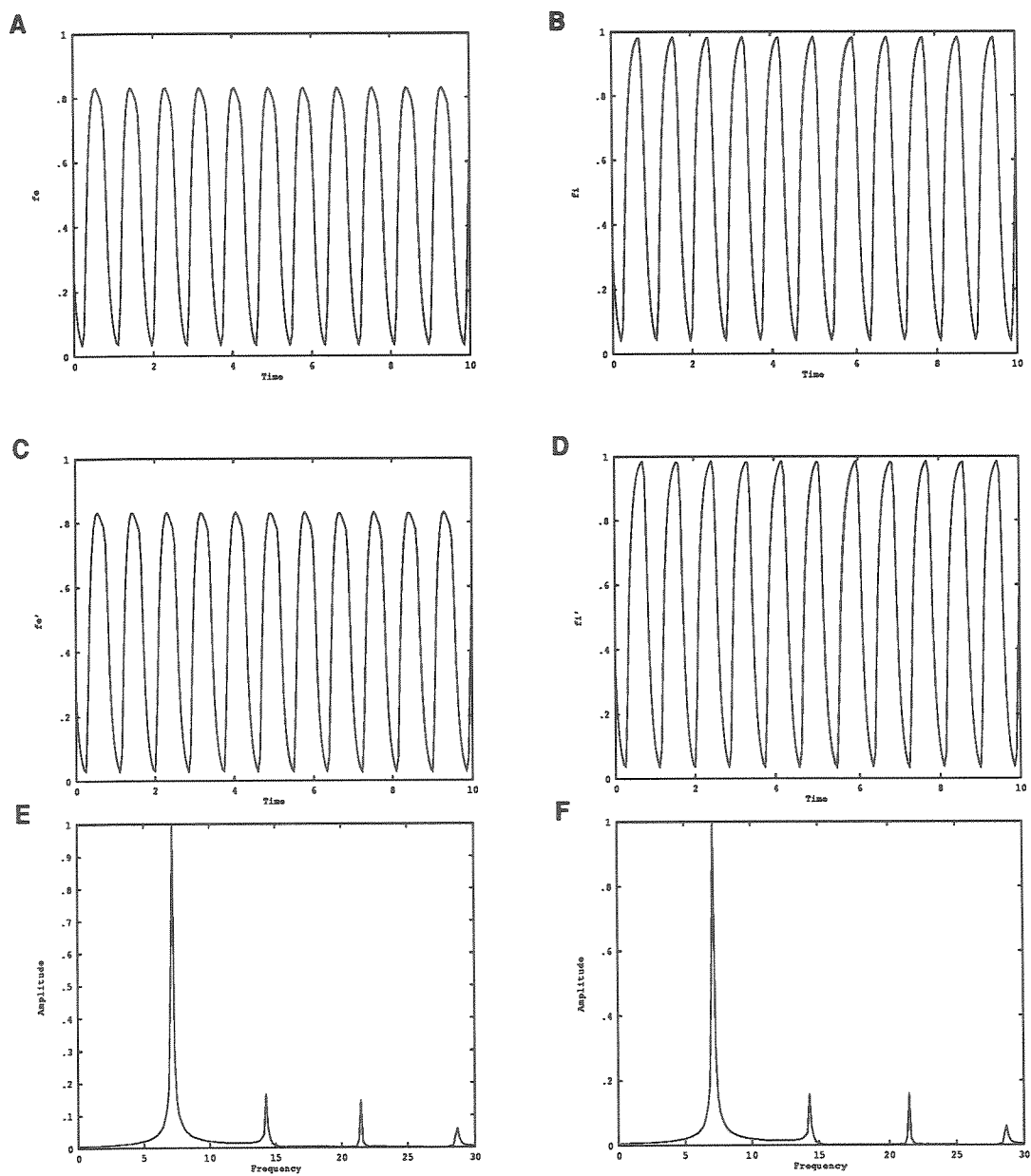


Figure 4.3.3: The amplitude and frequency of the oscillations in the two groups have similar characteristics after reentry is introduced. The fraction of neurons firing per unit time for group G : (A) f_e vs. t and (B) f_i vs. t . The fraction of neurons firing per unit time for group G' : (C) f'_e vs. t , (D) f'_i vs. t . The frequency spectra of (E) group G and (F) group G' are identical. The intrinsic frequencies are the same as in Fig. 4.3.1.

4.4 Frequency-Amplitude-Phase Relations

In order to study the origin and characteristics of the synchronization of the activity of the neuronal groups G and G' , the nonlinear differential equations are reduced to nonlinear algebraic equations governing the frequency-amplitude-phase relations of the oscillations using the method of harmonic balance (Bogoliubov and Mitropolsky, 1961; Gelb and Velde, 1967). The derivation of the relations is outlined in this section— the details may be found in Appendix 4A.

Neglecting the higher harmonics, solutions to Eqns. 4.2.1 - 4.2.4 may be approximated by

$$f_e(t) = \bar{f}_e + f_{e0} \sin(\omega t) \quad (4.4.1)$$

$$f_i(t) = \bar{f}_i + f_{i0} \sin(\omega t - \theta_i) \quad (4.4.2)$$

$$f'_e(t) = \bar{f}'_e + f'_{e0} \sin(\omega t - \theta'_e) \quad (4.4.3)$$

$$f'_i(t) = \bar{f}'_i + f'_{i0} \sin(\omega t - \theta'_e - \theta'_i) \quad (4.4.4)$$

where θ_i , θ'_e and θ'_i are the phase differences (assumed to be constant) between f_e and f_i , f_e and f'_e , and f_e and f'_i respectively. The origin of the piece-wise linear sigmoid (Eqn. 4.2.9) is shifted to the threshold in order to make it symmetric:

$$\begin{aligned} \sigma^*(x^*) &= mx^* & |x^*| < \delta \\ &0.5 & x^* > \delta \\ &-0.5 & x^* < -\delta \end{aligned} \quad (4.4.5)$$

where $x^* = x - \chi$, m is the slope of the sigmoid, and δ is the saturation point with $m\delta = \frac{1}{2}$. Eqns. 4.2.1 - 4.2.4 and Eqns. 4.2.5 - 4.2.8 are modified to

$$T_e \dot{f}_e(t) = -f_e(t) + (1 - \int_{t-\tau_e}^t f_e(t') dt')(0.5 + \sigma_e^*(x_e^*)) \quad (4.4.6)$$

$$T_i \dot{f}_i(t) = -f_i(t) + 0.5 + \sigma_i^*(x_i^*) \quad (4.4.7)$$

$$T_e' \dot{f}_e'(t) = -f_e'(t) + (1 - \int_{t-r_e}^t f_e'(t') dt')(0.5 + \sigma_e^{*'}(x_e^{*'})) \quad (4.4.8)$$

$$T_i' \dot{f}_i'(t) = -f_i'(t) + 0.5 + \sigma_i^{*'}(x_i^{*'}) \quad (4.4.9)$$

$$x_e^*(t) = C f_e(t) + C_r f_e'(t - t_r') - C f_i(t - t_d) + P - \chi_e \quad (4.4.10)$$

$$x_i^*(t) = C f_e(t) + C_r f_e'(t - t_r') - C f_i(t - t_d) + Q - \chi_i \quad (4.4.11)$$

$$x_e^{*'}(t) = C f_e'(t) + C_r f_e(t - t_r) - C f_i'(t - t_d') + P' - \chi_e' \quad (4.4.12)$$

$$x_i^{*'}(t) = C f_e'(t) + C_r f_e(t - t_r) - C f_i'(t - t_d') + Q' - \chi_i' \quad (4.4.13)$$

where χ_e , χ_i , χ_e' , and χ_i' are the respective thresholds of the subpopulations.

Using the method of harmonic balance (Gelb and Velde, 1967), the response of the nonlinear sigmoid to an input of the form $x^*(t) = B + A \sin(\omega t + \theta)$, where B is the bias and A the amplitude, is approximated as follows:

$$\begin{aligned} \sigma(x^*(t)) &\sim BF_B(\sigma, B, A) + AF_A(\sigma, B, A) \sin(\omega t + \theta) \\ &\quad + AF_A^\dagger(\sigma, B, A) \cos(\omega t + \theta) \quad (4.4.14) \\ F_B(\sigma, B, A) &= \frac{1}{2\pi B} \int_0^{2\pi} \sigma(B + A \sin(\psi)) d\psi \\ F_A(\sigma, B, A) &= \frac{1}{\pi A} \int_0^{2\pi} \sigma(B + A \sin(\psi)) \sin(\psi) d\psi \\ F_A^\dagger(\sigma, B, A) &= \frac{1}{\pi A} \int_0^{2\pi} \sigma(B + A \sin(\psi)) \cos(\psi) d\psi \end{aligned}$$

F_B and F_A are the nonlinear gain for the bias and sinusoidal components respectively. The nonlinear equations then reduce to the following algebraic equations when the amplitude of the input to the sigmoid is large compared to the bias (this requires excitation of the subpopulations at the threshold, i.e., $P \sim \chi_e$, $Q \sim \chi_i$, $P' \sim \chi_e'$, and $Q' \sim \chi_i'$) but the harmonics are still weak (see Appendix B.1):

$$\bar{f}_e = 0.5(1 - \bar{f}_e r_e) + \frac{2B_e}{\pi A_e} (1 - \bar{f}_e r_e) \quad (4.4.15)$$

$$\omega T_e f_{e0} = \frac{2}{\pi}(1 - \bar{f}_e r_e) \sin(\theta_{ae}) \quad (4.4.16)$$

$$f_{e0} = \frac{2}{\pi}(1 - \bar{f}_e r_e) \cos(\theta_{ae}) \quad (4.4.17)$$

$$\bar{f}_i = 0.5 + \frac{2B_i}{\pi A_i} \quad (4.4.18)$$

$$\omega T_i f_{i0} = \frac{2}{\pi} \sin(\theta_{ai} + \theta_i) \quad (4.4.19)$$

$$f_{i0} = \frac{2}{\pi} \cos(\theta_{ai} + \theta_i) \quad (4.4.20)$$

$$\bar{f}'_e = 0.5(1 - \bar{f}_e r_e) + \frac{2B'_e}{\pi A'_e}(1 - \bar{f}'_e r_e) \quad (4.4.21)$$

$$\omega T'_e f'_{e0} = \frac{2}{\pi}(1 - \bar{f}'_e r_e) \sin(\theta'_{ae} + \theta'_e) \quad (4.4.22)$$

$$f'_{e0} = \frac{2}{\pi}(1 - \bar{f}'_e r_e) \cos(\theta'_{ae} + \theta'_e) \quad (4.4.23)$$

$$\bar{f}'_i = 0.5 + \frac{2B'_i}{\pi A'_i} \quad (4.4.24)$$

$$\omega T'_i f'_{i0} = \frac{2}{\pi} \sin(\theta'_{ai} + \theta'_i) \quad (4.4.25)$$

$$f'_{i0} = \frac{2}{\pi} \cos(\theta'_{ai} + \theta'_i) \quad (4.4.26)$$

where

$$\tan(\theta_{ae}) = -\frac{C_r f'_{e0} \sin(\theta'_e + \omega t'_r) - C f_{i0} \sin(\theta_i + \omega t_d)}{C f_{e0} + C_r f'_{e0} \cos(\theta'_e + \omega t'_r) - C f_{i0} \cos(\theta_i + \omega t_d)} \quad (4.4.27)$$

$$\tan(\theta'_{ae}) = -\frac{C f'_{e0} \sin(\theta'_e) + C_r f_{e0} \sin(\omega t_r) - C f'_{i0} \sin(\theta'_i + \omega t'_d)}{C f'_{e0} \cos(\theta'_e) + C_r f_{e0} \cos(\omega t_r) - C f'_{i0} \cos(\theta'_i + \omega t'_d)} \quad (4.4.28)$$

$$\tan(\theta_{ai}) = \tan(\theta_{ae}) \quad (4.4.29)$$

$$\tan(\theta'_{ai}) = \tan(\theta'_{ae}) \quad (4.4.30)$$

The coefficients, B_e , B_i , B'_e , and B'_i , are the bias and A_e , A_i , A'_e , and A'_i the amplitudes of the activities of the respective subpopulations.

In the next section we attempt to gain some insight into the nonlinear interaction of the excitatory and inhibitory signals from the two groups by analyzing Eqns. 4.4.15 - 4.4.30.

4.5 Nonlinear Theory

In considering a nonlinear theory of synchronization two points may first be noted. When one of the groups is driven (much) below its threshold for excitation oscillations are neither excited in the group nor induced by reentry because of the strongly dissipative nature of activity in an unexcited group (Wilson and Cowan, 1972). Specifically, the nonlinear gain for the sinusoidal component of the input to the sigmoid is zero. Hence, the synchronization is input driven. Eqns. 4.4.15 - 4.4.30 represent the approximate frequency-amplitude-phase relations of synchronized oscillations when the subpopulations are driven close to their respective thresholds. Secondly, when the excitatory cells are not refractory ($r_e = 0$) the bias component of the input into the sigmoid is large, so that no oscillations occurred in the present model when reentrant signals are introduced. With a nonzero refractory period oscillations occurred because of suppressed excitatory activity (see Eqn. 4.5.3 below). As discussed in the previous chapter, refractoriness in the excitatory neurons is an aiding factor in the existence of intrinsic oscillations in groups as well, because it causes suppression of excitatory activity and places the fixed point in a regime wherein the slope of the sigmoid at the fixed point is nonzero, so that delayed inhibition can induce oscillations. Refractoriness in excitatory cells is particularly necessary when there are reentrant excitatory signals. The important effect of refractoriness in excitatory cells has been noted by (Sporns et al., 1989) in their detailed simulations.

In the present discussion, we select the critical variables in the system to be the inhibitory delay times t_d and t'_d , and the reentry delay times t'_r and t_r ; the reason being that it allows us to study the effects of the relative phases of the interacting signals. As shown in the previous chapter, the phase of a

signal arriving due to a delay τ , when the ongoing oscillation has a frequency ω , is $\omega\tau$, and this (hidden) phase plays an important role in the origin and characteristics of the oscillations and, as will we see, in synchronization as well. Except as noted, the remaining parameters are as mentioned in Section 4.2.

For $T_e = T'_e = T_i = T'_i = T$, it is easy to show that $\theta_i = \theta'_i = 0$, $f_{e0} = f'_{e0}$, $f_{i0} = f'_{i0}$, $\bar{f}_e = \bar{f}'_e$, and $\bar{f}_i = \bar{f}'_i$. From Eqns. 4.4.16, 4.4.17, 4.4.22, 4.4.23, 4.4.27 and 4.4.29, the frequency of the synchronized oscillation, ω , and the phase difference, θ'_e , between the excitatory components f'_e and f_e of the two groups are given by,

$$\omega T = -\frac{\frac{C_r}{C} \frac{f_{e0}}{f_{i0}} \sin(\theta'_e + \omega t'_r) - \sin(\omega t_d)}{\frac{f_{e0}}{f_{i0}} + \frac{C_r}{C} \frac{f_{e0}}{f_{i0}} \cos(\theta'_e + \omega t'_r) - \cos(\omega t_d)} \quad (4.5.1)$$

$$\frac{\omega T - \tan(\theta'_e)}{1 + \omega T \tan(\theta'_e)} = -\frac{\frac{f_{e0}}{f_{i0}} \sin(\theta'_e) + \frac{C_r}{C} \frac{f_{e0}}{f_{i0}} \sin(\omega t_r) - \sin(\theta'_e + \omega t'_d)}{\frac{f_{e0}}{f_{i0}} \cos(\theta'_e) + \frac{C_r}{C} \frac{f_{e0}}{f_{i0}} \cos(\omega t_r) - \cos(\theta'_e + \omega t'_d)} \quad (4.5.2)$$

These relations indicate the importance of the phases of the interacting signals. The effective phase of a signal has two components, one typically referred to as the ‘phase difference’, for example, θ'_e due to synaptic coupling, and the other explicitly due to delay in activation of the signal, for example $\omega t'_r$. The phase difference, θ'_e , between the excitatory components, $f_e(t)$ and $f'_e(t)$, is exactly zero only when there is a certain symmetry: if the frequencies of oscillation are exactly the same and the coupling is symmetric both in strength and delay. Arbitrarily small phase differences are possible when the intrinsic frequencies of the groups approach each other, i.e., $\Omega \rightarrow \Omega'$. The effect of the excitatory signal is weighted by $\frac{f_{e0}}{f_{i0}}$, and the reentrant signal by $\frac{C_r}{C} \frac{f_{e0}}{f_{i0}}$ with respect to the inhibitory signal. The ratio of the mean intergroup to intragroup connection strength therefore determines the influence of the reentrant signal.

With the approximation $\bar{f}_e \sim f_{e0}$ (see Fig. 4.3.3), and the relations, $\frac{f_{e0}}{f_{i0}} = 1 - r_e \bar{f}_e$, $f_{e0} = \frac{2}{\pi\sqrt{1+\omega^2 T^2}}(1 - r_e \bar{f}_e)$ and $f_{i0} = \frac{2}{\pi\sqrt{1+\omega^2 T^2}}$, the following

expression for $\frac{f_{e0}}{f_{i0}}$ is obtained:

$$\frac{f_{e0}}{f_{i0}} \sim \frac{1}{1 + \frac{2r_e}{\pi\sqrt{1+\omega^2T^2}}} \quad (4.5.3)$$

If $\omega T < 1$, as is typical in the present discussion, it follows that $\frac{f_{e0}}{f_{i0}} \sim \frac{1}{1+\kappa r_e}$, where $\frac{\sqrt{2}}{\pi} \leq \kappa \leq \frac{2}{\pi}$. The ratio of the amplitude of the excitatory and inhibitory neurons firing per unit time scales inversely with the refractoriness of the excitatory neurons and underlies the suppression of excitatory activity necessary for integrating the excitatory signals from (possibly several) other groups.

From Eqns. 4.5.1 - 4.5.3, we note that synchronization is achieved by adjusting the amplitudes and phases of the various excitatory and inhibitory components as well as the frequency of the coherent oscillation.

In the simulations of Sporns et al. (1989), it has been observed that reentrant signaling reduces the frequency of oscillation. Similar results are also noted with numerical experiments on Eqns. 4.2.1 - 4.2.8, (see Section 4.3). For a simple case it is possible to prove, analytically, that the introduction of reentry reduces the frequency of synchronized oscillation, and the decrease is proportional to $\frac{C_r}{C}$, the ratio of the mean intergroup to intragroup synaptic strength. The result is essentially an extension of the proof given in the previous chapter about the decline of the frequency with increasing ratio of recurrent excitation to inhibition. Consider Eqns. 4.5.1 - 4.5.3 with $t_d = t'_d$ and $t_r = t'_r = 0$. The intrinsic frequencies of oscillation of the two groups without reentrant connections ($C_r = 0$) are identical in this case. With the above approximations, the phase difference θ'_e is identically zero and the frequency of oscillation simplifies to,

$$\omega T = \tan(\theta_{ae}) = \frac{\sin(\omega t_d)}{\frac{f_{e0}}{f_{i0}}(1 + \frac{C_r}{C}) - \cos(\omega t_d)} \quad (4.5.4)$$

Theorem 3.7.1 is useful here and we restate it for convenience:

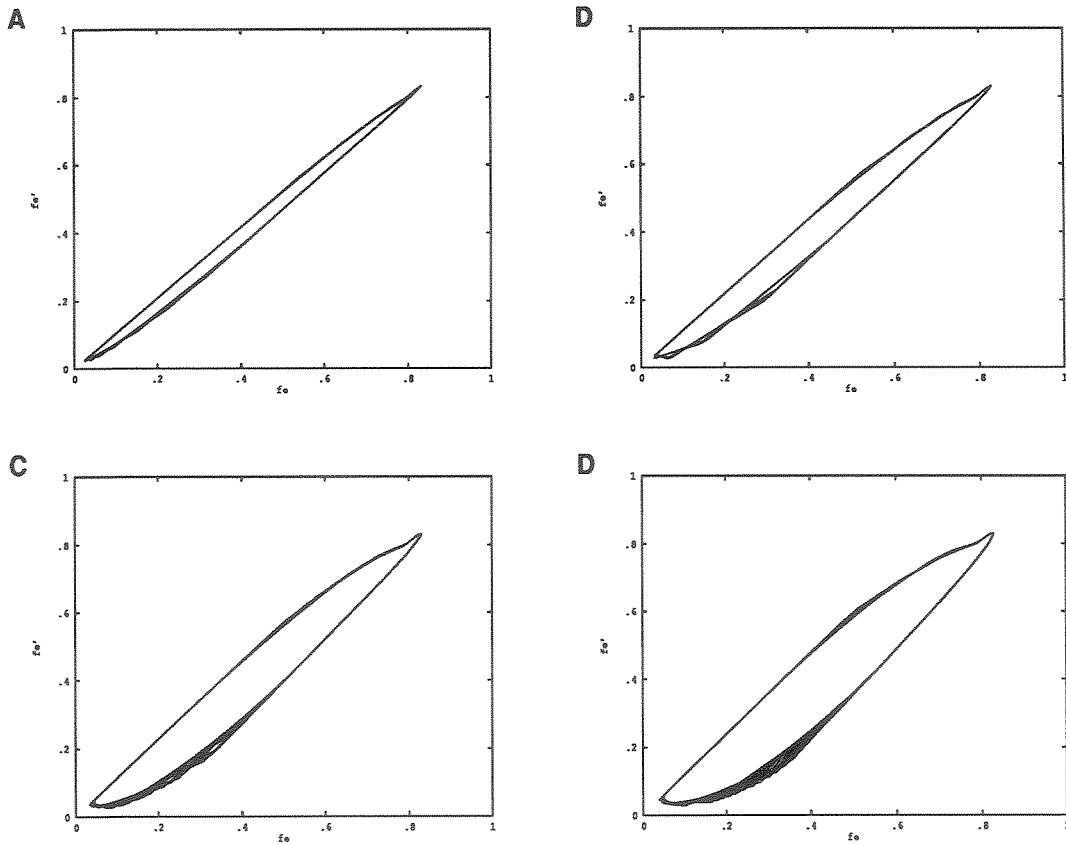


Figure 4.5.1: Increasing the difference in the intrinsic frequencies of the groups, by selectively increasing the inhibitory delay in one of the groups, causes an increasing phase shift between the excitatory components, f_e' and f_e . The frequency of the the group G' is fixed at $\Omega' = 8.28$, ($t_d' = 0.2$), with the frequency of the group G varied as follows: (A) $\Omega = 8.59$, ($t_d = 0.19$), (B) $\Omega = 8.90$, ($t_d = 0.18$), (C) $\Omega = 9.05$, ($t_d = 0.17$), and (D) $\Omega = 9.36$, ($t_d = 0.16$).

C_r	ω (num.)	ω (theory)
0.0	8.28	8.94
0.5	8.13	8.71
1.0	7.97	8.47
1.5	7.67	8.23
2.0	7.52	8.00
2.5	7.21	7.77
3.0	6.90	7.53

Table 4.5.1: The frequency of the synchronized oscillation decreases when reentry is introduced and the decrease is proportional to the reentrant connection strength, C_r . In this example, the intrinsic frequencies are identical, $\Omega = \Omega' = 8.28$, corresponding to inhibitory delays, $t_d = t'_d = 0.2$. The reentrant signals have no delay, $t_r = t'_r = 0$.

Theorem 4.5.1 *For $x > 0$, the frequency of oscillation given by $T\omega = \frac{\sin(\omega t_d)}{x - \cos(\omega t_d)}$ monotonically decreases as x increases.*

Let $x = \frac{f_{e0}}{f_{i0}}(1 + \frac{C_r}{C})$. Assume that the frequency of oscillation increases as $\frac{C_r}{C}$ increases. Then in Eqn. 4.5.3, $\frac{f_{e0}}{f_{i0}}$ increases so that x increases. This contradicts Theorem 3.7.1. Hence we have shown that the frequency of oscillation, ω , decreases when reentry is introduced and, moreover, ω decreases monotonically with increasing $\frac{C_r}{C}$. Table 4.5.1 compares the numerical and theoretical results for the frequency of oscillation of the groups as a function of C_r .

The above result is proven only for zero reentrant delay, $t_r = t'_r = 0$. Consider the effect of nonzero delay in the arrival of reentrant signals, with the same approximations as above, but $t_r = t'_r \neq 0$. In this case also, the phase difference between the excitatory components of the two groups, θ'_e is zero. Note however that because of the delay, t_r , the reentrant signal now has a ‘hidden phase shift’, ωt_r . It is straightforward to show that the frequency of

t_r	ω (num.)	ω (theory)
0.00	7.98	8.47
0.05	7.67	8.28
0.10	7.82	8.20
0.15	7.82	8.25
0.20	7.82	8.45
0.25	8.13	8.78
0.30	8.74	9.19
0.35	9.36	9.50
0.40	9.36	9.63

Table 4.5.2: The frequency of synchronized oscillation first decreases with increasing reentry delay, t_r , and then increases as the excitatory reentrant signal arrives out of phase with the inhibitory signal. The intragroup inhibitory signal have delays $t_d = t'_d = 0.2$, and the the intrinsic frequencies of the group are identical, $\Omega = \Omega' = 8.28$. Here $\frac{C_r}{C} = \frac{1}{5}$.

oscillation is given by

$$\omega T = \tan(\theta_{ae}) = -\frac{\frac{C_r}{C} \frac{f_{e0}}{f_{i0}} \sin(\omega t_r) - \sin(\omega t_d)}{\frac{f_{e0}}{f_{i0}} + \frac{C_r}{C} \frac{f_{e0}}{f_{i0}} \cos(\omega t_r) - \cos(\omega t_d)} \quad (4.5.5)$$

with $\frac{f_{e0}}{f_{i0}}$ given by Eqn. 4.5.3. The frequency depends on the phase shifts ωt_d and ωt_r of the inhibitory and reentrant signals with the latter weighted by $\frac{C_r}{C}$, the ratio of the mean intergroup to intragroup connection strength. When $t_r \sim t_d$, the two signals are out of phase and qualitatively different behavior could be expected. For $t_r \ll t_d$, the frequency is lowered by reentrant signals, as proven for the case of $t_r = 0$ above, however for t_r close to and greater than t_d , the frequency can increase. Table 4.5.2 compares the theoretical and numerical frequencies as a function of t_r . As predicted, the frequency of oscillation decreases for small reentry delays and upon further increase in delay, increases, clearly showing a lack of monotonicity.

Hence, the relative phases of the incoming signals are critical in determining the frequency of the oscillation. From the symmetry in the example

considered above, the phase difference, θ'_e , between the excitatory components of the two groups is constrained to be zero, and no other changes ensue. However, as we note below, for the more realistic case of groups with differing intrinsic frequencies, functionally important features emerge when the phase difference θ'_e is not strictly zero.

Next consider the case of differing inhibitory delays in the groups, $t_d \neq t'_d$, so that the frequencies of the two groups are different. Let the reentry delays be zero, $t_r = t'_r = 0$. The frequency of oscillation is obtained by solving

$$\omega T = -\frac{\frac{C_r}{C} \frac{f_{e0}}{f_{i0}} \sin(\theta'_e) - \sin(\omega t_d)}{\frac{f_{e0}}{f_{i0}} + \frac{C_r}{C} \frac{f_{e0}}{f_{i0}} \cos(\theta'_e) - \cos(\omega t_d)} \quad (4.5.6)$$

$$\frac{\omega T - \tan(\theta'_e)}{1 + \omega T \tan(\theta'_e)} = -\frac{\frac{f_{e0}}{f_{i0}} \sin(\theta'_e) - \sin(\theta'_e + \omega t'_d)}{\frac{f_{e0}}{f_{i0}} \cos(\theta'_e) + \frac{C_r}{C} \frac{f_{e0}}{f_{i0}} - \cos(\theta'_e + \omega t'_d)} \quad (4.5.7)$$

Eqns. 4.5.6 and 4.5.7 indicate that the groups phase lock by adjusting the phase difference, θ'_e , and the frequency, ω . The ratio of amplitudes of excitatory and inhibitory neurons firing per unit time, $\frac{f_{e0}}{f_{i0}} \sim \frac{1}{1+\kappa r_e}$ (Eqn. 4.5.3), typically changes little (unless ωT changes substantially).

When the frequency of the oscillation in one of the groups is selectively increased by reducing the inhibitory signal delay, t_d , so that the mismatch in the intrinsic frequencies of the groups increases, the phase difference, θ'_e , increases as indicated in Table 4.5.3. The phase portraits (Fig. 4.5.1) confirm this result. The sign of the theoretically derived phase difference shows that the activity in the group with the higher frequency (G) leads the activity in group G' . Note that the phase difference can become arbitrarily small as the frequencies of the groups approach each other, i.e., $\Omega \rightarrow \Omega'$. The frequency of the synchronized oscillation also increases with the intrinsic frequency of oscillation of the group G , emphasizing the cooperative nature of the interaction mediated by reentrant connections. In the present example, note that there is a negligible phase

t_d	ω (Ω) (num.)	ω (Ω) (theory)	θ'_e (theory)
0.20	7.52 (8.28)	8.00 (8.94)	0.0
0.19	7.52 (8.59)	8.12 (9.25)	0.10
0.18	7.67 (8.90)	8.24 (9.58)	0.20
0.17	7.82 (9.05)	8.37 (9.94)	0.30
0.16	7.98 (9.36)	8.51 (10.33)	0.41
0.15	8.13 (9.82)	8.67 (10.76)	0.52
0.14	8.28 (10.12)	8.85 (11.24)	0.66
0.13	8.44 (10.58)	9.09 (11.76)	0.84

Table 4.5.3: The phase difference between the excitatory components of the groups, θ'_e increases as the frequency mismatch between the groups increases. ω is the frequency of synchronized oscillations, and Ω , the intrinsic frequency of one of the groups (shown in brackets). Ω' , the intrinsic frequency of the other group is fixed at 8.28. Ω is selectively increased by decreasing the inhibitory delay, t_d . The synchronized frequency, ω , also increases with Ω .

difference between the excitatory and inhibitory components within a group because of symmetric intragroup connectivity and identical decay rates for the excitatory and inhibitory components.

When reentrant connections are introduced, phase locked oscillations, such as those described above, occur even when the frequencies of the two groups without reentrant signaling differ by as much as 35%. However, if the frequencies of the groups differ by 50% or more, synchronization is more complicated. Let, for example, the intragroup inhibitory delays be $t_d = 0.1$ and $t'_d = 0.3$ so that the frequencies of the two groups differ considerably: $\Omega = 12.27$ and $\Omega' = 6.60$. In this case, when reentry is introduced, the spectral peaks occur at a frequency of $\omega = 6.75$, close to, (1) the intrinsic frequency of G' , and (2) a subharmonic of G (Fig. 4.5.2). The cross correlation between the activity of the groups is reduced because of the complex spectra which contain non-overlapping frequency peaks. These results suggest a role for the complex

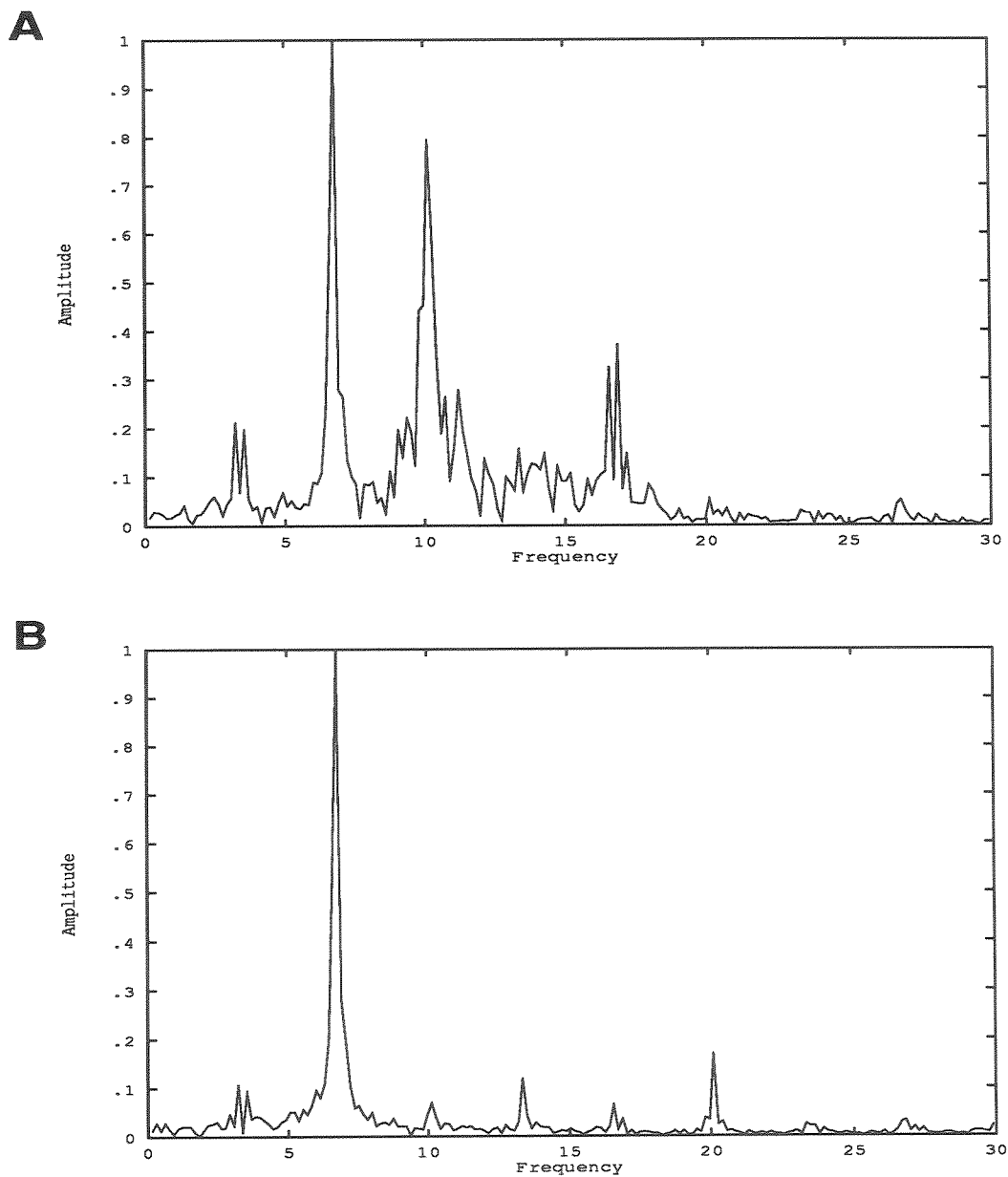


Figure 4.5.2: When the intrinsic frequencies of the groups differ by over 50%, subharmonic resonance establishes partial synchrony. (A) The frequency spectrum for group G shows a subharmonic ($\omega = 6.75$) whose frequency is close to half its intrinsic frequency; (B) The group G' has a frequency spectrum with its dominant frequency close to its intrinsic frequency. The intrinsic frequencies of the groups are $\Omega = 12.27$, ($t_d = 0.1$) and $\Omega' = 6.60$, ($t'_d = 0.3$).

harmonics that can circulate in the system – they establish partial synchrony when the disparity in the frequencies is large or when the intrinsic oscillations of the groups contain strong harmonics.

Consider next the effect of increasing the reentry delay in order to understand the effect of signals interacting with different phases. In particular, we wish to investigate the effect of the phases of the reentrant and inhibitory signals when the intrinsic frequencies of the groups are not the same. Let the reentry delays be symmetric, i.e., $t_r = t'_r$. The frequency and phase, θ'_e , of the oscillation are given by,

$$\omega T = -\frac{\frac{C_r}{C} \frac{f_{e0}}{f_{i0}} \sin(\theta'_e + \omega t_r) - \sin(\omega t_d)}{\frac{f_{e0}}{f_{i0}} + \frac{C_r}{C} \frac{f_{e0}}{f_{i0}} \cos(\theta'_e + \omega t_r) - \cos(\omega t_d)} \quad (4.5.8)$$

$$\frac{\omega T - \tan(\theta'_e)}{1 + \omega T \tan(\theta'_e)} = -\frac{\frac{f_{e0}}{f_{i0}} \sin(\theta'_e) + \frac{C_r}{C} \frac{f_{e0}}{f_{i0}} \sin(\omega t_r) - \sin(\theta'_e + \omega t'_d)}{\frac{f_{e0}}{f_{i0}} \cos(\theta'_e) + \frac{C_r}{C} \frac{f_{e0}}{f_{i0}} \cos(\omega t_r) - \cos(\theta'_e + \omega t'_d)} \quad (4.5.9)$$

As the reentry delay, t_r , is increased, the theoretical results indicate that the phase difference θ'_e between the groups increases and then abruptly jumps by almost 160° . Concomitantly, the frequency decreases and then jumps to a higher value. Further increase of the delay is accompanied by a decrease in frequency and an increase in the phase difference (see Table 4.5.4). This phenomenon is similar to the jump resonance observed in other nonlinear systems (Stoker, 1950; Guckenheimer and Holmes, 1983) and is characterized by abrupt changes in phase, amplitude, and frequency. At the transition region, the behavior of the system can be quite complex, and the theory is no longer valid since the phase, θ'_e , is no longer constant. The following functionally important characteristics are noted in this region: (1) lost phase coherence, (2) persistent transients, and (3) reduced cross correlation between the groups. Reductions of 50% in the cross correlation have been observed (Fig. 4.5.3). The frequency spectra (Fig. 4.5.4) also indicate that the underlying activity is asynchronous.

t_r	ω (num.)	ω (theory)	θ'_e (theory)
0.00	7.60	8.24	0.19
0.05	6.90	7.85	0.26
0.06	6.90	7.80	0.29
0.12	9.97	10.27	- 2.49
0.15	9.82	10.21	- 2.74
0.20	9.51	9.79	- 2.84

Table 4.5.4: The phase difference, θ'_e , between the excitatory and inhibitory components of the two groups and the synchronized frequency, ω , jump abruptly as the reentry delay, t_r , is increased causing the inhibitory and reentrant signals to arrive out of phase. In this example, the frequencies of the two groups are $\Omega = 8.89$ and $\Omega' = 8.28$, corresponding to inhibitory signal delays, $t_d = 0.18$ and $t'_d = 0.2$.

Numerical experiments indicate that the size of the transition region increases with the mismatch in the intrinsic frequencies (Ω and Ω') of the groups. Thus, depending on the phases of the interacting signals, the oscillatory activity of the groups can be either synchronized or desynchronized. Even when the frequencies of the groups are exactly the same, asymmetry in reentry delays, i.e., $t_r \neq t'_r$, can cause a nonzero phase difference between the excitatory components of the groups, as may be seen from Eqns. 4.5.1 and 4.5.2 with $t_d = t'_d$. For small differences in the delays, the phase difference, θ'_e , is small. However, as the mismatch increases, the oscillations display the jump bifurcation described above wherein discontinuous changes in frequency and phase occur. Table 4.5.5 compares the theoretical and numerical results on the frequency and phase changes when t'_r is increased with t_r constant. In this case also, persistent transients are observed near the transition region, and the cross correlation between the groups can decrease substantially even though the intrinsic frequencies of the groups are exactly the same. The desynchronization of the oscillations in this case points to the emergent features of phasic signaling.

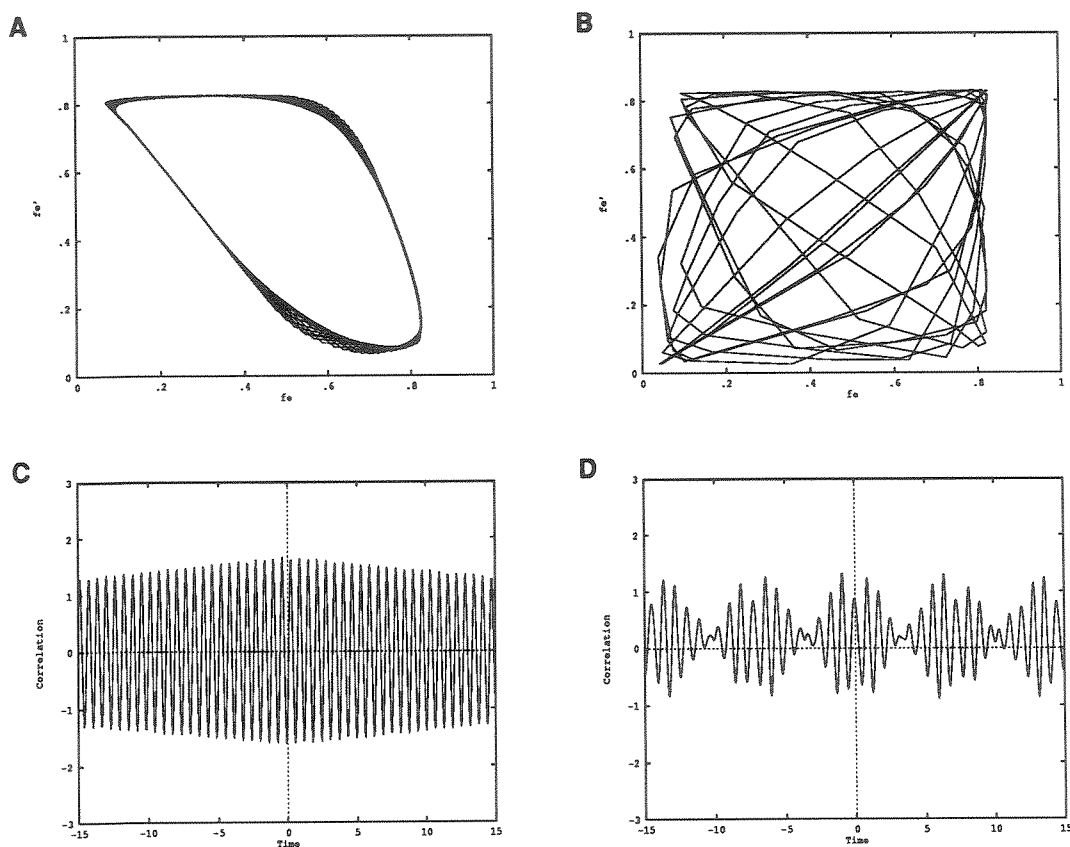


Figure 4.5.3: Desynchronization and resynchronization of the oscillatory activity occurs when the delay in the reentrant signal is increased. (A) The phase difference, θ'_e , between f_e and f'_e , the fraction of excitatory neurons firing per unit time, jumps abruptly by almost 150° as predicted theoretically. (B) In the transition region, phase coherence is lost. (C) The cross correlation after the transition is much greater than the cross correlation at the transition, (D). The reentry delays are $t_r = t'_r = 0.15$ after the transition and $t_r = t'_r = 0.1$ at the transition point. The intrinsic frequencies of the groups are, $\Omega = 9.82$, ($t_d = 0.15$) and $\Omega' = 8.28$ ($t'_d = 0.2$). The cross correlations are normalized with respect to the mean and standard deviation of the post transition activity (C).

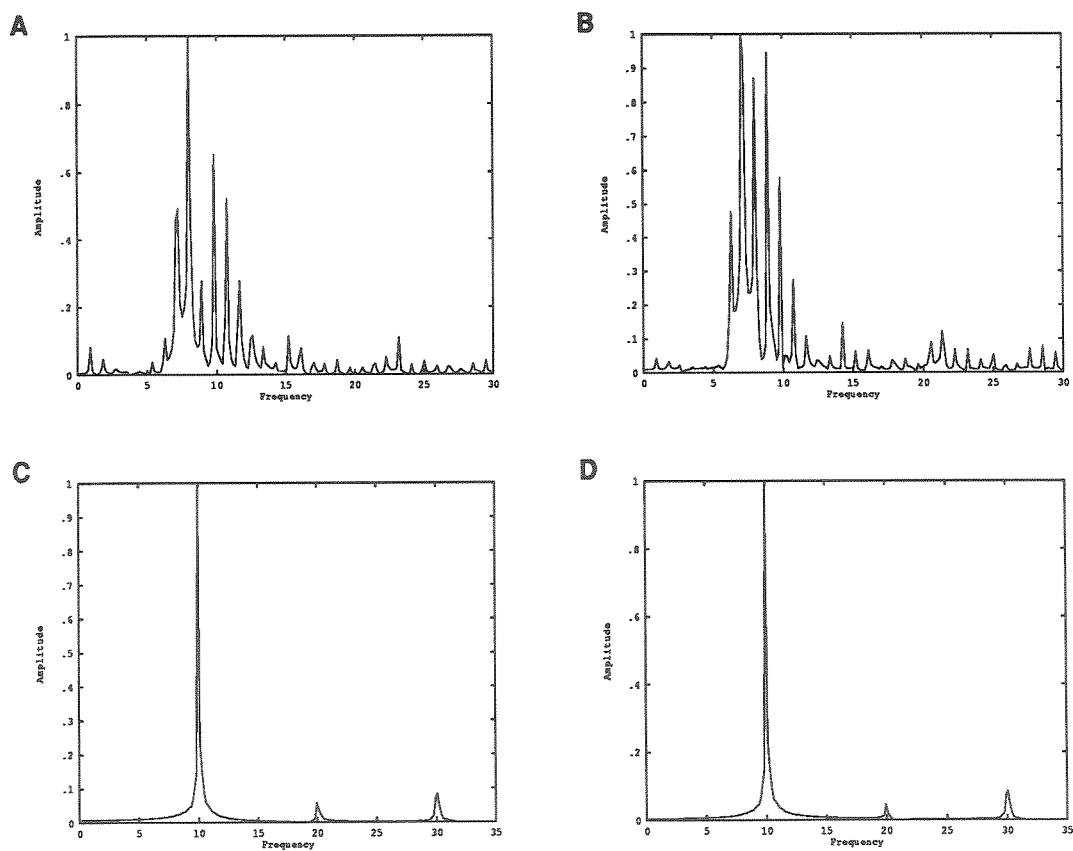


Figure 4.5.4: The spectra during desynchronized activity and after resynchronization. (A) Spectrum of the oscillatory activity of G and (B) spectrum of the oscillatory activity of G' while activity is desynchronized indicate complex non-overlapping frequencies. (C) Spectrum of G and (D) spectrum of G' after resynchronization indicate the basis of the restored synchrony.

t_r	ω (num.)	ω (theory)	θ'_e (theory)
0.00	7.52	8.00	0.0
0.05	7.21	7.79	0.19
0.10	7.21	7.61	0.38
0.15	7.21	7.48	0.56
0.20	7.52	10.25	- 2.12
0.22	9.82	10.21	-2.01
0.30	9.66	9.97	- 1.65
0.40	9.36	9.56	- 1.22

Table 4.5.5: The synchronized frequency, ω , and the phase difference, θ'_e , between the excitatory components of the two groups jump abruptly as the mismatch in reentry times increases even when the frequencies of the two groups are exactly the same. The delay in the excitatory signal from the group G , t_r , is increased with the delay of the signal from G' to G kept fixed at $t'_r = 0$.

These results emphasize the critical role of the relative phases of the interacting signals and the functionally important role of delay induced phase shifts.

All of the above results, derived for identical excitatory and inhibitory activity decay time scales, $T_e = T_i$, also hold for the more realistic case of slowly decaying inhibitory activity, $T_e < T_i$ which we consider next. Here we will only sketch some results for the sake of completeness. For simplicity, we set $T_e = T'_e$, $T_i = T'_i$, and $t_r = t'_r = 0$. The following relations can be easily shown: (1) $f_{e0} = f'_{e0}$, (2) $f_{i0} = f'_{i0}$ and, (3) $\theta'_i - \theta'_e = \theta_i$. When $T_e \neq T_i$, the phase difference θ_i between the excitatory and inhibitory components within a group is no longer zero, $\tan(\theta_i) = \frac{\omega(T_i - T_e)}{1 + T_e T_i \omega^2}$. With the approximation $f_{e0} \sim \bar{f}_e$, the ratio of the amplitudes of the excitatory and inhibitory neurons firing per unit time, can be obtained from Eqns. 4.4.16, 4.4.17, 4.4.19, and 4.4.20,

$$\frac{f_{e0}}{f_{i0}} = \sqrt{\frac{1 + \omega^2 T_i^2}{1 + \omega^2 T_e^2}} \frac{1}{1 + \frac{2T_e}{\pi \sqrt{1 + \omega^2 T_e^2}}} \quad (4.5.10)$$

If $\omega T_e < 1$, as is typical in the present discussion, it follows that $\frac{f_{e0}}{f_{i0}} \sim \sqrt{\frac{1+\omega^2 T_i^2}{1+\omega^2 T_e^2}} \frac{1}{1+\kappa r_e}$, where $\frac{\sqrt{2}}{\pi} \leq \kappa \leq \frac{2}{\pi}$. The ratio of the amplitude of the excitatory and inhibitory neurons firing per unit time (1) scales inversely with the refractoriness of the excitatory neurons, and (2) depends on the decay times, T_e and T_i , and the frequency in a nontrivial manner. The frequency-amplitude-phase relations are obtained from Eqns. 4.4.16, 4.4.17, 4.4.22, and 4.4.23,

$$\omega T_e = -\frac{\frac{C_r}{C} \frac{f_{e0}}{f_{i0}} \sin(\theta'_e) - \sin(\theta_i + \omega t_d)}{\frac{f_{e0}}{f_{i0}} + \frac{C_r}{C} \frac{f_{e0}}{f_{i0}} \cos(\theta'_e) - \cos(\theta_i + \omega t_d)} \quad (4.5.11)$$

$$\frac{\omega T_e - \tan(\theta'_e)}{1 + \omega T_e \tan(\theta'_e)} = -\frac{\frac{f_{e0}}{f_{i0}} \sin(\theta'_e) - \sin(\theta'_e + \theta_i + \omega t'_d)}{\frac{f_{e0}}{f_{i0}} \cos(\theta'_e) + \frac{C_r}{C} \frac{f_{e0}}{f_{i0}} - \cos(\theta'_e + \theta_i + \omega t'_d)} \quad (4.5.12)$$

For $t_d = t'_d$, it follows that $\theta'_e = 0$ and $\theta'_i = \theta_i$. It may be noted that the phase difference θ_i reflects intragroup asymmetries (for example, differences in excitatory and inhibitory decay time periods) whereas θ'_e reflects intergroup asymmetries (for example, differences in forward and backward connection strengths).

In agreement with the results obtained for $T_i = T_e$, we find (1) the theoretically determined phase difference increases as the difference between the intrinsic frequencies of the groups increases, and (2) the frequency of the synchronized oscillation decreases in comparison to $\max(\Omega, \Omega')$ (if not both Ω and Ω') (Table 4.5.6).

When the frequencies between the groups differ by more than 50%, circulating subharmonics establish partial synchrony. For the particular case illustrated in Fig. 4.5.5, $\Omega = 7.823$ and $\Omega' = 4.449$, the frequencies differ by more than 50%. After reentry is introduced, the peak amplitudes occur at $\omega = 6.903$ for the group G , and $\omega' = 4.602$ for G' , so that $\frac{\omega}{\omega'} = \frac{3}{2}$. The generation of subharmonics, (notice that a subharmonic at $\omega_{sub} = 2.3$ circulates in both the groups), seems to underlie this process. The cross correlation is reduced due to the complex spectrum with nonoverlapping frequency spectra. We may

t'_d	$\omega (\Omega')$ (num.)	$\omega (\Omega')$ (theory)	$\theta'_e(\text{theory})$
0.10	6.44 (7.82)	7.11 (9.18)	0.00
0.15	6.29 (6.90)	6.88 (8.00)	0.09
0.20	6.14 (6.14)	6.51 (7.04)	0.26
0.25	5.98 (5.68)	6.15 (6.28)	0.44
0.30	5.98 (5.22)	5.81 (5.67)	0.65

Table 4.5.6: The phase difference, θ'_e , between the excitatory components of the groups increases as mismatch between the frequencies increases. Here the inhibitory signal decays slower than the excitatory signal ($T_e = 0.1$, $T_i = 0.2$). Note that in comparison to the case of $T_e = T_i$, (Table 4.5.3), the phase differences are smaller. The frequency of the synchronized oscillation, ω , decreases as the intrinsic frequency Ω' (shown in brackets), is selectively reduced by increasing the inhibition delay t'_d in group G' . $\Omega = 7.82$ is constant, corresponding to inhibitory delay $t_d = 0.1$.

note that for the same values of the delay in inhibitory feedback, t_d and t'_d , the intrinsic frequencies of oscillation of the two groups differ progressively less as the inhibitory decay time T_i is increased. Hence slowly decaying inhibition gives the oscillation a certain robustness as far as establishing coherency is concerned because typically 1 : 1 phase locking takes place; moreover, the phase differences are smaller as well. However, this observation is not valid if the intrinsic oscillations in the groups contain strong harmonics.

To summarize, the phase difference between the excitatory components of the groups G and G' is exactly zero only when the frequencies of oscillation of the two groups are identical and there is symmetry in the coupling and time delays of the reentrant signals. However, the phase difference can be arbitrarily small when the frequencies of the two groups are close. If the inhibitory signals are slowly decaying, the frequency differences can be small for a wide range of parameters (for example, the inhibitory signal delay, the reentrant signal delay, or the connection strengths). The phase difference between the groups (1) increases with the frequency mismatch, and (2) depends

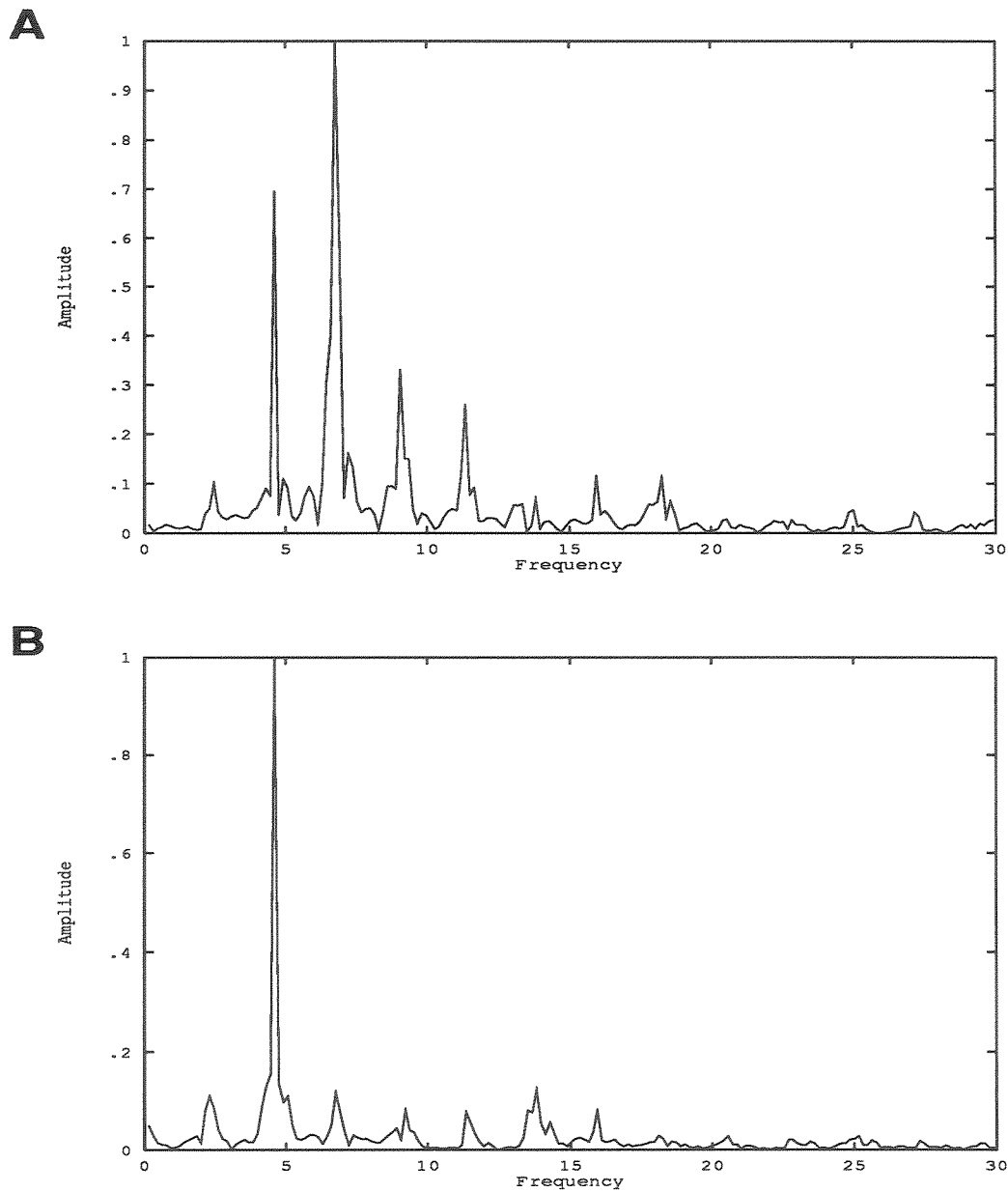


Figure 4.5.5: Circulating subharmonics establish partial synchrony when the intrinsic frequencies of the groups differ by over 50%. In this case the inhibitory signal decays slower than the excitatory signal ($T_e = 0.1$, $T_i = 0.2$). The intrinsic frequencies of the groups are $\Omega = 7.823$ ($t_d = 0.1$), and $\Omega' = 4.449$, ($t'_d = 0.4$). (A) The frequency spectrum shows that the group with the larger intrinsic frequency has a dominant frequency at $\omega = 6.903$, and (B) the group G' has a frequency spectrum with the dominant frequency at $\omega' = 4.602$ so that $\frac{\omega}{\omega'} = \frac{3}{2}$. In this example, $C = 6$.

on the reentry delay in a complicated way: it increases with increasing reentry, loses phase coherence, and then jumps by almost 150° . The frequency decreases with the introduction of reentry for small reentry delay times, and the decrease is proportional to the mean reentrant synaptic strength. However, as the delay in the reentrant signal is increased and the reentrant signal arrives out of phase with the inhibitory signal, the frequency can jump abruptly to a higher value. At the transition region, phase coherence is lost and the cross correlation between the activities of the groups can decrease by up to at least 50%. When the frequencies of the groups differ by more than 50%, partial synchrony is established by subharmonic resonance.

4.6 Other Models

We briefly consider some hypothetical models describing the collective behavior of interacting groups of neurons in order to elucidate the critical nonlinear ingredients for synchronization. The first model we consider has a multiplicative type of nonlinearity, wherein the inhibition shunts the excitatory activity in both the excitatory and inhibitory subpopulations:

$$T_e \dot{f}_e(t) = -f_e(t) + (1 - \int_{t-r_e}^t f_e(t') dt') * \sigma_{ee}(C f_e(t) + C'_r f'_e(t - t'_r) + P) \\ * (1 - \sigma_{ie}(C f_i(t - t_d) + Q)) \quad (4.6.1)$$

$$T_i \dot{f}_i(t) = -f_i(t) + (1 - \int_{t-r_i}^t f_i(t') dt') * \sigma_{ei}(C f_e(t) + C'_r f'_e(t - t'_r) + P) \\ * (1 - \sigma_{ii}(C f_i(t - t_d) + Q)) \quad (4.6.2)$$

with similar equations for the group G' . The terms $(1 - \sigma_{ie})$ and $(1 - \sigma_{ii})$, where σ_{ie} and σ_{ii} are the standard sigmoids, model shunting inhibition. Stable oscillations are observed in each group but there is no synchronization of activity when reentry is introduced. This suggests that nonlinear summation of

the excitatory and inhibitory components, lacking in the above model, may be essential for synchronization. Such a mechanism would be consistent with the fact that cells sum up input in a nonlinear manner. The Wilson-Cowan model is precisely of this type and, as we have noted, replaces the nonlinear summation of excitatory and inhibitory voltages by the renormalized population variables for the fraction of excitatory and inhibitory neurons firing per unit time, $f_e(t)$ and $f_i(t)$. A simple modification of Eqn. 4.6.2 so that the inhibitory subpopulation provides the locus for the nonlinear summation of the excitatory and inhibitory components:

$$T_i \dot{f}_i(t) = -f_i(t) + (1 - \int_{t-r_i}^t f_i(t') dt') * \\ * \sigma_{ii}(C f_e(t) + C'_r f'_e(t - t'_r) - C f_i(t - t_d) + Q) \quad (4.6.3)$$

is sufficient to synchronize the activity of the two neuronal groups.

The locus of nonlinear summation of the excitatory and inhibitory components in the subpopulations may be the inhibitory interneurons for the following reasons, (1) the slow graded nature of the postsynaptic potential of these neurons could enable the integration of the delayed reentrant signals, and (2) most inhibitory interneurons, but only a small fraction of the excitatory neurons, participate in the rhythmic population oscillations at a given time (Traub et al., 1989).

4.7 Discussion

Reentrant signaling induces phase locking between neuronal groups with small intrinsic frequency mismatch. In this case, the frequency spectra of the activity of the groups shows complete overlap reflecting the increase in the cross-correlation between the activities of the groups. When the intrinsic

frequencies of the groups differ by over 50%, however, partial synchrony is established by circulating sub-harmonics.

The synchronization is input driven because of the strongly dissipative nature of the activity in an unexcited group (or one excited subthreshold). In the model considered, refractoriness in the excitatory neurons, which suppresses the number of excitatory neurons firing per unit time is critical for generating oscillations when reentry is introduced. The number of excitatory neurons firing per unit time scales inversely with the refractoriness. In the presence of several interacting signals, refractoriness provides dynamic stability.

Nonlinear summation of excitatory and inhibitory signals, mediated by the reciprocal connections, is critical for establishing synchrony between groups. The locus of such interaction may be the inhibitory interneurons whose firing is much better correlated with the population activity than that of excitatory neurons (Traub et al., 1989). One-way signaling can also induce synchronization but such a scheme suffers from two deficiencies: (1) the phase difference between the excitatory components of the groups is much greater than when reentrant signaling is present, and (2) the mismatch in the intrinsic frequencies of the groups is restricted to about 10%. In general, as one may expect, synchronization is more robust with reentrant signaling. However, one-way signaling may help either to establish coherency when reciprocal connections are not possible, or reciprocal connectivity exists and the (weaker) pathway is strengthened by the coherency established by the (stronger) pathway, thus suggesting developmental implications.

Synchronization is achieved by dynamically adjusting the amplitudes and phases of the various excitatory and inhibitory components as well as the frequency of the coherent oscillation. The (relative) phase of the interacting

signals has two components, one usually referred to as the ‘phase difference’, for example, θ'_e above due to synaptic coupling, or θ_i due to the mismatch in the excitatory and inhibitory decay times, and the other explicitly due to delay in activation of the signal, for example $\omega t'_e$ above. These phases are important in determining the frequency of the oscillation. The phase difference between the excitatory components of the groups, θ'_e is strictly zero only when there is a certain symmetry: if the frequencies of oscillation are exactly the same and the coupling is symmetric both in strength and delay. Arbitrarily small phase differences are possible as the intrinsic frequencies of the groups approach each other, i.e., $\Omega \rightarrow \Omega'$. For small reentry delays, the phase difference between groups increases with increasing mismatch in the intrinsic frequencies of the groups. Reentrant signaling reduces the frequency of oscillation when the reentry delay is small compared to the delay in the inhibition, typically by about 10%, in agreement with the detailed computer simulations of (Sporns et al., 1989). This decrease is proportional to $\frac{C_r}{C}$, the ratio of the mean intergroup to intragroup synaptic strength.

However, as the reentry delay increases, the reentrant signal arrives out of phase with the inhibitory signal, and the frequency and phase difference between the activity of the two groups undergo a jump bifurcation– the phase changes abruptly by about 180° , and the frequency of the synchronized oscillation increases (by as much as 40%). At the transition region, phase coherence is lost thereby reducing the cross correlation. We may term this desynchronization. An extreme example of this process is the desynchronization of the oscillations of two groups of neurons with identical intrinsic frequencies when the reentry delay times are asymmetric.

Desynchronization of oscillatory responses in the present case does not

require synaptic modification as in (von der Malsburg and Schneider, 1986), nor is it the result of decreased or residual interaction. Desynchronization is a consequence of signals not arriving with the proper phase relationships. A simple mechanism to achieve this, as we have noted, is by delayed reentrant signaling. The role of delays in desynchronizing oscillatory responses has been noted in a recent computer simulation (Schillen and Konig, 1990).

The jump bifurcation delineates two delay related time windows: (1) in which correlated activity can take place and (2) in which the oscillations are decorrelated. These time windows share some of the characteristics of the atemporal or neutral time windows discussed in the context of transduction of signals by Poppel et al. (1990).

The synchronization, desynchronization, and resynchronization of the oscillations represents a correlation dependent non-Boolean switching mechanism. Such a switching mechanism differs from the on-off response and the idea of a 'set cell' (Evarts et al., 1984), digital switches (McCulloch and Pitts, 1943) and analog computations (Koch and Poggio, 1987).

We predict that similar results will be found for the more realistic cases of time courses of the signals such as the alpha form ($te^{-t/\tau}$). By varying the time courses of the signals using neurotransmitters (Marder et al., 1987) it is possible to dynamically control the spatiotemporal correlations even as the groups signal to each other. This is a specific example of what might be termed neurotransmitter logic (Finkel and Edelman, 1987). Such a logic differs fundamentally from Boolean logic wherein the specific time courses of signals are not relevant: as long as inputs arrive within a narrow time window, a logical operation is performed.

The phase of a signal arriving from a neuronal group depends on

the time delay, the synaptic coupling, and frequency of the ongoing oscillation. The interaction of signals with different phases in turn influences the characteristics of the ongoing oscillations. The frequency of the underlying activity itself is a signature of the global activity of (possibly) several groups acting coherently. In addition, signals can selectively influence the oscillations and the cross-correlation between the activity of neuronal groups. Moreover, depending on the phases of the interacting signals, the oscillatory activity of the groups can be either synchronized or desynchronized. The mechanisms of synchronization, desynchronization, and phasic signaling discussed above provide dynamic linkage between coactive neuronal groups thereby enabling the distributed neural system to operate in a highly parallel manner.

Chapter 5

Topological Effects

5.1 Introduction

The dynamical sampling of the environment leads to the activation of certain localized populations (neuronal groups) at a given time. Following further sampling, still other groups of neurons are likely to be recruited with a fraction of the previously active groups still active. In higher animals these interactions are further compounded by the presence of preparatory sets which involve endogenously activated neuronal groups (Evarts et al., 1984; Edelman, 1987). Thus, the set of neuronal groups that are active is continually changing and forms a global mapping that is dynamic (Edelman, 1989).

A particular subset of the global mapping is an n -tuple: n neuronal groups coupled in varied topologies (Edelman, 1989). In order to gain insight into some aspects of signaling between neuronal groups forming a global mapping, we consider the triadic interaction of neuronal groups. This problem is important to study because signals are constantly being mapped between primary, secondary and association areas in the brain. Several examples of such interaction may be given: mapping through intermediate areas linking the prefrontal cortex and the motor cortex (Fuster, 1986), various visual areas (Zeki and Shepp, 1988), the cortex-hippocampus-cortex loop and the basal ganglia-cortex-thalamus loop (Alexander et al., 1986). Such interactions may involve complete closure in circulating the signals as in the triangular or a partial

closure as in the series interaction.

In the previous chapter we noted the role of coherent oscillations in signaling in a distributed system and the emergent features thereof. The present study seeks to extend and generalize some of the results obtained with the diadic interaction. We will be mainly concerned with the asymptotic behavior of three interacting neuronal groups which we will attempt to generalize to more global mappings. The discussion here is mainly concerned with the effects of nonlinearly interacting signals, i.e. the nonlinear summation of signals giving rise to overall integration. It is also the simplest mapping in which the effect of topology can be studied. Although the details of the connectivities between and within the groups are relevant, it is believed that the distinction between gross mapping topologies (triangular vs. series) is the more important. Significant differences are found between these mapping topologies as a result of differences between the open and closed circulation of signals.

A study of the triadic interaction gives clues as to what might happen in more complex settings (e.g. the interaction of several neuronal groups). In particular, an important question that must be answered is whether the effect of additionally recruited groups is not merely to modulate the diadic oscillatory activity but to substantially alter the characteristics of the oscillations.

The setting for studying the triadic interaction may be viewed in two ways: (1) a study of three interacting groups in its own right and (2) a study of the dynamic changes caused by third group on the dyadic interaction of the neuronal groups. The main dynamical interaction can then be understood in terms of the nonlinear interaction of signals with different phases. In particular, the delay involved in mapping the activity from one region to another contributes significantly to the phase. The main problem here is to investigate

the role of time delays in dynamically correlating and decorrelating the oscillatory activity of neuronal groups and to ask whether the phenomena observed in the diadic interaction extend to more general cases and how these changes reflect global mapping.

The outline of this Chapter is as follows: in Section 5.2, a mathematical model is described to investigate the interaction of coherent excitatory and inhibitory signals from three groups. In Section 5.3, (an approximate) nonlinear theory is described along with results from numerical experiments in order to ascertain the important phenomena that can accrue from the aforementioned triadic interaction. Section 5.4 summarizes and concludes the discussion with a generalization to possible global temporal effects in neural systems.

5.2 Mathematical Model

We will be concerned with the interaction of excitatory and inhibitory signals generated by the coherent oscillations in three neuronal groups; the oscillatory signals being generated by the interaction of excitatory and inhibitory neurons within a neuronal group. To study the dynamics of the aggregate, in the mathematical model the nonlinear summation of excitatory and inhibitory voltages is renormalized to represent the nonlinear summation of coherent excitatory and inhibitory signals from and within the three neuronal groups. For the study of certain critical aspects of the nonlinear interaction of coherent signals, the model is an adequate one. Each neuronal group is represented by two population variables $f_e(t)$ and $f_i(t)$, the fraction of excitatory and inhibitory neurons firing per unit time. Because (1) the neurons in a group are tightly coupled and localized and (2) single cells may fire asynchronously while the population firing is collectively synchronized (Traub et al., 1989; Sporns

et al., 1989), these variables are used in describing the aggregate dynamics. The model is a straightforward extension of the models developed in Chapters 3 and 4.

Fig. 5.2.1 is a schematic illustration of the inter- and intragroup connectivity between three neuronal groups G_0 , G_1 , and G_2 , where E and I represent the excitatory and inhibitory subpopulations of G , E' and I' , and E'' and I'' the corresponding subpopulations of G' . (*Notation:* Throughout this Chapter, the unprimed variables refer to G , the primed ones to G' and the double primed ones to G''). Following Wilson and Cowan (1972), the fraction of excitatory and inhibitory cells firing per unit time, $f_e(t)$, and $f_i(t)$ for the group G_0 , $f'_e(t)$, and $f'_i(t)$, for the group G_1 , and $f''_e(t)$, and $f''_i(t)$, for the group G_2 at time t are given by the following time coarse-grained and spatially averaged nonlinear differential equations,

$$T_e \dot{f}_e(t) = -f_e(t) + (1 - \int_{t-r_e}^t f_e(t') dt') \sigma_e(x_e) \quad (5.2.1)$$

$$T_i \dot{f}_i(t) = -f_i(t) + (1 - \int_{t-r_i}^t f_i(t') dt') \sigma_i(x_i) \quad (5.2.2)$$

$$T'_e \dot{f}'_e(t) = -f'_e(t) + (1 - \int_{t-r'_e}^t f'_e(t') dt') \sigma_e(x'_e) \quad (5.2.3)$$

$$T'_i \dot{f}'_i(t) = -f'_i(t) + (1 - \int_{t-r'_i}^t f'_i(t') dt') \sigma_i(x'_i) \quad (5.2.4)$$

$$T''_e \dot{f}''_e(t) = -f''_e(t) + (1 - \int_{t-r''_e}^t f''_e(t') dt') \sigma_e(x''_e) \quad (5.2.5)$$

$$T''_i \dot{f}''_i(t) = -f''_i(t) + (1 - \int_{t-r''_i}^t f''_i(t') dt') \sigma_i(x''_i) \quad (5.2.6)$$

$$x_e(t) = C_1 f_e(t) + C_r f'_e(t - t_r) + C''_r f''_e(t - t''_r) - C_2 f_i(t - t_d) + P$$

$$x_i(t) = C_3 f_e(t) + C_r f'_e(t - t_r) + C''_r f''_e(t - t''_r) - C_4 f_i(t - t_d) + Q$$

$$x'_e(t) = C'_1 f'_e(t) + C_r f_e(t - t_r) + C'_r f''_e(t - t''_r) - C'_2 f'_i(t - t'_d) + P'$$

$$x'_i(t) = C'_3 f'_e(t) + C_r f_e(t - t_r) + C'_r f''_e(t - t''_r) - C'_4 f'_i(t - t'_d) + Q'$$

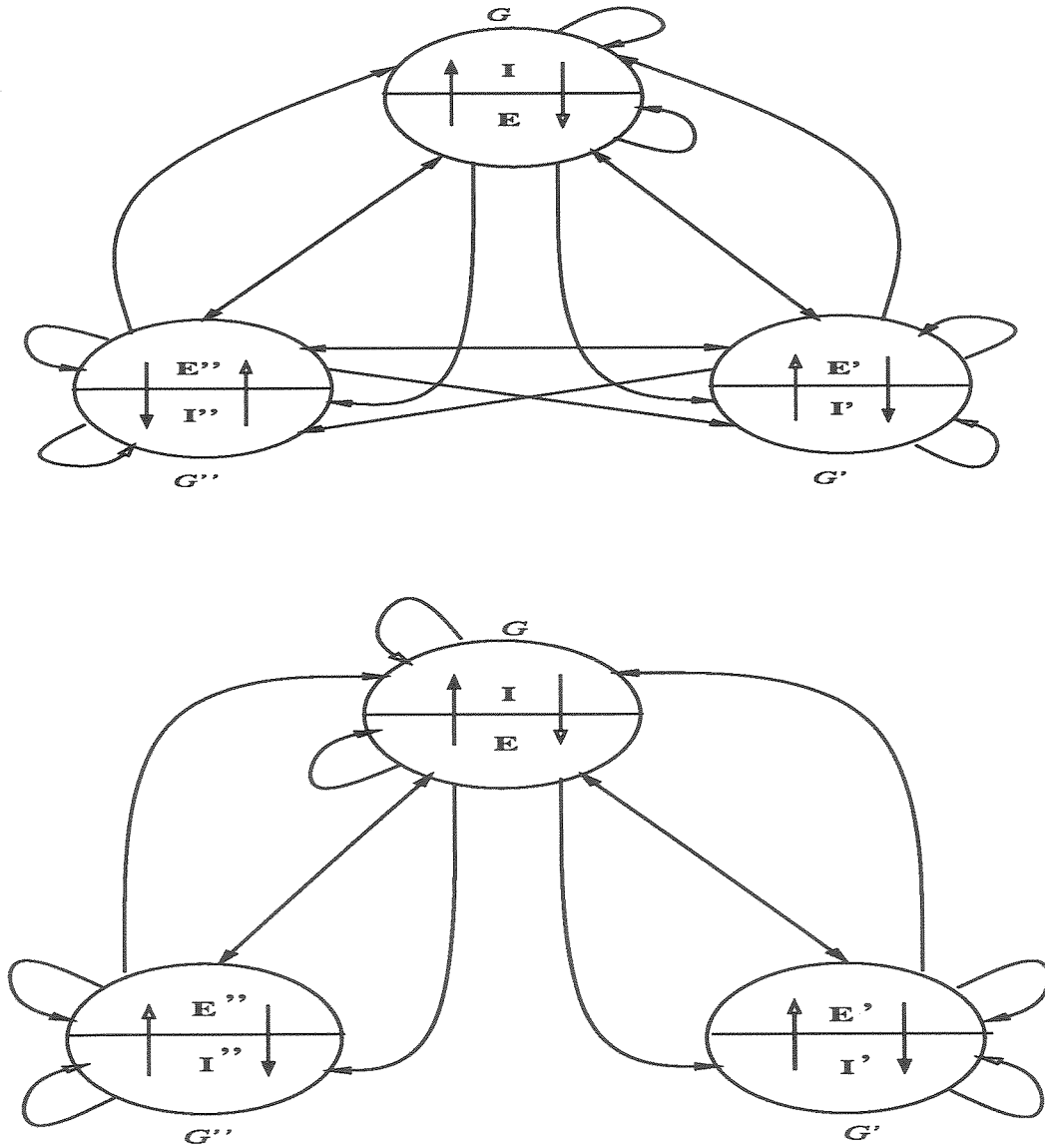


Figure 5.2.1: Two distinct topologies of triadic neuronal group interactions. (A) Triangular 'closed loop' and (B) Series 'open loop' interaction of neuronal groups G , G' , and G'' . In each group E and I represent the excitatory and inhibitory subpopulations. The excitatory connections are indicated with filled arrows and the inhibitory ones with unfilled arrows. The inter-group signaling is entirely excitatory.

$$\begin{aligned}
x_e''(t) &= C_1'' f_e''(t) + C_r'' f_e(t - t_r'') + C_r' f_e'(t - t_r') - C_2'' f_i'(t - t_d'') + P'' \\
x_i''(t) &= C_3'' f_e''(t) + C_r'' f_e(t - t_r'') + C_r' f_e'(t - t_r') - C_4'' f_i'(t - t_d'') + Q''
\end{aligned}$$

where x_e , x_i , x_e' , x_i' , and x_e'' , x_i'' are the activities and $\sigma_e(x_e)$, $\sigma_i(x_i)$, $\sigma_e(x_e')$, $\sigma_i(x_i')$, $\sigma_e(x_e'')$, and $\sigma_i(x_i'')$ are the responses (outputs) of the respective subpopulations. The sigmoids have the standard form,

$$\sigma(x) = \frac{1}{1 + \exp(-\beta(x - \chi))}$$

where β and χ are respectively the sigmoid nonlinearity and threshold and represents nonlinear saturation of the net activation of the respective subpopulation. Consider, for example, the equation for the fraction of excitatory cells firing per unit time, $f_e(t)$ (Eqn. 5.2.1) for the subpopulation represented by E . The time scale of decay of activity in the absence of external excitation is T_e , and r_e is the absolute refractory period of the excitatory cells. The change in the fraction of cells firing depends on (1) the decay in activity and (2) the fraction of cells that are not refractory and are active. The fraction of cells that are not refractory at time t is $(1 - \int_{t-r_e}^t f(t') dt')$ and the fraction of cells that are active is given by the sigmoid σ_e as a function of the average activity of the cells, $x_e(t)$. C_1 , C_2 , C_r and C_r'' are the mean synaptic strengths mediating the E to E , I to E , E' to E , and E'' to E subpopulation interactions respectively, and P is the (constant) external input. The inhibitory signal arrives with a delay, t_d , and the reentrant signal with a delay, t_r' . The delay could be due to either delay in chemical activation or delay in transmission, or both, as discussed above. A nonzero intragroup inhibitory delay t_d , t_d' , and t_d'' are essential to the present study because in the absence of such a delay, strong feedback coupling is required (Wilson and Cowan, 1972). Strong feedback coupling causes generation of strong harmonics which makes the theoretical analysis extremely

difficult. Inhibition delays, expressed, for example by $GABA_A$ and $GABA_B$, provide a large dynamic range for the oscillations (Traub et al., 1989). Any delay in the recurrent excitation within the neuronal group has been ignored as small compared to the delay in the inhibitory and reentrant signals. Consistent with the theory of neuronal group selection (Edelman, 1987), we assume that the mean intragroup synaptic strength is greater than the intergroup synaptic strength, i.e., $C > C_r$. Refractoriness in the inhibitory neurons is neglected, and is not critical for the phenomena we wish to study. Similar considerations hold for each of the other subpopulations.

For the mathematical analysis of Eqns. 5.2.1 - 5.2.8, it is necessary to approximate the sigmoid with a piecewise linear function as in Chapter 3:

$$\sigma(x) = \begin{array}{ll} 1.0 & x > \chi + \delta \\ 0.0 & x < \chi - \delta \\ m(x - \chi) + 0.5 & |x - \chi| < \delta \end{array} \quad (5.2.7)$$

where $\chi + \delta$ is the saturation point, and m is the slope of the sigmoid with $\delta m = \frac{1}{2}$. The approximation preserves the nonlinear saturation characteristics of the original sigmoid.

Two final notes are in order pertaining to the following discussion:

Parameters: Except as noted, the following default parameters are used in quoting the results of the numerical studies of Eqns. 5.2.1 - 5.2.8, $T_e = T_i = T'_e = T'_i = T''_e = T''_i = 0.1$, $m_e = m_i = 0.5$, $\chi_e = \chi_i = 4.0$, $P = Q = P' = Q' = 4.0$, $r_e = r'_e = r''_e = 0.5$, $r_i = r'_i = r''_i = 0.0$, $C_1 = C_2 = C_3 = C_4 = C'_1 = C'_2 = C'_3 = C'_4 = C''_1 = C''_2 = C''_3 = C''_4 = C = 6.0$, $C_r = 2.0$, $C'_r = 2.0$, $C''_r = 2.0$.

Notation: The intrinsic frequencies of the two groups (without reentry) will be denoted by Ω , Ω' and Ω'' and the (common) synchronized frequency of the three groups by ω .

Although the model could be made even more general, the simplifications have been chosen to keep the model analytically tractable.

We distinguish between the triangular (Fig. 5.2.1a) and the series ($C'_r = 0$) interactions (Fig. 5.2.1b). It will be seen that the broken symmetry in the latter case leads to several distinct phenomena.

5.3 Analytic and Numerical Results

The mathematical model described in the previous section is studied both analytically and using numerical simulations. A nonlinear theory based on the averaging technique of Bogoliubov-Krylov-Mitropolsky (Bogoliubov and Mitropolsky, 1961; Gelb and Velde, 1967; Guckenheimer and Holmes, 1983) is particularly useful in understanding the relationships between the frequency, amplitude, and phase of the oscillations. These relations, though approximate, reproduce most of the behavior, aid in searching the solution space for bifurcations and provide insights into the nature of the triadic interaction. Besides, the relations provide a self-consistent method to evaluate the phase differences between the various intra- and inter-group excitatory and inhibitory components of the activities of the groups.

Neglecting the higher harmonics, solutions to Eqns. 5.2.1 – 5.2.6 may be approximated by

$$f_e(t) = \bar{f}_e + f_{e0} \sin(\omega t) \quad (5.3.1)$$

$$f_i(t) = \bar{f}_i + f_{i0} \sin(\omega t - \theta_i) \quad (5.3.2)$$

$$f'_e(t) = \bar{f}'_e + f'_{e0} \sin(\omega t - \theta'_e) \quad (5.3.3)$$

$$f'_i(t) = \bar{f}'_i + f'_{i0} \sin(\omega t - \theta'_e - \theta'_i) \quad (5.3.4)$$

$$f''_e(t) = \bar{f}''_e + f''_{e0} \sin(\omega t - \theta''_e) \quad (5.3.5)$$

$$f_i''(t) = \bar{f}_i'' + f_{i0}'' \sin(\omega t - \theta_e'' - \theta_i'') \quad (5.3.6)$$

where θ_i , θ_i' , and θ_i'' , are the phase differences (assumed to be constant) between the intra-group excitatory and inhibitory components f_e and f_i , f_e' and f_i' , f_e'' and f_i'' respectively; θ_e' and θ_e'' are the phase differences (assumed to be constant) between the intragroup components f_e and f_e' , and f_e and f_e'' respectively.

Assuming threshold excitation of each of the subpopulations ($P = \chi_e$ etc.) and identical excitatory and inhibitory decay rates $T_e = T_e' = T_e'' = T_i = T_i' = T_i'' = T$, it is easy to show that (1) $\theta_i = \theta_i' = \theta_i'' = 0$ because the input into the excitatory subpopulation is equal to the input into the inhibitory subpopulation and (2) $f_{e0} = f_{e0}' = f_{e0}''$, $f_{i0} = f_{i0}' = f_{i0}''$, $\bar{f}_e = \bar{f}_e' = \bar{f}_e''$, and $\bar{f}_i = \bar{f}_i' = \bar{f}_i''$. With these approximations, the frequency of the synchronized oscillation, ω , and the phase differences, θ_e' (between groups G and G') and θ_e'' (between groups G and G'') are given by,

$$\omega T = \frac{\frac{C_r}{C} \frac{f_{e0}}{f_{i0}} \sin(\theta_e' + \omega t_r) + \frac{C_r''}{C} \frac{f_{e0}}{f_{i0}} \sin(\theta_e'' + \omega t_r'') - \sin(\omega t_d)}{\frac{f_{e0}}{f_{i0}} + \frac{C_r}{C} \frac{f_{e0}}{f_{i0}} \cos(\theta_e' + \omega t_r) + \frac{C_r''}{C} \frac{f_{e0}}{f_{i0}} \cos(\theta_e'' + \omega t_r'') - \cos(\omega t_d)} \quad (5.3.7)$$

$$\frac{\omega T - \tan(\theta_e')}{1 + \omega T \tan(\theta_e')} = \frac{\frac{f_{e0}}{f_{i0}} \sin(\theta_e') + \frac{C_r}{C} \frac{f_{e0}}{f_{i0}} \sin(\omega t_r) + \frac{C_r'}{C} \frac{f_{e0}}{f_{i0}} \sin(\theta_e'' + \omega t_r') - \sin(\theta_e' + \omega t_d')}{\frac{f_{e0}}{f_{i0}} \cos(\theta_e') + \frac{C_r}{C} \frac{f_{e0}}{f_{i0}} \cos(\omega t_r) + \frac{C_r'}{C} \frac{f_{e0}}{f_{i0}} \cos(\theta_e'' + \omega t_r') - \cos(\theta_e' + \omega t_d')} \quad (5.3.8)$$

$$\frac{\omega T - \tan(\theta_e'')}{1 + \omega T \tan(\theta_e'')} = \frac{\frac{f_{e0}}{f_{i0}} \sin(\theta_e'') + \frac{C_r''}{C} \frac{f_{e0}}{f_{i0}} \sin(\omega t_r'') + \frac{C_r'}{C} \frac{f_{e0}}{f_{i0}} \sin(\theta_e' + \omega t_r') - \sin(\theta_e'' + \omega t_d'')}{\frac{f_{e0}}{f_{i0}} \cos(\theta_e'') + \frac{C_r''}{C} \frac{f_{e0}}{f_{i0}} \cos(\omega t_r'') + \frac{C_r'}{C} \frac{f_{e0}}{f_{i0}} \cos(\theta_e' + \omega t_r') - \cos(\theta_e'' + \omega t_d'')} \quad (5.3.9)$$

Using the approximation $\bar{f}_e \sim f_{e0}$, the ratio of the excitatory to the inhibitory

cells firing per unit time is given by

$$\frac{f_{e0}}{f_{i0}} \sim \frac{1}{1 + \frac{2r_e}{\pi\sqrt{1+\omega^2 T^2}}} \quad (5.3.10)$$

The derivation follows closely the calculations in Chapters 3 and 4 and therefore are not repeated here. The above, somewhat general results, will be simplified as special cases are considered. It may however be noted that (1) the relative effect of each reentrant signal is weighted by (a) ratio of the intergroup to intragroup connection strength and (b) the ratio of the excitatory to inhibitory neurons firing per unit time, (2) the relative phases of the signals depends on the asymmetries as well as the time delays.

The triadic interaction was studied in its two variant forms: the triangular interaction with $C_r = C'_r = C''_r$ and the series interaction with $C_r = C'_r$ and $C''_r = 0$. The two cases are compared and contrasted to study differences in mapping topology. For a wide range of parameters, the oscillatory activity of the groups with disparate frequencies is synchronized just as for the diadic interaction. We will be mostly concerned with the behavior of the system in terms of the effect of G'' on the oscillatory activity of groups GG' .

5.3.1 Triangular Reentry

First consider the case of triangular interaction of groups with identical intrinsic frequencies. In the present study, this is achieved by setting the (intragroup) inhibitory delays to be identical, $t_d = t'_d = t''_d$.

Effect of introducing reentry With the introduction of reentrant signaling between the three groups, the frequency of oscillation decreases when the reentry delays are small. The drop is even greater than the one for the

diadic interaction. This result may be proven for the simpler case of the zero reentry delays and identical frequencies of the groups. From Eqns. 5.3.7 - 5.3.10, the (common) frequency of the three groups then simplifies to

$$\omega T = \frac{\sin(\omega t_d)}{(1 + 2\frac{C_r}{C})\frac{f_{e0}}{f_{i0}} - \cos(\omega t_d)} \quad (5.3.11)$$

Let $x = (1 + 2\frac{C_r}{C})\frac{f_{e0}}{f_{i0}}$. Assume that the frequency of oscillation increases as $\frac{C_r}{C}$ increases. Then in Eqn. 5.3.10, $\frac{f_{e0}}{f_{i0}}$ increases so that $x = \frac{f_{e0}}{f_{i0}}(1 + 2\frac{C_r}{C})$ increases. This contradicts Theorem 3.7.1. Hence, the frequency of oscillation, ω , decreases when reentry is introduced and, furthermore, ω decreases monotonically with increasing $\frac{C_r}{C}$ (Table 5.3.1). Moreover, the factor of 2 in the expression for x implies that the decrease is greater than the one for diadic interaction under the same conditions (see also Section 4.5).

The reason for the drop in the frequency is that when the reentry delays are small, and the phase differences θ'_e and θ''_e are small, the reentrant excitatory signals arrive in phase with the excitatory signal within the group thereby prolonging the excitatory activity within the group. Hence, the decrease in frequency is proportional to the strength and the number (two, in the present case) of the excitatory reentrant signals (modulated by the connection strengths).

Effect of reentry delays If the reentry delay is increased, the reentrant excitatory signals can arrive out of phase with the delayed inhibitory signal resulting in a large jump in the frequency. In this case, the frequency is given by

$$\omega T = -\frac{2\frac{C_r}{C}\frac{f_{e0}}{f_{i0}}\sin(\omega t_r) - \sin(\omega t_d)}{\frac{f_{e0}}{f_{i0}} + 2\frac{C_r}{C}\frac{f_{e0}}{f_{i0}}\cos(\omega t_r) - \cos(\omega t_d)} \quad (5.3.12)$$

C_r	ω (num.)	ω (theory)
0.0	8.13	9.12
0.5	7.82	8.76
1.0	7.21	8.41
1.5	6.60	8.05
2.0	5.98	7.69

Table 5.3.1: Reentrant signaling reduces the frequency of the synchronized oscillation; the decrease is proportional to the sum of the reentrant excitatory connection strengths. In this example, the intrinsic frequencies are identical, $\Omega = \Omega' = \Omega'' = 8.13$, corresponding to inhibitory intra-group delays, $t_d = t'_d = t''_d = 0.2$; the reentrant signals have no delay, $t_r = t'_r = t''_r = 0$; and $C_r = C'_r = C''_r$.

The factor of 2 implies that the effect of the reentrant signal is identical to that in the diadic interaction with twice the connection strength. A comparison of the diadic and triadic interactions shows that the jump in the frequency is larger for the triadic interaction, as predicted theoretically (Table 5.3.2). The large jump for the triadic interaction is due to the greater suppression of the frequency when the signals arrive in phase, as noted above. Due to the symmetry of connectivities, connection strengths, and delays, the phase differences between the groups are identically zero and so there is loss of phase coherence of the synchronized oscillatory activity.

Effect of reentry delay mismatch Mismatch in the delay in signals arriving from G'' can result in a phase difference between G and G' . Furthermore, changing the reentrant signal delay between G'' and G can differentially alter the phase difference between G and G' . To consider a simple example, let $t_d = t'_d = t''_d$, so that the frequencies of the groups are identical, and $t_r = t'_r = 0.0$, so that the phase difference θ''_e between G and G'' is constrained to be zero, and $\theta'_e \neq 0$. As t''_r is increased, the phase difference θ'_e does not

t_r	ω (num.)	ω (theory)	ω (num.)	ω (theory)
0.00	5.98	7.69	7.21	8.41
0.005	5.98	7.08	7.21	8.37
0.10	5.68	6.66	7.06	7.98
0.15	5.52	6.48	7.06	8.04
0.20	5.52	6.72	7.21	8.33
0.25	5.68	8.31	8.90	8.93
0.30	5.52	10.73	8.44	9.65
0.35	10.58	11.17	9.82	10.09
0.40	10.43	10.93	9.82	10.15

Table 5.3.2: The frequency of synchronized oscillation first decreases with increasing reentry delay, t_r , and then increases as the excitatory reentrant signal arrives out of phase with the inhibitory signal; a comparison of the results for the cases of three and two groups. The intragroup inhibitory signal have delays $t_d = t'_d = t''_d = 0.2$, and the intrinsic frequencies of the group are identical, $\Omega = \Omega' = \Omega'' = 8.13$, and $\frac{C_r}{C} = \frac{2}{6}$.

vary much except when a jump bifurcation occurs when the frequency also changes substantially thereby causing a large jump in the phase. This result is in agreement with the observation (see Chapter 4) that asymmetries in general (see also the case of the series interaction below) give rise to phase differences. Moreover, the phase differences can reflect global mapping and delay effects.

The nonlinear nature of the relationship between frequency and phase also implies that, because of the jump bifurcation, small local changes in the parameters can cause large changes in the global characteristics of the oscillatory activity. The result also illustrates the possibility of differential amplification of phases and will be further elaborated below when groups with differing intrinsic frequencies are considered.

Effect on desynchronization: Reinforcement As noted in the introduction, when the reentry delay between two groups with differing intrinsic

frequencies is increased, the oscillatory response can be desynchronized before the jump bifurcation occurs. The size of the desynchronized region is proportional to the frequency mismatch between the groups. What is the effect of additional excitatory signals arriving from G'' ? Additional signals could cause resynchronization of the oscillatory activity, i.e. the phase coherence and cross-correlation between G and G' are restored. On the other hand, it is also possible that the correlated diadic oscillatory activity could be decorrelated. In view of the importance of such dynamic control in distributed neural systems, a discussion of such interactions is pursued in some detail.

Let $t_d = t''_d \neq t'_d$ and $t_r = t'_r$ and $t''_r = 0$. The intrinsic frequencies of groups G and G' , then, differ and the phase difference between these groups is nonzero $\theta'_e \neq 0$. By symmetry, $\theta''_e = 0$ and $\Omega'' = \Omega$. The frequency-amplitude-phase relations then simplify to

$$\omega T = -\frac{\frac{C_r}{C} \frac{f_{e0}}{f_{i0}} \sin(\theta'_e + \omega t_r) - \sin(\omega t_d)}{\frac{f_{e0}}{f_{i0}} (1 + \frac{C_r}{C}) + \frac{C_r}{C} \frac{f_{e0}}{f_{i0}} \cos(\theta'_e + \omega t_r) - \cos(\omega t_d)} \quad (5.3.13)$$

$$\frac{\omega T - \tan(\theta'_e)}{1 + \omega T \tan(\theta'_e)} = -\frac{\frac{f_{e0}}{f_{i0}} \sin(\theta'_e) + 2 \frac{C_r}{C} \frac{f_{e0}}{f_{i0}} \sin(\omega t_r) - \sin(\theta'_e + \omega t'_d)}{\frac{f_{e0}}{f_{i0}} \cos(\theta'_e) + 2 \frac{C_r}{C} \frac{f_{e0}}{f_{i0}} \cos(\omega t_r) - \cos(\theta'_e + \omega t'_d)} \quad (5.3.14)$$

An examination of the equations shows the reentry scaling factors, $(1 + \frac{C_r}{C})$ in Eqns. 5.3.13 and 5.3.14 and 2 in Eqn. 5.3.14, in comparison with the diadic interaction. Thus, G'' can dynamically control the phase of the oscillations of groups G and G' in a complex and highly nonlinear manner as already seen before. What is new in the present case is that not only is the point at which the jump bifurcation occurs altered by the interaction, but desynchronization is prevented. As an example, let $\Omega = 8.13$ ($t_d = 0.2$) and $\Omega = 7.21$ ($t'_d = 0.25$), then for $0.1 < t_r < 0.15$, the oscillatory activity of G and G' (sans G'') are decorrelated. With a secondary signal from G'' , as the reentry delay $t_r = t'_r$ is increased, although (by symmetry) $\theta''_e = 0$ is constant, the phase difference θ'_e

t_r	ω (num.)	ω (theory)	θ'_e (theory)
0.0	5.98	7.39	0.37
0.1	5.82	9.13	-2.40
0.15	8.13	9.26	-3.08
0.20	7.98	8.93	-3.03
0.25	7.67	8.55	-2.98
0.30	7.67	8.18	-2.93

Table 5.3.3: The frequency and phase undergo a jump bifurcation as the reentry delay is increased. The intrinsic frequencies of the groups G and G'' are different. Due to a reinforcing signal from G'' , the desynchronizing temporal window is eliminated in this example. Note also that the delay at which the jump occurs is smaller than the case in Table 5.3.2, where the intrinsic frequencies are exactly the same; the jump being smaller as well. The intrinsic frequencies are $\Omega = \Omega'' = 8.13$ and $\Omega' = 7.21$. The reentry delays are constrained $t_r = t'_r$ and $t''_r = 0$ so that the phase difference between the groups are $\theta''_e = 0$.

jumps by about 180° , along with the frequency at a delay of $t_r = 0.2$. (Table 5.3.3). In the present case, desynchronization is not observed.

‘Reinforcement’ from G'' effectively decreases the size of the desynchronized region and in the above example, actually eliminates it. The synchronization is particularly robust when the intrinsic frequency of G'' satisfies $\min(\Omega, \Omega') \leq \Omega'' \leq \max(\Omega, \Omega')$.

Thus, triangular mapping alters the size of the decorrelated region and suggests the general tendency of the completely connected n-couple to synchronize the activity in a stable manner by efficiently circulating the signals in a closed loop.

Dynamic Control of Cross-Correlation If the intrinsic frequency of G'' is such that the mean frequency mismatch between the groups is increased, the cross correlation between the groups G and G' can be dynamically con-

$t'_r = t''_r$	<i>Correlation</i>
0.00	0.78
0.10	0.75
0.15	0.59
0.20	0.50
0.25	0.21
0.30	0.63
0.35	0.71

Table 5.3.4: The relative correlation of groups G and G' can be controlled by phasic signaling from the group G'' in a robust manner when the introduction of the new group increases the mean frequency mismatch. The base line correlation is for the diadic interaction of G and G' with $t_r = 0$; the corresponding correlation when $t_r = 0.15$ (the delay in the present case as well) is 0.30. The intrinsic frequencies of the groups are $\Omega = 8.13$, $\Omega' = 7.21$, and $\Omega'' = 9.664$, corresponding to inhibitory delays $t_d = 0.2$, $t'_d = 0.25$, and $t''_d = 0.15$.

trolled by the signals originating from G'' . Consider the case where the oscillatory activity of the groups G and G' are decorrelated due to a non-zero reentry delay t_r . When the signals from G'' have zero delay, the signals arrive in phase with the excitatory signals within the groups and this provides a reinforcing effect. However, as the delay in these signals increases, the signals arrive out of phase, and the oscillations can be desynchronized. Following a jump bifurcation, the oscillations are resynchronized with a $\sim 180^\circ$ phase shift between the excitatory components of the groups G and G' and between G' and G'' , thereby resulting in phase-frustration where the phases between G'' and G shows a knotted structure. In the context of the present delay differential equations, the nature of the knotty structure is not understood. The main result of interest, however, is that the dyadic cross-correlation can be dynamically controlled with the delay in reentrant signaling from G'' for the reasons explained above (Table 5.3.4).

Differential amplification of phases A simpler example of the differential changes in phase has already been considered. In a more general setting, differential amplification of phases can occur. For example, suppose the reentry delay t_r'' between the groups G and G'' is increased, how is the phase difference between G and G' , θ'_e , affected? To consider an example, let the intrinsic frequencies of the groups be different (due to differing intra group inhibitory delays), and a delay mismatch with $t_r = t_r' = 0$ and variable t_r'' . In this case, the both the phases are nonzero:

$$\frac{\frac{C_r}{C} \frac{f_{e0}}{f_{i0}} \sin(\theta'_e) + \frac{C_r}{C} \frac{f_{e0}}{f_{i0}} \sin(\theta''_e + \omega t_r'') - \sin(\omega t_d)}{\frac{f_{e0}}{f_{i0}} + \frac{C_r}{C} \frac{f_{e0}}{f_{i0}} \cos(\theta'_e) + \frac{C_r}{C} \frac{f_{e0}}{f_{i0}} \cos(\theta''_e + \omega t_r'') - \cos(\omega t_d)}{\omega T} = - \quad (5.3.15)$$

$$\frac{\omega T - \tan(\theta'_e)}{1 + \omega T \tan(\theta'_e)} = - \frac{\frac{f_{e0}}{f_{i0}} \sin(\theta'_e) + \frac{C_r}{C} \frac{f_{e0}}{f_{i0}} \sin(\theta''_e)^\dagger - \sin(\theta'_e + \omega t'_d)}{\frac{f_{e0}}{f_{i0}} \cos(\theta'_e) + \frac{C_r}{C} \frac{f_{e0}}{f_{i0}} + \frac{C_r}{C} \frac{f_{e0}}{f_{i0}} \cos(\theta''_e) - \cos(\theta'_e + \omega t'_d)}{\omega T} = - \quad (5.3.16)$$

$$\frac{\frac{f_{e0}}{f_{i0}} \sin(\theta''_e)^\ddagger + \frac{C_r}{C} \frac{f_{e0}}{f_{i0}} \sin(\omega t_r'') + \frac{C_r}{C} \frac{f_{e0}}{f_{i0}} \sin(\theta'_e) - \sin(\theta''_e + \omega t''_d)}{\frac{f_{e0}}{f_{i0}} \cos(\theta''_e) + \frac{C_r}{C} \frac{f_{e0}}{f_{i0}} \cos(\omega t_r'') + \frac{C_r}{C} \frac{f_{e0}}{f_{i0}} \cos(\theta'_e) - \cos(\theta''_e + \omega t''_d)}{\omega T} = - \quad (5.3.17)$$

If the frequency does not change much, the effect of varying t_r'' on the phase θ'_e is a second order effect as may be seen by comparing the terms marked \dagger and \ddagger in the above equations (note that t_r'' does not occur in Eqn. 5.3.17). Therefore, the primary effect is on the phase θ''_e . However, when the jump bifurcation occurs, the phase difference θ'_e also increases (because of a large concomitant change in the frequency) while the phase difference θ''_e jumps by almost 180° . Similar results hold for the more general case: when, for example, the delay t_r is increased, it is primarily the phase difference θ'_e that is affected; however, when the jump bifurcation occurs, abrupt jumps in θ''_e occur.

In this manner, local changes can result in global changes due to the highly nonlinear nature of the interaction. Moreover, these changes show differential ordering in phase as the latencies of signals are varied.

Integration of disparate time scales When the frequencies of the groups differ by over 50%, partial synchrony is established by circulating subharmonics; the degree of synchronization is however small due to the presence of several complex non-overlapping subharmonics (see Chapter 4). The introduction of a third group with an intermediate frequency causes robust synchronization, by effectively minimizing the frequency mismatch. As an example, consider the case where the intrinsic frequencies of the groups are $\Omega = 12.58$, $\Omega' = 5.52$, and $\Omega'' = 7.21$. In the absence of signals from G'' , the cross correlation between G and G' is small (Fig. 5.3.1 A).

However, following the introduction of excitatory signals from G'' to G and G' the cross correlation between the groups G and G' as well as the cross correlation between the three groups increases substantially (Fig. 5.3.1). The origin of this phenomena can be understood by examining the overlap in the frequency spectra of the oscillatory activity of the groups (Fig. 5.3.2). By robustly circulating intermediate frequencies ($\omega = 5.98$), which are close to the intrinsic frequency of G'' , and its harmonics, the overlap in the frequency spectrum is considerably increased. In comparison to the diadic interaction, it may be noted that the complex subharmonics (see Fig. 4.5.2) have been quenched. There is a small differential effect in the cross-correlation $[GG''] \sim [GG'] \sim 0.7 < [G'G''] = 1.0$, (Fig. 5.3.1 B, C, and D). In the case of the series interaction, where the harmonics are not circulated as effectively, the cross-correlation can show significant differential effects, as will be shown below.

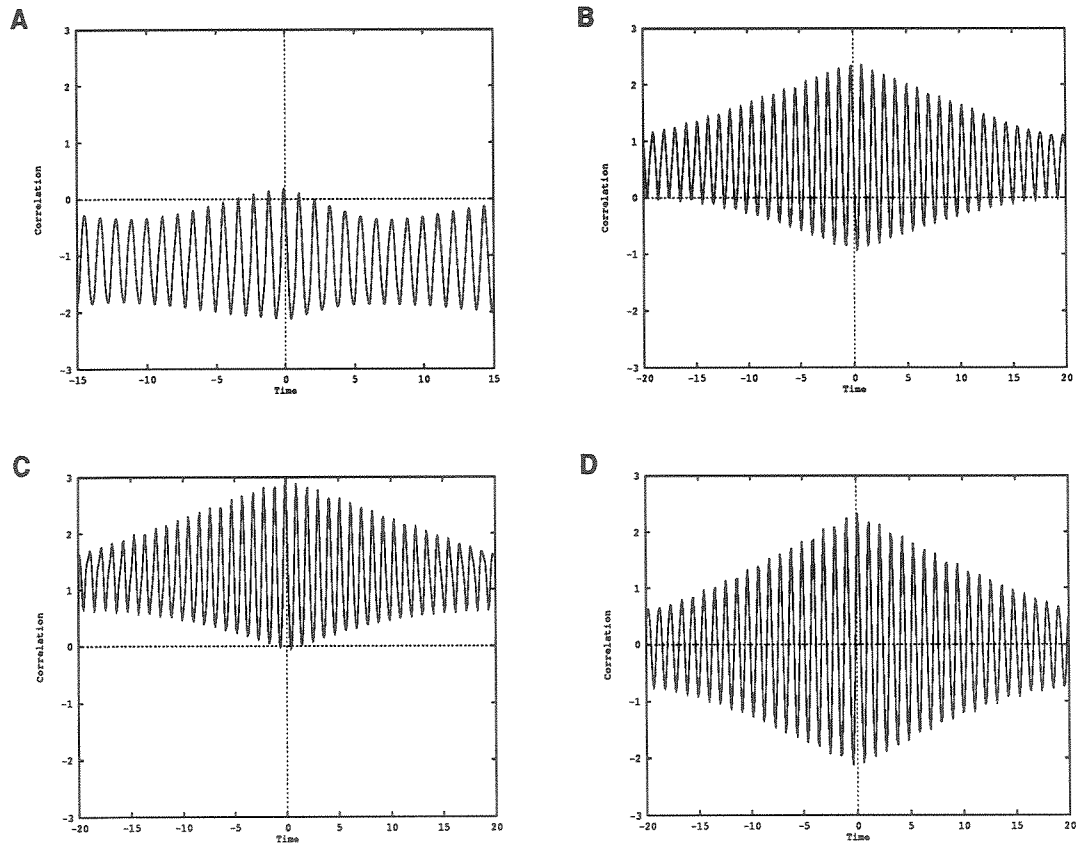


Figure 5.3.1: Triangular reentrant signaling increases the cross-correlation of diadic interactions when the intrinsic frequencies of the groups are disparate. The cross-correlations between the excitatory activities of groups (A) G and G' without signals from G'' , (B) G and G' , (C) G and G'' , and (D) groups G' and G'' . There is a small differential effect in the cross-correlation: $GG' \sim GG'' < G'G''$. The intrinsic frequencies of the groups are $\Omega = 12.58$, $\Omega' = 5.52$, and $\Omega'' = 7.21$.

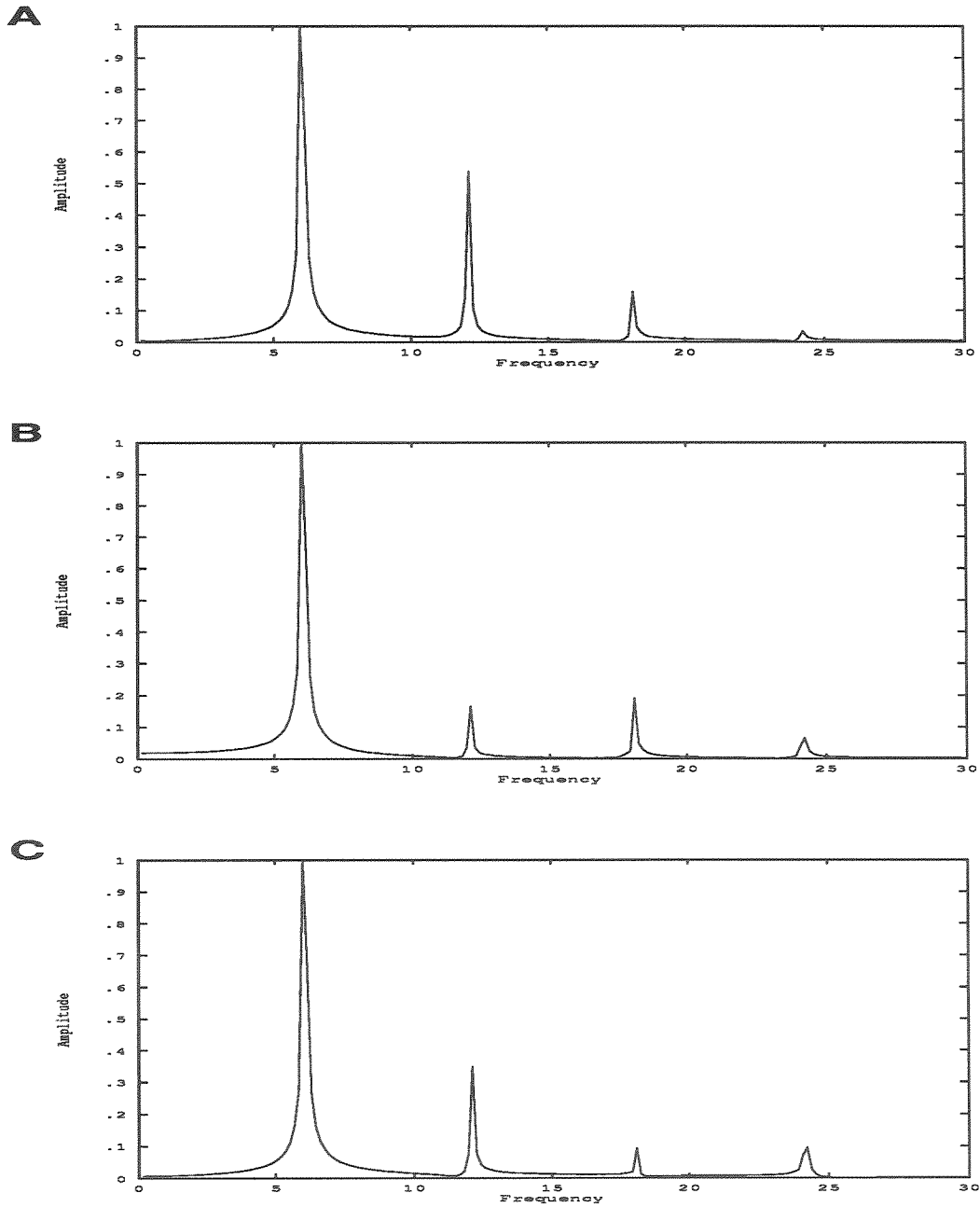


Figure 5.3.2: The frequency spectra for groups (A) G , (B) G' , and (C) G'' . The complex subharmonics, present in the diadic interaction of neuronal groups with widely disparate intrinsic frequencies, have been eliminated thereby resulting in the large cross-correlation indicated in Fig. 5.3.1. The pairwise overlap in the spectra indicates the degree of cross-correlation.

Thus, triangular interaction provides a robust way to integrate oscillatory activity over several time scales.

5.3.2 Series Reentry

Many of the differences between the series and triangular interactions arise from (1) the broken symmetry which can result in large phase differences θ'_e and θ''_e due to input mismatch even when the intrinsic frequencies of the groups are identical and (2) the inability to circulate signals as effectively.

Effect of introducing reentry As a simplification, let the intrinsic frequencies of the groups be identical with $t'_d = t''_d$ and $t_r = t''_r$. By symmetry, $\theta'_e = \theta''_e$. The frequency-amplitude-phase relations are given by

$$\omega T = -\frac{2\frac{C_r}{C}\frac{f_{e0}}{f_{i0}}\sin(\theta'_e + \omega t_r) - \sin(\omega t_d)}{\frac{f_{e0}}{f_{i0}} + 2\frac{C_r}{C}\frac{f_{e0}}{f_{i0}}\cos(\theta'_e + \omega t_r) - \cos(\omega t_d)} \quad (5.3.18)$$

$$\frac{\omega T - \tan(\theta'_e)}{1 + \omega T \tan(\theta'_e)} = -\frac{\frac{f_{e0}}{f_{i0}}\sin(\theta'_e) + \frac{C_r}{C}\frac{f_{e0}}{f_{i0}}\sin(\omega t_r) - \sin(\theta'_e + \omega t_d)}{\frac{f_{e0}}{f_{i0}}\cos(\theta'_e) + \frac{C_r}{C}\frac{f_{e0}}{f_{i0}}\cos(\omega t_r) - \cos(\theta'_e + \omega t_d)} \quad (5.3.19)$$

Input mismatch between G on one hand and G'' and G' on the other due to the asymmetry in the mapping topology results in nonzero phase differences between the groups as may be readily seen from Eqns. 5.3.18 and 5.3.19. As the reentry delay $t_r = t''_r$ is increased, although no desynchronization is observed, persistent transients are observed which cause a decrease in the cross-correlation between the groups. Note that this happens even though the frequencies of the groups are identical. From Table 5.3.5, comparing the results with the case of the triangular interaction, it may be noted that the jump in frequency is much smaller in the present case. This is because in the present case, at small delays reentry does not depress the frequency to the same extent as in the triangular interaction. The reentrant signals arrive with non-zero

t_r	ω (num.)	ω (theory)	θ_e (theory)
0.00	7.06	8.20	- 0.27
0.05	7.06	7.98	- 0.55
0.10	9.66	9.79	- 2.08
0.15	9.64	10.10	- 2.79
0.20	9.36	9.70	- 2.96
0.25	8.90	9.24	- 3.11
0.30	8.28	8.80	- 3.21

Table 5.3.5: In the case of the series interaction, the frequency and phase undergo a jump bifurcation at a lower value of the reentry delay, compared to the triangular interaction. As predicted theoretically, the jump in frequency is also smaller. Although the intrinsic frequencies are identical and other parameters symmetric, the asymmetry in mapping can result in a large phase difference as shown. The intrinsic frequencies of the groups are $\Omega = \Omega' = \Omega'' = 8.13$.

phase difference with respect to the intra-group excitatory signal; consequently, the jump bifurcation occurs at a lower value of the reentry delay in the present case.

Effect on synchronized and desynchronized activity Reentrant signals from G'' can decorrelate the oscillatory activity of G and G' in a robust manner even if G'' decreases the mean frequency mismatch between the groups. For example, as $\Omega'' \rightarrow \Omega$, i.e. the intrinsic frequency of the group G'' approaches that of G , desynchronization of the oscillations occurs resulting in a decrease of over 50% in the cross-correlation between the groups (Table 5.3.6). Similar results are obtained for $\Omega' < \Omega'' < \Omega$. For example, with $\Omega = 8.13$, $\Omega' =$, and $\Omega'' = 7.21$ ($t_d = 0.2$, $t'_d = 0.3$, and $t''_d = 0.25$) – for $0.15 < t''_r < 0.3$, the oscillatory activities of G and G' are uncorrelated.

If the oscillatory activity of the G and G' is desynchronized due to non-zero reentry delay t_r between them, signals from G'' reinforce the oscillations

t_r''	<i>Correlation</i>
0.00	0.79
0.05	0.67
0.10	0.56
0.15	0.58
0.20	0.36
0.25	0.81
0.30	0.74

Table 5.3.6: Signals from G'' can decorrelate diadic interactions in a robust manner. For $0.1 < t_r'' < 0.20$, phase coherence between G and G' is completely lost thereby resulting in a decrease of the cross-correlation by over 50%. Around $t_r'' = 0.25$, synchrony is restored following a jump bifurcation. The base line correlation is for the diadic interaction of G and G' with $t_r = 0$. The intrinsic frequencies of the groups are $\Omega = \Omega'' = 8.13$ and $\Omega' = 7.21$, corresponding to inhibitory delays $t_d = t_d'' = 0.2$ and $t_d' = 0.25$.

for small delay but desynchronize the oscillations. In the presence of delays, as has already been noted, the decorrelation is quite drastic (Table 5.3.7).

Thus, there exist broad time delays, for signals from G'' , in which the correlated activity of two neuronal groups can be desynchronized; the range of the time delay windows is even broader than the case of the diadic interaction. Numerical studies further indicate that this range of these time delays (for which the oscillatory activity is decorrelated) increases with (a) the frequency mismatch between G and G' and (b) the proximity of the frequency of G'' to that of G .

For the triangular interactions, it may be noted, under the same constraints, the oscillatory activity is approximately synchronized even as the jump bifurcation occurs.

There is, however, no selective entrainment, i.e., it is not the case that the oscillatory activity of G'' and G are correlated while that of G' and G are

t_r''	Correlation
0.00	0.78
0.10	0.53
0.15	0.63
0.20	0.31
0.25	0.34
0.30	0.37
0.35	0.58
0.40	0.61

Table 5.3.7: Signals from G'' can partially correlate diadic interactions for small delay and robustly decorrelate the oscillations for larger delay. For $0.20 < t_r'' < 0.30$, phase coherence between G and G' is completely lost thereby resulting in a decrease of the cross-correlation by over 70%. Around $t_r'' = 0.32$, synchrony is restored following a jump bifurcation. The parameters are the same as in Table 5.3.6.

decorrelated. The reason for this seems to be that when the frequencies of the groups are not widely different, the signals are circulated through G , i.e., G provides efficient throughput.

Selective correlation If the intrinsic frequencies of the groups differ widely, selective correlation of the oscillatory activities is possible wherein an ordering of the cross-correlations between the groups – $[GG''] > [GG'] > [G'G'']$ – occurs. Such selective correlation is established by circulating harmonics. As an example, let the intrinsic frequencies be $\Omega = 12.58$, $\Omega' = 5.52$, and $\Omega'' = 7.21$, circulating harmonics from G'' . Because the intrinsic frequencies differ by more than 50%, the cross correlation between the activities of G and G' sans G'' is small, as we have already seen. However, when the group G'' is introduced, the cross-correlation shows the aforementioned differential effects (Fig. 5.3.3): $[GG''] = 1.0$, $[GG'] = 0.56$, and $[G'G''] = 0.2$. The correlation is least among the groups G' and G'' which are not directly connected. This

result may be simply understood by comparing pairwise the overlap in the frequency spectra of the three groups (Fig. 5.3.4). It may also be noted that the serial interaction is not as efficient as the triangular interaction in circulating intermediate frequencies. As the spectra indicate, the frequency throughput can be small – (1) the primary frequency of G'' ($\omega = 7.36$) circulates in G but not in G' and (2) the primary frequency of G' ($\omega = 5.68$) circulates in G but not in G'' . These mechanisms may be useful in integrating activity over several time scales without slowing down the responses to a common low frequency in contradistinction to the triangular interaction discussed above.

Thus, in the series interaction, G'' can selectively correlate the activity of the diadic ($[GG']$) interaction even as the signals circulate continuously.

5.4 Discussion

The aim of the preceding analysis has been to consider the effect of the mapping topology on the integration of oscillatory signals, including synchronization, desynchronization and dynamic switching of frequency, phase, and amplitude and the emergence of delay related temporal windows in distributed neural systems. Towards this end, the triangular and series triadic interaction of neuronal groups (Fig. 5.2.1) has been studied with particular emphasis on the dynamic control of diadic interaction by a third neuronal group. The results confirm that synchronization, desynchronization, and resynchronization obtained for the case of the dyadic interaction are not specific to it but are general emergent features of signaling in distributed neural systems. Furthermore, these effects are dependent on the topology of the mapping and are accompanied by both qualitative and quantitative changes.

For a wide range of parameters, the oscillatory activity of the groups

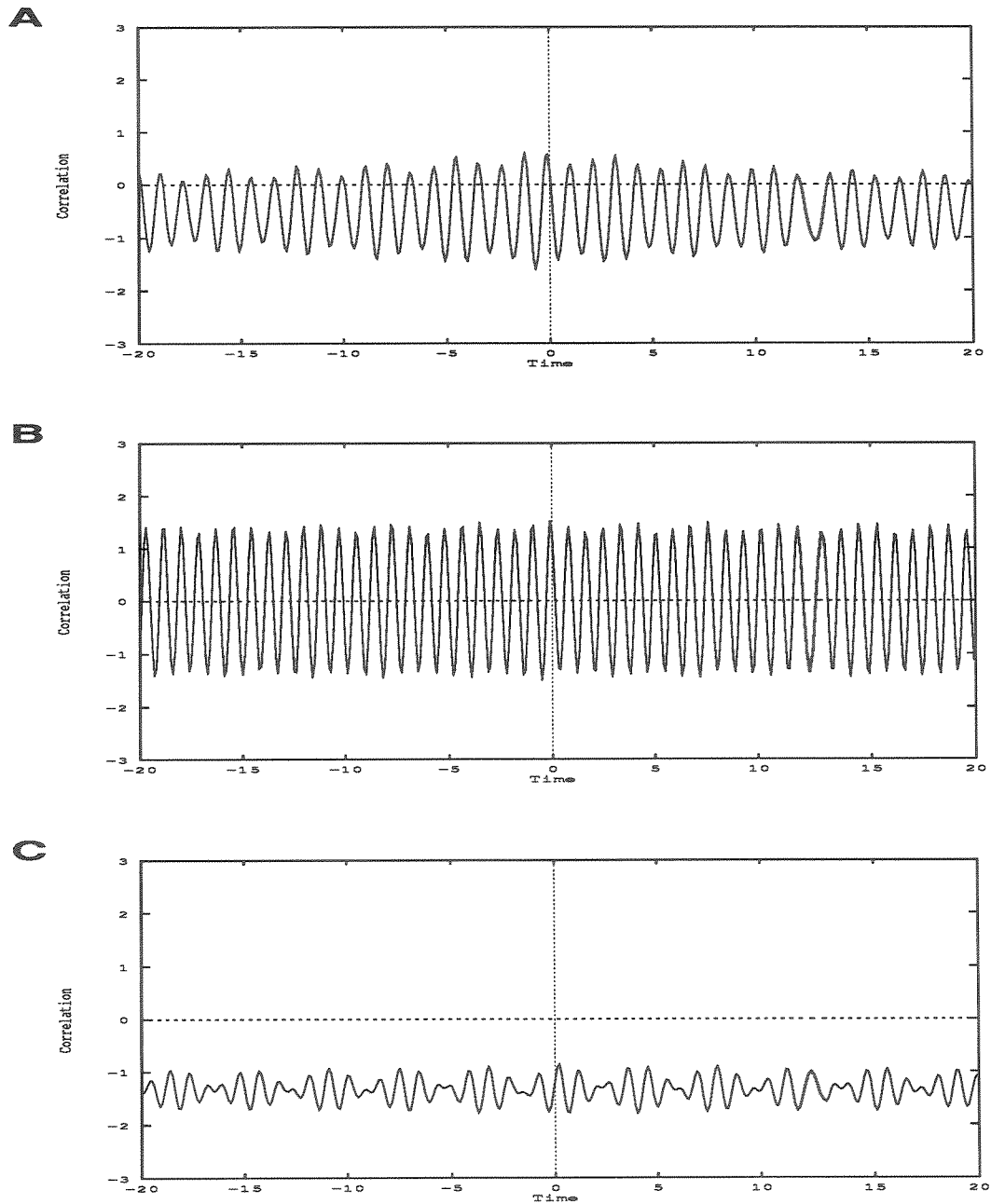


Figure 5.3.3: In the case of series reentrant signaling, frequency mismatch between the groups can result in selective differential cross-correlation. The cross-correlations between (A) G and G' , (B) G and G'' , and (C) G' and G'' clearly indicates an ordering: $GG'' > GG' > G'G''$. The intrinsic frequencies of the groups are the same as in Fig. 5.3.1.

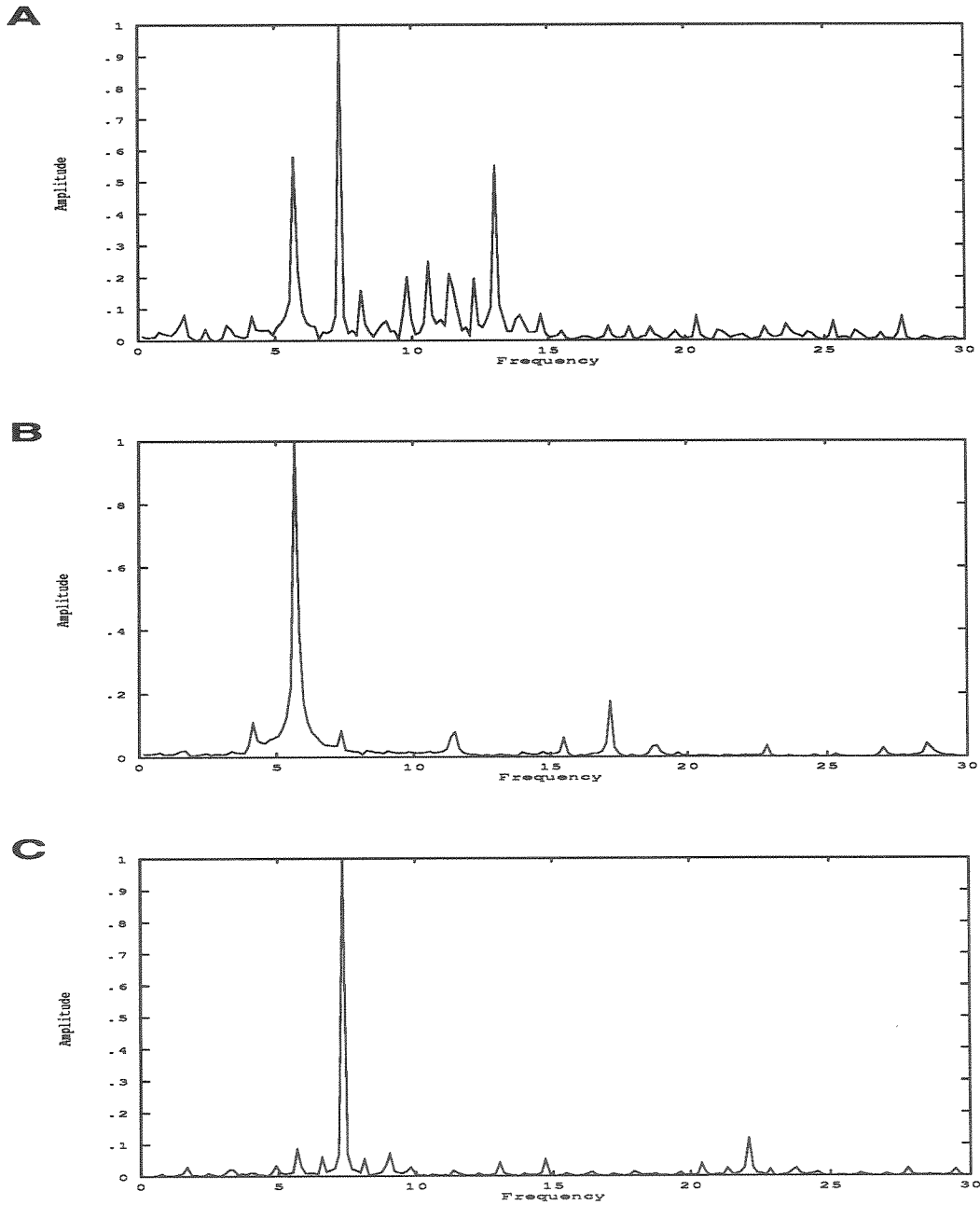


Figure 5.3.4: The frequency spectra for groups (A) G , (B) G' , and (C) G'' engaged in series reentrant signaling. By comparing, pairwise, the overlap in the spectra, it is easy to understand the origin of the differential cross-correlation effects shown in Fig. 5.3.3.

is synchronized with a large cross correlation. With the introduction of reentry, the frequency of oscillation decreases when the reentry delays and phase differences between the groups are small. The decrease is proportional to the strength of the two excitatory reentrant signals incident onto a group. The frequency decreases even further compared to the drop with two synchronized groups. This is because the excitatory signals arriving in phase prolong the excitatory activity within the group. In the case of the series interaction, even in a perfectly symmetric case (identical intrinsic frequencies and reentrant connection strengths) and the phase differences between the groups are nonzero due to the input mismatch between G' , G'' and G . Consequently, the decrease in the frequency is not as large.

A consequence of the larger frequency decrease in the case of the triangular interaction is that the jump bifurcation occurs for larger value of delay in the reentrant signal, compared to the series interaction (see Tables 5.3.2 and 5.3.4). Moreover, in the series interaction, with identical frequencies, although no desynchronization is observed, persistent transients are observed which cause a decrease in the cross-correlation between the groups. These results indicate the destabilizing nature of the 'open loop' series interaction. The nature of this destabilization will be further clarified in the following discussion.

Signals from G'' can dynamically control the phase of the oscillations of groups G and G' . The effects vary considerably depending on the mapping topology and whether the introduction of G'' increases the mean frequency mismatch between the groups.

In the case of the triangular interaction, if the mean frequency mismatch is not increased, differential changes in phase can occur as the latencies of specific signals are varied. For example, if the delay between G and G'' is

changed, the phase difference between those groups changes while there is little change between the phase differences of G and G' . However, when the jump bifurcation occurs, an approximately 180° change in θ_e'' is accompanied by a large jump in θ_e . In this manner, because of the jump bifurcation local changes can result in global changes. These alterations in phase may underlie dynamic switching of states, if by states we mean the relative phases of the activities of the neuronal groups.

An important characteristic of the oscillatory activity in the foregoing analysis is that the desynchronization of G, G' is obviated by what might be termed 'reinforcement' from G'' . This is a direct consequence of the decrease in the size of the desynchronized region. The result suggests that such closed loop mapping as in the triangular mapping may synchronize the activity in a stable manner.

For increases in mean frequency mismatch between the groups, the signals from G'' can control the cross-correlation between the groups G and G' in a robust manner (Table 5.3.4).

In the case of the series interaction, the behavior is qualitatively different. Even without an increase in the mean mismatch of the intrinsic frequencies of the groups, desynchronization of correlated diadic interactions occurs in a robust manner. Furthermore, there exist broad time delays, t_r'' , for which the oscillatory activity is desynchronized. When the diadic oscillations are desynchronized, the size of these windows is even broader than the one for the diadic interaction. For these reasons, the 'open loop' series mapping may be termed destabilizing.

When the intrinsic frequencies of the groups are widely different, then partial synchrony is established by subharmonic resonance (Chapter 4). The

Feature	Triangular	Series
Reinforcement	strong	weak
Desynchronizing windows	narrow	broad
Phase differences	small	large
Integration	efficient	weak
Circulation of harmonics	strong	weak
Selective correlation	strong	weak

Table 5.4.1: The differences between triangular and series interaction of neuronal groups suggest stabilizing and destabilizing topologies respectively.

introduction of a third group with an intermediate frequency causes much more robust synchronization. In the case of the triangular interaction, each harmonic is circulated in every group (Fig. 5.3.3), whereas in the series interaction, not all harmonics circulate in all groups. This gives rise to distinct phenomena in the two cases. In the former, it provides a robust way to integrate oscillatory activity over several time scales. In the latter, an ordering of the cross-correlations between the groups. Thus selective correlation is possible.

The differences between the triangular and series triadic interactions, summarized in Table 5.4.1, suggest that in the presence of delays, there are stabilizing and destabilizing topologies.

Several themes emerge from the foregoing analysis. First, closed loop (multiconnected) n-tuple mapping can integrate the oscillatory activity over several time scales. It is therefore suggested that efficient integration of the cortical activity where the frequencies are around 40 Hz. with hippocampal activity where the theta rhythm has a frequency of 4 Hz., can be achieved by mapping through secondary regions with intermediate frequencies. Moreover, the primary frequency is likely to be closer to the frequency of the intermediate region.

Second, the dynamic interaction of neuronal groups is metastable: the metastability arises from two sources (1) the dynamic recruitment of new groups as the input into the system varies by sensory or motor sampling (Edelman, 1987) and (2) the dynamic switching of phase when the oscillatory activity is uncorrelated. The underlying reason for the metastability is the jump bifurcation wherein rhythmic activity can be either desynchronized or synchronized by newly recruited neuronal groups which are activated by recurrent or incoming signals. Such metastable activity, we may argue, is necessary to prevent stereotypical and over-generalized responses. It is therefore possible that "... an identical stimulus can trigger one behavior at one moment and another behavior at another moment" (Evarts et al., 1984). While it is as yet hard to relate these results to the experimental results from the responses of single cells, the results are in agreement with the observation that the underlying global interaction is not a simple modulation of signals (Haenny et al., 1988).

Third, there exist broad temporal delay windows and mapping topologies for which the oscillatory activity of specific neuronal groups can be decorrelated (with complete loss of phase coherence). As already noted, the origin of these time windows lies in the demarcation of the synchronized and desynchronized activity by the jump bifurcation. Specifically, it is implied that given a mapping configuration, there exist, for specific signals, time delays $t_{r1} < t_r < t_{r2}$ for which the global activity is correlated and delays $t_{r2} < t_r < t_{r3}$ for which the activities are decorrelated. Thus there are distinct time windows for synchronization and desynchronization. This suggests that only signals arriving within a certain time window are likely to be correlated. Such mechanisms may provide additional timing constraints. These time windows are of an atemporal and neutral nature (Poppel et al., 1990).

Consideration of timing effects in neural systems have dealt with the mismatch between the arrival times of excitatory and inhibitory signals (Koch et al., 1983). The results obtained here argue for a more global consideration of timing effects in neural systems. This is particularly true in view of the fact that the frequency is not just the time inverse of the delay but depends on the the intrinsic circuit properties such as connection strengths and the time courses of decay of the signals as well as the topology of the mapping. By varying the time courses of specific signals onto specific targets, neurotransmitters and neuromodulators (Marder et al., 1987) may play an important part in the global signaling. The effect of recruiting additional groups and altering delays is not merely to modulate the oscillatory activity, but to alter the characteristics of the oscillatory activity in the robust manner discussed above. Hence, like global mapping, global temporal effects are dynamic and metastable. Given the complex nature of the oscillatory and decorrelated activity that is possible, particularly in the presence of delays, it may not be necessary to evoke notions of clocks or multiclocks (Kristofferson, 1984) in distributed neural systems.

Chapter 6

Summary, Predictions, and Concluding Remarks

6.1 Summary

This thesis has studied some of the fundamental processes underlying the functioning of complex neural systems. Neuronal groups serve as the locus for the generation of coherent oscillatory signals. This oscillatory signal is the basis of signaling in the distributed system. The origin and characteristics of population oscillations and their role in and implications for signaling in distributed neural systems formed the focus of the theoretical analysis.

A phase shift between the excitatory and inhibitory components underlies the generation of oscillations. Delay in inhibition and slowly decaying inhibitory signals readily result in such phase shift. The time period of the oscillations is different from any one time scale in the system; for example, for a wide range of parameters $\omega T_e \ll 1$ and $\omega t_d \ll 1$, where T_e is decay time scale of the excitatory activity and t_d is the inhibitory delay. In agreement with the detailed computer simulation of Traub et. al (1988, 1990), it has been found that a large dynamic range for the frequency of the oscillations as the time course of the inhibitory signal is varied. When the frequency is low, the refractory period is large, or the activity is high, strong second and third harmonics can be generated. Experimental evidence for this result has recently been obtained in a study of tactile frequency discrimination in monkeys (Mountcastle et al., 1990).

The oscillatory activity of neuronal groups can be synchronized or desynchronized by nonlinear summation of reentrant signals with the ongoing oscillatory activity within a group. Self-consistent frequency-amplitude-phase relations derived show that the frequency, phase, and cross-correlation of the synchronized response depend critically on the relative phases of the interacting signals. The phase difference between the activities of the groups increases with increasing mismatch in the intrinsic frequencies of the groups and can be arbitrarily small when the intrinsic frequencies of the groups are close. The small phase differences found experimentally (Gray et al., 1989) suggest that signaling between the spatially separated neuronal groups must be reciprocal with roughly equal mean forward and backward connection strengths; otherwise, the input mismatch would have resulted in large phase differences.

Reentrant signaling reduces the frequency of oscillation when the reentry delay is small; this is in agreement with the computer simulations of several thousand neurons organized into neuronal groups (Sporns et al., 1989). However, when the reentry delay is increased, the reentrant signal arrives out of phase with the intragroup inhibitory signal, and the frequency and phase difference between the activity of the two groups undergo large abrupt jumps: the frequency increases by about 50% and the phase difference flips by about 180° . At the transition region, phase coherence is lost, and the oscillations are desynchronized. Such a desynchronization of the oscillatory response has been reported in a computer simulation of interacting neurons (Schillen and Konig, 1990). Therefore, delay in signaling can act as (phasic) switching mechanism for correlating and decorrelating the oscillatory activity.

The triangular and series reentrant interaction of coherent oscillatory signals indicates important topological effects of mapping in distributed neural

systems. It is found that the triangular interaction (1) results in strong reinforcement of the oscillatory response, (2) can prevent the decorrelation of the diadic oscillatory activity, and (3) can aid in the integration of the oscillatory activity over several time scales by efficiently circulating harmonics. Series interaction, on the other hand, provides weak reinforcement, and can selectively decorrelate diadic neuronal group interactions. Synchronization, desynchronization, and the dynamic switching of phases and frequency as well as the size of the decorrelating time delay windows depend on both the local circuit properties and the mapping topology.

Delay in signaling can act as switch. Switching as discussed here is the result of continuous signaling and not a *ON – OFF* response – it is correlation dependent. It is important to note that the desynchronization of oscillatory activity does not result from decreased or residual interaction: it is a consequence of signals not arriving with the proper phase relationships. The switching is dynamic – it occurs even as signals are being transmitted and circulated. It is quite possible that such switching may also be induced by variable inputs, changes in connection strengths or other parameters since they all affect the phases of the interacting signals. It is important to note that switching is topology dependent as well.

The dynamic range frequency, amplitude, and phase range of multiple interacting neuronal groups implies that it is not necessary to evoke the idea of clocks or multiple clocks (Wiener, 1961; Kristofferson, 1984). We may reiterate that since the frequency depends on the global mapping, the typical time scale of neuronal activity in the system, $O(\omega^{-1})$ changes dynamically and furthermore the change is dependent on the set of neuronal groups that are selected to be active at a given time. The metastable nature of the oscillations implies

that no ‘clock’ will be found. The desynchronization and resynchronization, if verified experimentally, would be manifestations of phasic signaling.

Since the brain is constantly under the dynamic control of neurotransmitters with complex time courses, the view that emerges, is that signaling in distributed neural systems is dynamic and metastable due to the modulation and switching effects discussed above. Real time dynamic control of the cross-correlation of the ongoing activity of neuronal groups is possible. Signaling can result in dynamic linkage (association and dissociation) of the groups. The ‘logic’ dictated by phasic reentrant signaling is thus fundamentally different from the Boolean switching operations. Timing and signaling in neural systems are part of the same physical process and have features quite distinct from timing and signaling in computer systems. The mechanisms discussed in this thesis, provide dynamic linkage between neuronal groups thereby enabling the distributed neural system to operate in a highly parallel manner without clocks, algorithms, and central control.

6.2 Predictions

The results obtained suggest that,

1. Phasic reentrant signaling in neural systems will lead to synchronization, desynchronization, and resynchronization of oscillatory responses with the characteristics as discussed above. The most obvious origin of these phenomena is delay in reentrant signaling. By cooling the axons mediating reentrant signaling, it should be possible to verify these phenomena.
2. Neural switching mechanisms as discussed above, are likely to be closely related to neural plasticity since both are cross-correlation dependent.

3. Dynamic fluctuations in frequency-amplitude-phase characteristics of the oscillations are likely. Due to the constant recruitment of new groups, their transient interactions, and the jump bifurcation, signaling will be metastable.
4. The degree of cross-correlation between coactive groups can be dynamically controlled by modulating the time courses of individual signals incident on specific targets. Such a function is likely to be performed by neurotransmitters and neuromodulators.
5. Integration of activity over disparate time scales is possible by closed loop mapping of multiply connected neuronal groups. The degree of integration achieved will depend upon, among other factors, the mapping topology. In particular, open loop mapping can be easily destabilized by delays.

6.3 Concluding Remarks

In conclusion, the broader theoretical implications of the results summarized above are discussed in this section. Given the enormous complexity of the system, the analysis is not without a degree of speculation.

6.3.1 Information in the Oscillations

A pure sine wave carries no information. In analog electronic communication, information is carried by either phase, amplitude, or frequency modulation (Tanenbaum, 1984).

In distributed neural systems, the oscillations and the dynamical correlations resulting from it are transient in nature. Additionally, turning on the

oscillations involves the process of recognition by the receptive field in the case of exogenous events.

Furthermore, the oscillations are never purely sinusoidal – and as we have seen, due to the nonlinear saturation characteristics of a population of neurons strong harmonics can be generated. Moreover, the harmonic content of the oscillations changes dynamically as the different neuronal groups are recruited. Synaptic modification, which has not been considered here, will further modulate the harmonic content of the oscillations.

Delay induced desynchronization and resynchronization of the oscillations results in dynamic changes in the characteristics of the oscillations. Thus, frequency, phase, and amplitude modulation arise from the same neural circuits. As we have seen, all three forms of modulation of the oscillatory signal can arise at the same time. In the foregoing analysis, the important effects of ‘noise’ and fine scale temporal effects such as event related potentials (Hillyard and Picton, 1987) have hardly been considered.

6.3.2 Switching and Gating

In a distributed neural system, switching gates signals along specific pathways. The need for dynamic switching mechanisms has been stressed by Evarts, Shinoda, and Wise (1984) who note that: (1) switching underlies selective attention and (2) switching allows for the flexible response to complex environmental stimuli by enabling the animal to select from a variety of possibilities. Neural switching allows selective gating of signals. Along with neural plasticity it provides the basis for adaptive behavior (Evarts et al., 1984).

A correlation dependent switching mechanism, such as the one discussed above, would meet an important condition that has been pointed out

by Evarts et al. (1984): that of a 'cycle time' during which the expected signal is matched to a postulated response and evaluated. Such a mechanism differs from the on-off response and the idea of a 'set cell' (Evarts et al., 1984) which could control the efficacy of a pathway through an inhibitory interneuron. Such a specific cell to cell signaling would be difficult in complex circuits. It also differs fundamentally from binary computations (McCulloch and Pitts, 1943) and analog computations (Koch and Poggio, 1987). Rather, it relies on the delayed time courses of specific signals involved in coherent oscillatory activity.

As discussed above, by varying the time courses of signals incident on specific targets, it is possible for the system to effectively gate the signals. Whether this is necessarily accompanied by synaptic modification is unclear. It is also not clear what the relation between decorrelation and synaptic change is. There are two possibilities: (1) with decorrelated oscillatory response, the mean synaptic strength between groups could decrease, or (2) the mean synaptic strength decreases when the oscillatory activities are out of phase with no change occurring when the oscillations are decorrelated. In either case, a critical relation between neural switching and neural plasticity is likely.

Dynamic switching techniques have been found to be useful in the design of new computer architectures (Hillis, 1985). However, in contradistinction to the schema in such machines, neural switching of the type postulated here, can be achieved without any routing algorithms. However, the actual gating of signals remains a significant challenge to understand.

6.3.3 Time Delays and Memory

In the old computer systems such as the EDVAC (Aspray and Burks, 1987), delay lines served the role of memory. In neural systems, delays provide

access to signals (and their transformations imposed by the neural circuitry and the extrinsic receptive field) till it is dissipated, and, therefore, serves as de facto memory. The results obtained in this study suggest that a delay, t_d , in signaling results in transforming the phase of the incoming oscillatory signal by ωt_d , where the frequency, ω , depends on the global mapping.

The implications of phase transformation of the signal for overall information processing remains to be investigated. Nevertheless, by providing delayed access to signals, the system provides a simple form of memory, one that may be important to maintain spatiotemporal continuity of the external world (Reeke et al., 1989).

Inclusion of delays may involve novel ideas of memory as well, quite distinct from the currently popular notions of associative memory (Hinton and Anderson, 1981; Hopfield, 1982; Hopfield, 1984). Some novel ideas involving oscillations and delayed inhibition have recently been proposed (Wang et al., 1990).

6.3.4 Time and Time Perception

It will be a considerable challenge to relate the notion of signaling and the temporal effects resulting therefrom to the psychological notion of timing, time perception, and time discrimination (Gibbon and Allan, 1984; Poppel, 1978). As has been noted by Staddon (1984), timing and memory call on the same processes. It seems unlikely, therefore, that these phenomena can be understood without relating it to memory, a topic beyond the scope of the present study.

With regard to temporal discrimination it may be noted that either because of delays in transduction of signals (Poppel et al., 1990) or the decor-

relation of the oscillatory activity as described in the previous section, there are likely to be time windows in which the ordering can be lost.

While the role of the rhythmic organization of temporal phenomena in decision and cognitive processes (Poppel, 1978) is far from clear, it is nevertheless suggested that the dynamical aspects of signaling involving coherent oscillatory signals possesses several positive characteristics for such a consideration: (1) dynamic control of the frequency-amplitude-phase of the oscillations by neurotransmitters and neuromodulators; (2) dynamic switching of frequency, amplitude, and phase; (3) straightforward integration of new signals; (4) integration of activity over disparate time scales; (5) dynamic control of the cross-correlation of spatially distributed oscillatory activity; and (6) metastable character of the oscillations prevents stereotypical and over generalized responses.

Appendix A

A.1

In this appendix we derive the stability conditions by linearizing Eqns. 3.2.5 and 3.2.6 for small r_e, r_i :

$$T_e \dot{f}_e(t) = -f_e(t) + (1 - \int_{t-r_e}^t f_e(t') dt') \sigma_e(x_e) \quad (\text{A.1.1})$$

$$T_i \dot{f}_i(t) = -f_i(t) + (1 - \int_{t-r_i}^t f_i(t') dt') \sigma_i(x_i) \quad (\text{A.1.2})$$

$$x_e = C_1 f_e(t) - C_2 f_i(t - t_d) + P$$

$$x_i = C_3 f_e(t) - C_4 f_i(t - t_d) + Q$$

Substituting $f_e = \bar{f}_e + e(t)$ and $f_i = \bar{f}_i + i(t)$ in Eqn. A.1.1 above, and neglecting second order terms we get,

$$\begin{aligned} T_e \dot{e}(t) = & -e(t)[1 + r_e \sigma_e(\bar{x}_e)] + [1 - r_e \bar{f}_e] C_1 e(t) \sigma'_e(\bar{x}_e) \\ & - [1 - r_e \bar{f}_e] C_2 i(t - t_d) \sigma'_e(\bar{x}_e) \end{aligned} \quad (\text{A.1.3})$$

Similarly for the inhibitory component,

$$\begin{aligned} T_i \dot{i}(t) = & -i(t)[1 + r_i \sigma_i(\bar{x}_i)] + [1 - r_i \bar{f}_i] C_3 e(t) \sigma'_i(\bar{x}_i) \\ & - [1 - r_i \bar{f}_i] C_4 i(t - t_d) \sigma'_i(\bar{x}_i) \end{aligned} \quad (\text{A.1.4})$$

These equations can be written in the simplified form :

$$\dot{e}(t) = -e(t) \kappa_e + C_1 \alpha_e \sigma'_e(\bar{x}_e) e(t) - C_2 \alpha_e \sigma'_e(\bar{x}_e) i(t - t_d) \quad (\text{A.1.5})$$

$$\dot{i}(t) = -i(t) \kappa_i + C_3 \alpha_i \sigma'_i(\bar{x}_i) e(t) - C_4 \alpha_i \sigma'_i(\bar{x}_i) i(t - t_d) \quad (\text{A.1.6})$$

where,

$$\begin{aligned}
T_e \kappa_e &= 1 + r_e \sigma_e(\bar{x}_e) \\
T_i \kappa_i &= 1 + r_i \sigma_i(\bar{x}_i) \\
T_e \alpha_e &= 1 - r_e \bar{f}_e \\
T_i \alpha_i &= 1 - r_i \bar{f}_i
\end{aligned}$$

With $e(t) \sim e_0 \exp(\lambda t)$ and $i(t) \sim i_0 \exp(\lambda t)$, the equations can be written as,

$$\begin{bmatrix} \lambda + \kappa_e - \alpha_e \sigma'_e(\bar{x}_e) C_1 & \alpha_e \sigma'_e(\bar{x}_e) C_2 \exp(-\lambda t_d) \\ -\alpha_i \sigma'_i(\bar{x}_i) C_3 & \lambda + \kappa_i - \alpha_i \sigma'_i(\bar{x}_i) C_4 \exp(-\lambda t_d) \end{bmatrix} \begin{bmatrix} e_0 \\ i_0 \end{bmatrix} = \begin{bmatrix} 0 \\ 0 \end{bmatrix}$$

The characteristic equation, obtained by setting the determinant to zero, is

$$\Delta(\lambda) = \lambda^2 + G\lambda + H + J \lambda \exp(-\lambda t_d) + I \exp(-\lambda t_d) = 0 \quad (\text{A.1.7})$$

where the coefficients G , H , I and J are:

$$\begin{aligned}
G(\bar{x}_e) &= (\kappa_e + \kappa_i - \alpha_e \sigma'_e(\bar{x}_e) C_1) \\
H(\bar{x}_e) &= \kappa_i (\kappa_e - \alpha_e \sigma'_e(\bar{x}_e) C_1) \\
I(\bar{x}_e, \bar{x}_i) &= \sigma'_e(\bar{x}_e) \sigma'_i(\bar{x}_i) \alpha_e \alpha_i (C_2 C_3 - C_1 C_4) \\
J(\bar{x}_i) &= \sigma'_i(\bar{x}_i) \alpha_i C_4 \\
\sigma'_e(\bar{x}_e) &= \beta_e / (4 \cosh^2(-\beta_e(\bar{x}_e - \chi_e))) \\
\sigma'_i(\bar{x}_i) &= \beta_i / (4 \cosh^2(-\beta_i(\bar{x}_i - \chi_i))) \\
\bar{x}_e &= C_1 \bar{f}_e - C_2 \bar{f}_i + P \\
\bar{x}_i &= C_3 \bar{f}_e - C_4 \bar{f}_i + Q
\end{aligned} \quad (\text{A.1.8})$$

A.2

In this Appendix, we prove Theorems 3.3.1, 3.3.2, and 3.3.3 concerning stability of the fixed points.

Theorem A.2.1 *For sufficiently large delay, t_d , if $H < 0$, the fixed point is unstable.*

Proof: Assume that there exists $\lambda = \lambda_p$ with positive real part. In the vicinity of λ_p , for large delay t_d , Eqn. 3.3.3 can be written as

$$\lambda^2 + G\lambda + H = 0 \quad (\text{A.2.1})$$

The roots of the above equation are $(-G \pm \sqrt{G^2 - 4H})/2$. If $H < 0$, one of the roots has a positive real part which implies that for sufficiently large delay the fixed point is unstable. This root is arbitrarily close to a solution of Eqn. 3.3.3, i.e., there exists a solution with positive real part. This completes the proof.

We next prove some results concerning stability of the fixed point in the general case. Rewrite Eqn. 3.3.3 by rescaling $\lambda \rightarrow \frac{\lambda}{t_d}$ (we assume $t_d \neq 0$ but may be arbitrarily small):

$$\Delta = \lambda^2 + Gt_d\lambda + Ht_d^2 + Jt_d\lambda \exp(-\lambda) + It_d^2 \exp(-\lambda) = 0 \quad (\text{A.2.2})$$

The stability can be studied by using the Michailov criterion (Kolmanovskii and Nosov, 1986). Let $\Delta(i\omega) = U(\omega) + iV(\omega)$, where U and V are real. From Eqn. 3B.3,

$$U(\omega) = -\omega^2 + Jt_d\omega \sin(\omega) + It_d^2 \cos(\omega) + Ht_d^2 \quad (\text{A.2.3})$$

$$V(\omega) = Gt_d\omega + Jt_d\omega \cos(\omega) - It_d^2 \sin(\omega) \quad (\text{A.2.4})$$

For asymptotic stability of the linear nth order equation, it is necessary and sufficient that the following condition be satisfied:

$$\arg\Delta(i\omega)|_{\omega=0}^{\infty} = n\frac{\pi}{2} \quad (\text{A.2.5})$$

The coefficients G , H , I and J depend on the slope of the sigmoid at the fixed point as well as the connectivities and time scales in the problem. No general necessary and sufficient conditions could be derived to show stability or instability of the fixed points. Instead we prove the following theorems which indicate the behavior of the system for particular conditions.

Theorem A.2.2 *A set of sufficient conditions for the stability of a fixed point is:*

(i) $t_d(H + I) > 0$ and (ii) $G - J > t_d|I|$.

Proof:

$$\begin{aligned} V(\omega) &= t_d G \omega + t_d J \omega \cos \omega - t_d^2 I \sin \omega \\ &\geq t_d G \omega - t_d J \omega - t_d^2 |I| \omega \\ &\geq t_d \omega (G - J - t_d |I|) \end{aligned} \quad (\text{A.2.6})$$

Therefore $V(\omega) > 0$ if $G - J - t_d |I| > 0$. This, together with the condition $t_d(H + I) > 0$, implies that $\arg\Delta(i\omega)|_{\omega=0}^{\infty} = \pi$. The proof of this statement follows:

1. There exists ω_1 such that $U(\omega_1) = 0$ since $U(\omega = 0) = H + I > 0$ and $U(\omega = \infty) = \infty$. Now, $V(\omega) > 0$ implies $\arg\Delta(i\omega)|_{\omega=0}^{\omega_1} = \pi/2$.

2. As $\omega \rightarrow \infty$, $\frac{V}{U} \rightarrow 0$. Hence $\arg\Delta(i\omega)|_{\omega_1}^{\infty} = \pi/2$.
3. Therefore $\arg\Delta(i\omega)|_{\omega=0}^{\infty} = \pi$.

This completes the proof.

Theorem A.2.3 *If $t_d(H + I) < 0$, the fixed point is unstable.*

Proof: From $U(\omega = 0) = t_d^2(H + I)$, $V(\omega = 0) = 0$ and $\omega \rightarrow \infty$, $\frac{V}{U} \rightarrow 0$, it follows that $\arg\Delta(i\omega)|_{\omega=0}^{\infty} = \pm 2n\pi$, $n = 0, 1, 2, \dots$. Since $\arg\Delta(i\omega)|_{\omega=0}^{\infty} \neq \pi$, the fixed point is asymptotically unstable.

A.3

We derive the harmonic feedback for the bias plus sinusoid input to the saturation nonlinearity. The main results are summarized at the end of the Appendix. Following the discussion in Section 3.4, the harmonic feedback for the input $x(t) = B + A \sin(\omega t)$ is,

$$f(x) \sim BF_B(f, A, B) + \sum_{k=1}^{\infty} [AF_A(f, A, B, k) \sin(\omega t) + AF_A^\dagger(f, A, B, k) \cos(\omega t)] \quad (\text{A.3.1})$$

$$F_A(f, A, B, k) = \frac{1}{\pi A} \int_0^{2\pi} f(B + A \sin(\theta)) \sin(k\theta) d\theta$$

$$F_A^\dagger(f, A, B, k) = \frac{1}{\pi A} \int_0^{2\pi} f(B + A \sin(\theta)) \cos(k\theta) d\theta$$

We will only consider the case of large amplitude oscillations in which case $\frac{\delta+B}{A} < 1$ and $\frac{\delta-B}{A} < 1$. For the piece-wise linear sigmoid, $F_A(f, A, B, k)$ can be evaluated as follows.

$$\pi AF_A(f, A, B, k) = \int_0^{2\pi} m f(B + A \sin(\theta)) \sin(k\theta)$$

$$\begin{aligned}
&= \int_0^{\psi_{10}} m(B + A \sin(\theta)) \sin(k\theta) d\theta + \int_{\psi_{10}}^{\psi_{11}} m\delta \sin(k\theta) d\theta \\
&+ \int_{\psi_{11}}^{\psi_{20}} m(B + A \sin(\theta)) \sin(k\theta) d\theta - \int_{\psi_{20}}^{\psi_{21}} m\delta \sin(k\theta) d\theta \\
&+ \int_{\psi_{21}}^{2\pi} m(B + A \sin(\theta)) \sin(k\theta) d\theta \quad (\text{A.3.2})
\end{aligned}$$

where,

$$\begin{aligned}
\psi_{10} &= \sin^{-1}\left(\frac{\delta-B}{A}\right) \\
\psi_{11} &= \pi - \psi_{10} \\
\psi_{20} &= \pi + \sin^{-1}\left(\frac{\delta+B}{A}\right) \\
\psi_{21} &= 2\pi - \sin^{-1}\left(\frac{\delta+B}{A}\right) \quad (\text{A.3.3})
\end{aligned}$$

Eqn. A.3.2 evaluates to,

$$\begin{aligned}
\pi AF_A(f, A, B, k) &= -\frac{mB}{k} \cos(k\theta)|_0^{\psi_{10}} \\
&+ \frac{mA}{2} \left[\frac{1}{k-1} \sin((k-1)\theta)|_0^{\psi_{10}} - \frac{1}{k+1} \sin((k+1)\theta)|_0^{\psi_{10}} \right] \\
&\quad - \frac{m\delta}{k} \cos(k\theta)|_{\psi_{10}}^{\psi_{11}} - \frac{mB}{k} \cos(k\theta)|_{\psi_{11}}^{\psi_{20}} \\
&+ \frac{mA}{2} \left[\frac{1}{k-1} \sin((k-1)\theta)|_{\psi_{11}}^{\psi_{20}} - \frac{1}{k+1} \sin((k+1)\theta)|_{\psi_{11}}^{\psi_{20}} \right] \\
&\quad + \frac{m\delta}{k} \cos(k\theta)|_{\psi_{20}}^{\psi_{21}} - \frac{mB}{k} \cos(k\theta)|_{\psi_{21}}^{2\pi} \\
&+ \frac{mA}{2} \left[\frac{1}{k-1} \sin((k-1)\theta)|_{\psi_{21}}^{2\pi} - \frac{1}{k+1} \sin((k+1)\theta)|_{\psi_{21}}^{2\pi} \right] \quad (\text{A.3.4})
\end{aligned}$$

We observe that the harmonics scale as $1/k$. A similar expression is obtained for $F_A^\dagger(f, A, B, k)$. The calculations are straightforward but tedious; we will therefore simply present the relevant results:

$$\begin{aligned}
\pi AF_A(f, A, B, k=3) &= \frac{2mB}{3} [\cos(3\delta^+) - \cos(3\delta^-)] + \frac{2m\delta}{3} [\cos(3\delta^+) + \cos(3\delta^-)] \\
&\quad + \frac{mA}{2} [(\sin(2\delta^+) + \sin(2\delta^-)) - \frac{1}{2}(\sin(2\delta^+) + \sin(2\delta^-))] \\
\pi AF_A^\dagger(f, A, B, k=2) &= mB[\sin(2\delta^+) + \sin(2\delta^-)] + m\delta[\sin(2\delta^+) - \sin(2\delta^-)] \\
&\quad + mA[\frac{1}{3}(\cos(3\delta^+) - \cos(3\delta^-)) - (\cos(2\delta^+) - \cos(2\delta^-))]
\end{aligned}$$

$$F_A(f, A, B, k = 2) = 0 \quad (\text{A.3.5})$$

where $\delta^+ = \sin^{-1}(\frac{\delta+B}{A})$ and $\delta^- = \sin^{-1}(\frac{\delta-B}{A})$. For $\frac{\delta+B}{A}, \frac{\delta-B}{A} \ll 1$, Eqns. A.3.5 may be simplified by using the approximations $\cos x \sim 1$ and $\sin x \sim x$,

$$F_A(f, A, B, k = 3) = \frac{2}{\pi A} \frac{1}{3} \quad (\text{A.3.6})$$

$$F_A(f, A, B, k = 2) = 0 \quad (\text{A.3.7})$$

$$F_A^\dagger(f, A, B, k = 2) = \frac{2}{\pi A} \frac{B}{A} \quad (\text{A.3.8})$$

We summarize the results of this Appendix:

1. The amplitude of the k^{th} harmonic is proportional to $1/k$.
2. The second harmonic is proportional to $\frac{B}{A}$ and is phase shifted by $\frac{\pi}{2}$.
3. The amplitude of the third harmonic can be up to a third of that of the fundamental.
4. When the bias B is zero, only the odd harmonics are present. (The calculations for $k = 2, 3$ extend to even and odd harmonics respectively).

A.4

The algebraic equations governing the frequency, amplitude and phase of oscillations for $r_e \neq 0$, $r_i = 0$ are derived. Let

$$\begin{aligned} f_e(t) &= \bar{f}_e + f_{e0} \sin(\omega t) \\ f_i(t) &= \bar{f}_i + f_{i0} \sin(\omega t - \theta_i) \end{aligned} \quad (\text{A.4.1})$$

be the form of the solution of

$$T_e \dot{f}_e(t) = -f_e(t) + I_e(t) * \sigma_e(C_1 f_e(t) - C_2 f_i(t - t_d) + P) \quad (\text{A.4.2})$$

$$T_i \dot{f}_i(t) = -f_i(t) + \sigma_i(C_3 f_e(t) - C_4 f_i(t - t_d)) \quad (\text{A.4.3})$$

$$I_e(t) = 1 - \int_{t-r_e}^t f_e(t') dt'$$

Then

$$\begin{aligned} I_e(t) &= 1 - \int_{t-r_e}^t [\bar{f}_e + f_{e0} \sin(\omega t')] dt' \\ &= (1 - \bar{f}_e r_e) - 2 \frac{f_{e0}}{\omega} \sin\left(\frac{\omega r_e}{2}\right) \sin\left(\omega t - \frac{\omega r_e}{2}\right) \end{aligned} \quad (\text{A.4.4})$$

The nonlinear response of the sigmoid is $BF_B + AF_A \sin(\omega t + \theta_{ae})$. The averaged response, taking into account the refractoriness, is $\langle I_e(t)(BF_B + AF_A \sin(\omega t + \theta_{ae})) \rangle$, where $\langle \rangle$ denotes the averages as in Eqn. 3.4.1. We now note that the effect of the sinusoidal term in Eqn. A.4.4 is to introduce a second harmonic proportional to $\frac{1}{\omega}$ when this averaging is carried out. Consistent with the neglect of higher harmonics, we neglect this last term in Eqn. A.4.4. (It can be shown under very general conditions that this is true. The reason being that when oscillations exist, the ratio of the bias to sinusoidal input to the sigmoid, $\frac{B_e}{A_e}$, is typically less than 1.)

With this approximation, proceeding exactly as in Section 3.5, the following relations may be easily shown :

$$\bar{f}_e = 0.5(1 - \bar{f}_e r_e) + (1 - \bar{f}_e r_e) B_e F_{B_e} \quad (\text{A.4.5})$$

$$\omega T_e f_{e0} = (1 - \bar{f}_e r_e) \sin(\theta_{ae}) A_e F_{A_e} \quad (\text{A.4.6})$$

$$f_{e0} = (1 - \bar{f}_e r_e) \cos(\theta_{ae}) A_e F_{A_e} \quad (\text{A.4.7})$$

$$\bar{f}_i = 0.5 + B_i F_{B_i} \quad (\text{A.4.8})$$

$$\omega T_i f_{i0} = A_i F_{A_i} \sin(\theta_{ai} + \theta_i) \quad (\text{A.4.9})$$

$$f_{i0} = A_i F_{A_i} \cos(\theta_{ai} + \theta_i) \quad (\text{A.4.10})$$

Appendix B

B.1

In this Appendix, the algebraic equations governing the frequency-amplitude-phase of the oscillation are derived. The refractoriness of the inhibitory neurons is neglected, i.e., $r_i = 0$.

With the approximations Eqns. 4.4.1 - 4.4.4 for the firing rates, the activities of the subpopulations, x_e^* , x_i^* , $x_e^{*'}$ and $x_i^{*'}$ (Eqns. 4.4.10 - 4.4.13) can be written as,

$$\begin{aligned} x_e^*(t) &= B_e + A_e \sin(\omega t + \theta_{ae}) \\ x_i^*(t) &= B_i + A_i \sin(\omega t + \theta_{ai}) \\ x_e^{*'}(t) &= B_e' + A_e' \sin(\omega t + \theta_{ae}') \\ x_i^{*'}(t) &= B_i' + A_i' \sin(\omega t + \theta_{ai}') \end{aligned}$$

where the bias and amplitude terms are,

$$\begin{aligned} B_e &= C \bar{f}_e + C_r \bar{f}'_e - C \bar{f}_i + P - \chi_e \\ B_i &= C \bar{f}_e + C_r \bar{f}'_e - C \bar{f}_i + Q - \chi'_i \\ B_e' &= C \bar{f}'_e + C_r \bar{f}_e - C \bar{f}'_i + P' - \chi'_e \\ B_i' &= C \bar{f}'_e + C_r \bar{f}_e - C \bar{f}'_i + Q' - \chi'_i \\ A_e \sin(\theta_{ae}) &= C_r f'_{e0} \sin(\theta'_e + \omega t'_r) - C f_{i0} \sin(\theta_i + \omega t_d) \\ A_e \cos(\theta_{ae}) &= C f_{e0} + C_r f'_{e0} \sin(\theta'_e + \omega t'_r) - C f_{i0} \cos(\theta_i + \omega t_d) \end{aligned} \tag{B.1.1}$$

$$\begin{aligned}
A_i &= A_e \\
A'_e \sin(\theta'_{ae}) &= C f'_{e0} \sin(\theta'_e) + C_r f_{e0} \sin(\omega t_r) - C f'_{i0} \sin(\theta'_i + \omega t'_d) \\
A'_e \cos(\theta'_{ae}) &= C f'_{e0} \cos(\theta'_e) + C_r f_{e0} \cos(\omega t_r) - C f'_{i0} \cos(\theta'_i + \omega t'_d) \\
A'_i &= A'_e
\end{aligned}$$

In order to study analytically the characteristics of the synchronization as a function of the phases of interacting signals, we use the simplification that each subpopulation is excited at its threshold, i.e., $P = \chi_e$, $Q = \chi_i$, $P' = \chi'_e$ and $Q' = \chi'_i$. This represents an adequate input drive to excite oscillations. The bias terms now depend only on the mismatch between the excitatory and inhibitory activity in the respective subpopulations.

For the piecewise linear saturation function (Eqn. 4.4.5), the nonlinear gain functions F_B and F_A for inputs of the form $x(t) = B + A \sin(\omega t + \theta)$ can be evaluated as in Chapter 3,

$$F_B(B, A) = \frac{2}{\pi A} \quad (\text{B.1.2})$$

$$F_A(B, A) = \frac{2}{\pi A} \quad (\text{B.1.3})$$

The integral involving refractoriness in Eqn. 4.4.6 can be easily evaluated:

$$\begin{aligned}
I_e(t) &= 1 - \int_{t-r_e}^t [\bar{f}_e + f_{e0} \sin(\omega t)] dt' \\
&= (1 - \bar{f}_e r_e) - 2 \frac{f_{e0}}{\omega} \sin\left(\frac{\omega r_e}{2}\right) \sin\left(\omega t - \frac{\omega r_e}{2}\right)
\end{aligned}$$

Consistent with the neglect of higher harmonics, terms of the order $\frac{f_{e0}}{\omega}$ may be neglected, so that $I_e(t) \sim (1 - \bar{f}_e r_e)$. Note that the role of the neglected sinusoidal term above is to introduce a second harmonic when the excitatory cells are refractory. With the nonlinear response from the sigmoid given by

$BF_B + AF_A \sin(\omega t + \theta_{ae})$, and substituting the nonlinear gain functions F_{Be} and F_{Ae} from Eqns. B.1.2 and B.1.3, we obtain,

$$I_e(t)\sigma_e^*(x_{e*}) = \frac{2B_e}{\pi A_e}(1 - \bar{f}_e r_e)[1 + \cos(\theta_{ae}) \sin(\omega t) + \sin(\theta_{ae}) \cos(\omega t)] \quad (\text{B.1.4})$$

Similarly, for the other subpopulations,

$$I'_e(t)\sigma_e^{*'}(x_{e*}) = \frac{2B'_e}{\pi A'_e}(1 - \bar{f}'_e r_e)[1 + \cos(\theta_{ae}) \sin(\omega t) + \sin(\theta_{ae}) \cos(\omega t)] \quad (\text{B.1.5})$$

$$\sigma_i^*(x_i^*) = \frac{2B_i}{\pi A_i}[1 + \cos(\theta_{ai}) \sin(\omega t) + \sin(\theta_{ai}) \cos(\omega t)] \quad (\text{B.1.6})$$

$$\sigma_i^{*'}(x_i^{*'}) = \frac{2B'_i}{\pi A'_i}[1 + \cos(\theta'_{ai}) \sin(\omega t) + \sin(\theta'_{ai}) \cos(\omega t)] \quad (\text{B.1.7})$$

Substituting Eqns. 4.4.1 - 4.4.4 and Eqns. B.1.4 - B.1.5 in Eqns. 4.4.6 - 4.4.13, and equating the coefficients of the bias, sin and cos components to zero, the necessary algebraic equations, Eqns. 4.4.15 - 4.4.30, are obtained.

Glossary

Cortex. The outer layer of the brain; occupies a large fraction of the mammalian brain. The cortex consists of modules each with four to six layers. Cortical areas include the somatosensory cortex, visual cortex, and motor cortex, each processing signals primarily related to a specific modality.

Cross-correlation. The cross-correlation of two functions $f(t)$ and $g(t)$ is defined as $C(\tau) = \int_{-\infty}^{\infty} f(t)g(t + \tau)dt$. This function is a measure of the extent to which the activities of groups overlap.

Decay Period. Time in which the activity drops to \exp^{-1} of the value at $t = 0$ when external excitation is removed.

Desynchronization. Loss of synchronization of the oscillatory activity of two or more neuronal groups induced by delayed reentrant signaling. Besides the decrease in cross-correlation, the phase coherence is lost and the frequency spectra show broad complex peaks.

EEG. Electroencephalogram: Electrical potentials recorded by placing electrodes in the brain or on the scalp. The field potential is generated by currents in neural circuits.

Fixed point. Time independent solution(s) to the differential equations.

Frequency Modulation. The process of changing the frequency of the oscillations. The changes are usually made in a manner such that they can be decoded to extract information from the oscillations. Similarly ideas apply to amplitude and phase modulation as well (Tanenbaum, 1984).

Frequency Spectrum. The power at each frequency present in the signal. For a signal $f(t)$, the power is defined as $P(\omega) = |S(\omega)|$, where $S(\omega) = \int_{-\infty}^{\infty} f(t) \exp(i\omega t) dt$. In the present models, the power spectra refer to those of the fraction of neurons firing per unit time.

Fundamental frequency The frequency at which the maximum of the power spectrum occurs.

$GABA_A$ and $GABA_B$. Fast and slow inhibitory neurotransmitters which alter the time course of the action of inhibition.

Hippocampus. A cortical structure that resembles the sea horse. The neural circuits of the hippocampus are simpler than most other cortical areas and therefore have been extensively modeled and studied. CA3 is one subdivision of the hippocampus.

Harmonic. Frequency component having a multiple frequency of the fundamental frequency.

Jump bifurcation. Large change in the frequency, amplitude, and phase of the oscillations as a system parameter is varied. This phenomenon is commonly observed in nonlinear electrical circuits with feedback (Gelb and Velde, 1967); see also pg. 174 in Guckenheimer and Holmes (1983).

Limit Cycle. Isolated closed trajectory in phase space corresponding to periodic solutions.

Neuron. A fundamental unit of the nervous system. It receives excitatory and inhibitory impulses from other neurons through long distance and local circuits on its cell bodies or processes called dendrites. These impulses are integrated (nonlinearly) to control impulses to other neurons.

Neuromodulators. Chemicals activated at the synapse that produce complex long-lasting effects on the postsynaptic neuron.

Neuronal Group. Localized population of neurons tightly connected to form a module in the distributed system. These groups are conjectured to be the fundamental *I/O* units of complex neural systems (Edelman, 1978). Examples of neuronal groups include the orientation columns (which respond optimally to bars placed at particular angles in the visual field and ocular dominance columns (which respond optimally to visual stimuli in the left or right half of the visual field).

Neurotransmitters. Chemicals released at the presynaptic terminal that bind to the postsynaptic receptors thereby transmitting information from one neuron to the other. The time course of the activation of receptors is critical in determining the characteristics of the population oscillations (Traub et al., 1989).

Population Oscillations. Rhythmic variation in the number of neurons firing per unit time in a localized population of neurons. The synchronized firing of all the neurons is not necessary; indeed, the firing of single neurons may be asynchronous (Traub et al., 1989).

Reciprocal Connections. The synaptic connections between neurons in different neuronal groups. These connections are long range compared to the recurrent connections (see below).

Recurrent Connections. The synaptic connections between neurons in the same neuronal group.

Reentrant Signaling. Two or more neuronal groups which are mutually

interconnected can supply one another with positive or negative feedback. Such mutual feedback can be delayed in time and may be continuous or intermittent (Edelman, 1978); see also Chapter 4 in Edelman (1989).

Refractory Period. Time during which the neuron can not fire due to hyperpolarization of the membrane potential.

Renormalization. The technique of replacing the complex response of a collection of units with the (simpler) response of the average in order to deduce the critical features associated with the global behavior of the dynamical system (Guckenheimer and Holmes, 1983).

Resynchronization. Synchronization of the oscillations following jump bifurcation. The phase difference between the activities of the groups flips by 180° , the frequency jumps by about 50%, and the amplitude shows a small increase as well. These changes underlie dynamic frequency, amplitude, and phase modulation of the oscillations.

Sigmoid. The nonlinear saturation function $\sigma(x) = \frac{1}{1 + \exp(-\beta(x - \chi))}$, where β and χ are respectively the sigmoid nonlinearity and threshold.

Subharmonic. Frequency components at a fraction of the fundamental frequency.

Synapse. Junction of two neurons by which neurons communicate either electrically or chemically. Synapses may be either excitatory or inhibitory.

Synaptic strength. The ability of a presynaptic neuron to excite or inhibit the postsynaptic neuron.

Synchronization. Groups with differing intrinsic frequencies can synchronize at the same frequency. Synchronization is accompanied by an increase in

the cross-correlation between the fraction of neurons firing per unit time for (two or more) groups, the phase plot indicates a limit cycle, and the frequency spectra show considerable overlap.

Time Course. The time course of a signal refers to the temporal form of activation of the signal. Time courses due to synaptic delays are typically of the form $\alpha(t) \sim t \exp^{-t/\tau}$; additionally, the transduction of signals can also be delayed due to transmission delays.

Bibliography

- Alexander, G. E., DeLong, M. R., and Strick, P. L. (1986). Parallel organization of functionally segregated circuits linking basal ganglia and cortex. *Annual Review of Neuroscience*, 9:357–381.
- an der Heiden, U. (1980). *Analysis of Neural Networks*, volume 35 of *Lecture Notes in Mathematics*. Springer, New York.
- Arbib, M. A. and Amari, S. (1989). *Dynamic Interactions in Neural Networks: Models and Data: Vol 1 Research Notes in Neural Computing*. Springer Verlag, New York.
- Aspray, W. and Burks, A., editors (1987). *Papers of John von Neumann on computing and computer theory*. MIT Press, Cambridge.
- Bernstein, N. (1967). *The co-ordination and regulation of movements*. Pergamon, Oxford.
- Bogoliubov, N. N. and Mitropolsky, Y. A. (1961). *Asymptotic Methods in the Theory of Nonlinear Oscillations*. Hindustan Publishing Corp., New Delhi.
- Brazier, M. A. B. (1977). *Electrical activity of the nervous system*. Pitman, London.
- Bressler, S. L. and Freeman, W. J. (1980). Frequency analysis of olfactory system EEG in cat, rabbit and rat. *Electroencephogr. Clin. Neurophysiol.*, 50:19–24.

- Bullier, J., McCourt, M. E., and Henry, G. H. (1988). Physiological studies on the feedback connection to the striate cortex from cortical areas 18 and 19 in the cat. *Exp. Brain Res.*, 70:90–98.
- Charniak, E. and McDermott, D. V. (1985). *Introduction to Artificial Intelligence*. Addison-Wesley, Reading, Mass.
- Cohen, A. H., Rossignol, S., and Grillner, S., editors (1987). *Neural Control of Rhythmic Movements in Vertebrates*. John Wiley, New York.
- Cowan, J. D. (1971). Stochastic models of neuroelectric activity. In Rice, S., Light, J., and Freed, K., editors, *Proc. Conf. Stat. Mech.*, Chicago. IUPAP, University of Chicago Press.
- DeYoe, E. A. and van Essen, D. C. (1988). Concurrent processing streams in monkey visual cortex. *Trends in Neuroscience*, 11-5:219–226.
- Eckhorn, R., Bauer, R., Jordan, W., Brosch, M., Munk, M., and Reitboeck, H. J. (1988). Coherent oscillations: A mechanism of feature linking in the visual cortex? *Biological Cybernetics*, 60:121–130.
- Edelman, G. M. (1978). Group selection and phasic reentrant signaling: A theory of higher brain function. In Edelman, G. M. and Mountcastle, V. B., editors, *The Mindful Brain: Cortical Organization and the Group Selective Theory of Higher Brain Function*. MIT Press, Cambridge.
- Edelman, G. M. (1987). *Neural Darwinism: The Theory of Neuronal Group Selection*. Basic Books, New York.
- Edelman, G. M. (1989). *The Remembered Present: A Biological Theory of Consciousness*. Basic Books, New York.

- Edelman, G. M. and Finkel, L. H. (1984). Neuronal group selection in the cerebral cortex. In Edelman, G. M., Gall, W. E., and Cowan, W. M., editors, *Dynamic Aspects of Neocortical Function*, pages 653–695. J. Wiley, New York.
- Evarts, E. E., Shinoda, Y., and Wise, S. P. (1984). *Neurophysiological Approaches to Higher Brain Functions*. J. Wiley, New York.
- Feldman, J. A. and Ballard, D. (1982). Connectionist models and their properties. *Cognitive Science*, 6:205–254.
- Finkel, L. H. and Edelman, G. M. (1987). Population rules for synapses in networks. In Edelman, G. M., Gall, W. E., and Cowan, W. M., editors, *Synaptic Function*, pages 711–757. J. Wiley, New York.
- Finkel, L. H. and Edelman, G. M. (1989). Integration of distributed cortical systems by reentry: a computer simulation of interactive functionally segregated visual areas. *Journal of Neuroscience*, 9-9:3188–3208.
- Freeman, W. J. and Skarda, C. A. (1985). Spatial EEG patterns, nonlinear dynamics, and perception: The neo-sherringtonian view. *Brain Res. Rev.*, 10:147–175.
- Frohlich, J. (1983). *Scaling and Self-similarity in Physics: Renormalization in Statistical Mechanics and Dynamics*. Birkhauser, Boston.
- Fuster, J. M. (1986). The prefrontal cortex and temporal integration. In Peters, A. and Jones, E. G., editors, *Cerebral Cortex, Vol:4*, pages 151–177. Plenum, New York.

- Gelb, A. and Velde, W. E. V. (1967). *Multiple Input Describing Functions and Nonlinear System Design*. McGraw-Hill, New York.
- Gibbon, J. and Allan, L. (1984). *Timing and Time Perception*. New York Academy of Science, New York.
- Goldman-Rakic, P. S. (1988). Topography of cognition: Parallel distributed networks in primate association cortex. *Annual Review of Neuroscience*, 14:137–156.
- Gray, C. M., Engel, A. K., and Singer, W. (1989). Oscillatory responses in cat visual cortex exhibit inter-columnar synchronization which reflects global stimulus properties. *Nature*, 338:334–337.
- Gray, C. M. and Singer, W. (1989). Stimulus-specific neuronal oscillations in orientation columns of the cat visual cortex. *Proc. Natl. Acad. Sci. USA*, 86:1698–1702.
- Guckenheimer, J. and Holmes, P. (1983). *Nonlinear Oscillations, Dynamical Systems, and Bifurcations of Vector Fields*. Springer-Verlag, New York.
- Haenny, P. E., Maunsell, J. H. R., and Schiller, P. H. (1988). State-dependent activity in monkey visual cortex, 2: Retinal and extraretinal factors in v4. *Exp. Brain Res.*, 69:245–259.
- Hebb, D. O. (1949). *The Organization of Behavior*. J. Wiley, New York.
- Hille, B. and Catterall, W. A. (1989). Electrical excitability and ionic channels. In Siegel, G., Agranoff, B., Albers, R. W., and Molinoff, P., editors, *Basic Neurochemistry: Molecular, Cellular, and Medical Aspects*. Raven Press, New York.

- Hillis, D. (1985). *The Connection Machine*. MIT, Cambridge.
- Hillyard, S. A. and Picton, T. W. (1987). Electrophysiology of cognition. In Plum, F., editor, *Handbook of Physiology: higher functions of the nervous system*, pages 519–584. American Physiological Society, Baltimore.
- Hinton, G. E. and Anderson, J. A., editors (1981). *Parallel Models of Associative Memory*. Erlbaum, Hillsdale, NJ.
- Hobson, J. A. and Steriade, M. (1986). *Neuronal Basis of Behavioral State Control*, pages 701–823. Handbook of Physiology, Vol:4, Section 1, The Nervous System. American Physiological Society, Bethesda, Md.
- Hopfield, J. J. (1982). Neural nets and physical systems with emergent collective computational properties. *Proc. Natl. Acad. Sci. USA*, 79:2554–2558.
- Hopfield, J. J. (1984). Neurons with graded response have collective computational properties like those of two-state neurons. *Proc. Natl. Acad. Sci. USA*, 3088–3092.
- Hubel, D. H. and Wiesel, T. N. (1977). Functional architecture of macaque monkey visual cortex. *Proc. Roy. Soc. Lond. [Biol.]*, 198:1–59.
- Kelso, J. A. S. and Tuller, B. (1984). A dynamical basis for action systems. In Gazzaniga, M. S., editor, *Handbook of Cognitive Neuroscience*. Plenum, New York.
- Koch, C. and Poggio, T. (1987). Biophysics of computation: Neurons, synapses, and membranes. In Edelman, G. M., Gall, W. E., and Cowan, W. M., editors, *Synaptic Function*. J. Wiley, New York.

- Koch, C., Poggio, T., and Torre, V. (1983). Nonlinear interactions in a dendritic tree: Localization, timing, and role in information processing. *Proc. Natl. Acad. Sci. USA*, 80:2799–2802.
- Kolmanovskii, V. B. and Nosov, V. R. (1986). *Stability of Functional Differential Equations*. Academic Press, London.
- Kopell, N. (1988). Toward a theory of modeling central pattern generators. In Cohen, A. H., Rossignol, S., and Grillner, S., editors, *Control of Rhythmic Movements in Vertebrates*. John Wiley, New York.
- Kristofferson, A. B. (1984). Quantal and deterministic timing in human duration discrimination. In Gibbon, J. and Allan, L., editors, *Timing and Time Perception*. New York Academy of Science, New York.
- Li, Z. and Hopfield, J. J. (1988). Modeling the olfactory bulb – coupled nonlinear oscillators. In Anderson, D. Z., editor, *Neural Information Processing Systems*, New York. AIP.
- Llinas, R. R. (1988). The intrinsic electrophysiological properties of mammalian neurons: A new insight into cns function. *Science*, 242:1654–1664.
- Marcus, C. M. and Westervelt, R. M. (1989). Stability of analog neural networks with delay. *Physical Review A*, 39:347–359.
- Marder, E., Hooper, J. S., and Eisen, H. (1987). Multiple neurotransmitters provide a mechanism for the production of multiple outputs from a single neuronal circuit. In Edelman, G. M., Gall, W. E., and Cowan, W. M., editors, *Synaptic Function*, pages 305–327. J. Wiley, New York.

- Marr, D. (1982). *Vision*. W. H. Freeman, New York.
- McCulloch, W. S. and Pitts, W. H. (1943). A logical calculus of the ideas immanent in nervous activity. *Bull. Math. Biophysics*, 5:115–133.
- Mees, A. I. (1981). *Dynamics of Feedback Systems*. John Wiley, New York.
- Mountcastle, V. B. (1978). An organizing principle for cerebral function: The unit module and the distributed system. In Edelman, G. M. and Mountcastle, V. B., editors, *The Mindful Brain: Cortical Organization and the Group Selective Theory of Higher Brain Function*. MIT Press, Cambridge.
- Mountcastle, V. B., Steinmetz, M. A., and Ramo, R. (1990). Frequency discrimination in the sense of flutter: Psychological measurements correlated with postcentral events in behaving monkeys. *Journal of Neuroscience*, 10 (9):3032–3044.
- Murray, J. D. (1989). *Mathematical Biology*. Springer Verlag, New York.
- Poppel, E. (1978). Time perception. In Tuber, H. and Held, R., editors, *Handbook of Sensory Physiology*. Springer-Verlag, New York.
- Poppel, E. and Logothetis, N. (1986). Neuronal oscillations in the human brain. *Naturwissenschaften*, 73:267–268.
- Poppel, E., Schill, K., and von Steinbuchel, N. (1990). Sensory integration within temporally neutral system states: A hypothesis. *Naturwissenschaften*, 77:89–91.
- Raibert, M. (1986). *Legged Robots that Balance*. MIT Press, Cambridge.

- Rand, R. H., Cohen, A. H., and Holmes, P. (1988). Systems of coupled oscillators as models of central pattern generators. In Cohen, A. H., Rossignol, S., and Grillner, S., editors, *Control of Rhythmic Movements in Vertebrates*. John Wiley, New York.
- Reeke, G. N. and Edelman, G. M. (1988). Real brains and artificial intelligence. In Graubard, S. R., editor, *The Artificial Intelligence Debate: False Starts, Real Foundations*. MIT, Cambridge.
- Reeke, G. N., Sporns, O., and Edelman, G. M. (1989). Synthetic neural modeling: Comparisons of population and connectionist approaches. In Pfeifer, R., Schreter, Z., Fogelman-Soulie, F., and Steels, L., editors, *Connectionism in Perspective*. North-Holland, Amsterdam.
- Rumelhart, D. and McClelland, J. (1986). *Parallel Distributed Processing: Explorations in the Microstructure of Cognition; Vol. 1: Foundations; Vol. 2: Psychological and Biological Models*. MIT, Cambridge.
- Schillen, T. B. and Konig, P. (1990). Coherency detection and response segregation by synchronizing and desynchronizing delay connections in a neuronal oscillator model. In *Proc. Int. Jnt. Conf. Neural Networks*, volume 2, pages 387–395.
- Shepherd, G. M. (1988a). A basic circuit of cortical organization. In Gazzaniga, M. S., editor, *Perspectives in memory research*. MIT Press, Cambridge.
- Shepherd, G. M. (1988b). *Neurobiology*. Oxford, New York, 2nd edition.

- Sporns, O., Gally, J. A., Reeke, G. N., and Edelman, G. M. (1989). Reentrant signaling among simulated neuronal groups leads to coherency in their oscillatory activity. *Proc. Natl. Acad. Sci. USA*, 86:7265–7269.
- Staddon, J. E. R. (1983). *Adaptive Behavior and Learning*. Cambridge Univ. Press, Cambridge.
- Steriade, M., Jones, E. G., and Llinas, R. R. (1990). *Thalamic Oscillations and Signaling*. J. Wiley, New York.
- Stoker, J. J. (1950). *Nonlinear Vibrations in Mechanical and Electrical Systems*. J. Wiley, New York.
- Tanenbaum, A. S., editor (1984). *Structured Computer Organization*. Prentice Hall, Englewood Cliffs, NJ.
- Thorpe, S. J. and Imbert, M. (1989). Biological constraints on connectionist modeling. In Pfeifer, R., Schreter, Z., Fogelman-Soulie, F., and Steels, L., editors, *Connectionism in Perspective*. North-Holland, Amsterdam.
- Traub, R. D., Miles, R., and Wong, R. K. S. (1988). Large scale simulations of the hippocampus. *IEEE Eng. Med. Biol. Mag.*, 7:31–34.
- Traub, R. D., Miles, R., and Wong, R. K. S. (1989). Model of the origin of rhythmic population oscillations in the hippocampal slice. *Science*, 243:1319–1325.
- Tuckwell, H. C. (1988). *Introduction to theoretical neurobiology; Vol. 1: Linear Cable Theory and dendritic structure, Vol. 2: Nonlinear and stochastic theories*. Cambridge Univ. Press, Cambridge.

- von der Malsburg, C. and Schneider, W. (1986). A neural cocktail-party processor. *Biological Cybernetics*, 54:29–40.
- von Neumann, J. (1956). Probabilistic logics and the synthesis of reliable organisms from unreliable components. In Shannon, C. E. and McCarthy, J., editors, *Automata Studies*. Princeton University Press, Princeton.
- Wang, D., Buhmann, J., and von der Malsburg, C. (1990). Pattern segmentation in associative memory. *Neural Computation*, 2:94–106.
- Wiener, N. (1961). *Cybernetics*. MIT Press, Cambridge.
- Wilson, H. R. and Cowan, J. D. (1972). Excitatory and inhibitory interactions in localized populations of model neurons. *Biophys. J.*, 12:1–24.
- Wilson, H. R. and Cowan, J. D. (1973). A mathematical theory of the functional dynamics of cortical and thalamic nervous tissue. *Kybernetik*, 13:55–80.
- Winograd, T. and Cowan, J. D. (1963). *Reliable Computation in the presence of noise*. MIT Press, Cambridge.
- Winston, P. H. and Brown, R. H., editors (1979). *Artificial Intelligence: An MIT Perspective; Volume 1: Expert Problem Solving, Natural Language Understanding, Intelligent Computer Coaches, Representation, and Learning; Volume 2: Understanding Vision, Manipulation, Computer Design, and Symbol Manipulation*. MIT, Cambridge.
- Wolfram, S. (1989). *Mathematica*. Addison-Wesley, Reading, Mass.
- Zeki, S. and Shepp, S. (1988). The functional logic of cortical connections. *Nature*, 335:311–317.

VITA

Ellikulath Vinod Menon was born on February 22, 1961, the son of Ellikulath Sathyavathi Menon and Achat Bhaskara Menon in Trichur, India. He attended the Indian Institute of Technology, Kharagpur, from 1979 to 1982, graduating with a degree in physics. He joined the Department of Physics at the University of Texas at Austin in 1984 and was engaged in research in statistical and plasma physics. In 1988, he transferred to the Department of Computer Sciences to pursue an interest in neural networks.

Permanent address: 7-54 Keerankulangara
Trichur, Kerala
India 680005

This dissertation was typeset¹ with \LaTeX by the author.

¹ \LaTeX document preparation system was developed by Leslie Lamport as a special version of Donald Knuth's \TeX program for computer typesetting. \TeX is a trademark of the American Mathematical Society. The \LaTeX macro package for The University of Texas at Austin dissertation format was written by Khe-Sing The.